530

International Atomic Energy Agency

INDC(SEC)-31/U

INDC

INTERNATIONAL NUCLEAR DATA COMMITTEE

FIFTH MEETING OF THE INTERNATIONAL NUCLEAR DATA COMMITTEE

TOPICAL DISCUSSION

ON

INELASTIC SCATTERING OF FAST NEUTRONS

January 1973

IAEA NUCLEAR DATA SECTION, KÄRNTNER RING 11, A-1010 VIENNA

INDC(SEC)-31/U

Fifth Meeting of the International Nuclear Data Committee

Topical Discussion

on

Inelastic Scattering of Fast Neutrons

January 1973

Table of Contents

A Multi-Angle Time-of-Flight Spectrometer

Y. Yamanouti and S. Tanaka

A multi-angle time-of-flight spectrometer for fast neutron scattering experiments in conjunction with the JAERI 5.5 MV Van de Graaff accelerator will be reported.

The spectrometer consists of four simultaneously operational detectors placed in 10° steps on a large turn table which is rotatable around the scattering sample. And the maximum flight paths are 8 m.

In the performance test, time spectra of neutrons elastically and inelastically scattered from carbon and iron in the energy regions around 20 MeV and below 8 MeV were observed over the angular range 30° to 155°. An overall time resolution of 2.5 nsec was obtained. And since it is very important to reduce background neutrons especially for the experiments in the region around 20 MeV, several shapes of shadow bars which intercept neutrons entering into detectors directly from the neutron source were tried and the optimum shape was found.

A Multi-Angle Time-of-Flight Spectrometer

Y. Yamanouti and S. Tanaka

Japan Atomic Energy Research Institute, Tokai-mura, Japan

The elastic and inelastic scattering neutron cross sections in the energy range 8 MeV to a few tens of MeV are very interesting for the investigation of the nuclear reaction mechanism, and recently have been also required for the nuclear fusion technology. However, we have few experimental data on the elastic and inelastic neutron scattering in this energy range except 14 MeV data, because of the peculiar difficulty of fast neutron measurements. In our laboratory, therefore, for the purpose of obtaining differential neutron scattering information in the energy range around 20 MeV, a time-of-flight spectrometer with four simultaneously operational detectors and with 8 m flight paths, which is used in conjuction with the JAERI 5.5 MV Van de Graaff accelerator, has been newly constructed and made operational.

Fig. 1 shows the experimental layout inclusive of the newly constructed time-of-flight spectrometer. 10 nsec wide pulsed beams with the pulse repetition rate of 1 MHZ produced in the high voltage terminal are accelerated through the acceleration tube of the Van de Graaff accelerator. After acceleration, finally about 1 nsec wide pulsed beams are formed at the neutron producing target by an electrostatic deflector and a time compression magnet of Mobley type. The observed pulse duration of deuteron beams at 5 MeV is about 1.5 nsec.

Fig. 2 shows the top view and vertical cross section of the collimator-shield system. Four detectors are placed in 10° steps on a large turn

table which is rotatable around the scattering sample. The range of scattering angles is -30° to +157° and the flight path of a detector is variable from 2 to 8 m, but simultaneous operation of four detectors is available at flight paths longer than 4 m. The collimator-shield system consists of four iron shadow bars, a collimator tank, four detector shield tanks and a large turn table. The collimator tank is necessary to reduce the air scattering and background neutrons scattered from the experimental equipments near the neutron source. The detector shield tanks are of nearly rectangular solid. These tanks are filled with paraffin.

Fig. 3 shows a block diagram of the electronics system which is designed to enable four neutron detectors to be used simultaneously. Electronics circuits are those of conventional time-of-flight technique with n-γ pulse shape discrimination. The neutron detector is a 12.7 cm in diameter, and 10.2 cm thick NE213 liquid scintillator optically coupled to an RCA C70133B photomultiplier tube. One of the output signals of each time-to-pulse-height-converter is used as a routing signal to a selective storage unit, and the other output signal is fed into an analog-to-digital-converter through a mixer. Finally time spectra from four detectors are stored in a 4096 channel pulse height analyzer. The overall time resolution of this spectrometer from measurements of the direct neutron time-of-flight spectra was 2.5 nsec (FWHM).

As a performance test to check up the design of the collimator-shield system and the operation of the electronics system, neutron time-of-flight spectra from a carbon sample together with sample-out background spectra were measured at various angles with 21.5 MeV neutrons. The obtained spectra are shown in figs. 4 and 5. In these spectra 1 channel corresponds to 0.5 nsec. 21.5 MeV neutrons are generated by the $T(d,n)^4He$ re-

action and average neutron flux at the center of scattering sample is about 1.3×10^6 $sec^{-1} \cdot cm^{-2}$. As shown in figures neutron backgrounds become comparable with the elastic and inelastic peaks at backward angles. The peak appeared in the background spectrum may be due to the neutrons elastically scattered from the edges of the collimator tank and shadow bars. In the energy range around 20 MeV the angular distributions of the elastically scattered neutrons have a tendency to show large cross sections at forward angles and to decrease rapidly with increasing scattering angle. Therefore, in this energy range neutron shielding is very difficult especially at backward angles. Since the shadow bar plays an important role to reduce neutron backgrounds, several shapes of the shadow bar which intercepts neutrons directly entering into the detectors from the neutron source were tried and optimum shape was found. Two time-of-flight spectra were measured at 50° by two detectors placed at different positions on the large turn table, and then the disagreement of the elastic cross sections obtained from these two spectra was within 6 percent of the obtained cross section. Fig. 6 shows a photograph of the spectrometer. The results of the performance tests have shown that this spectrometer is capable for obtaining the differential elastic and inelastic scattering information with overall time resolution 2.5 nsec in the energy range around 20 MeV.

Figure captions

Fig. 1 Experimental layout inclusive of the newly constructed time-of-flight spectrometer.

Fig. 2 Top view and vertical cross section of the collimator-shield system.

Fig. 3 Block diagram of the electronics system which is designed to enable four neutron detectors to be used simultaneously.

Fig. 4 Time-of-flight spectra for the $^{12}C(n,n)^{12}C$ and $^{12}C(n,n')^{12}C$ reactions obtained at 30° to 60°.

Fig. 5 Time-of-flight spectra for the $^{12}C(n,n)^{12}C$ and $^{12}C(n,n')^{12}C$ reactions obtained at 85° to 115°.

Fig. 6 Photograph of the spectrometer.

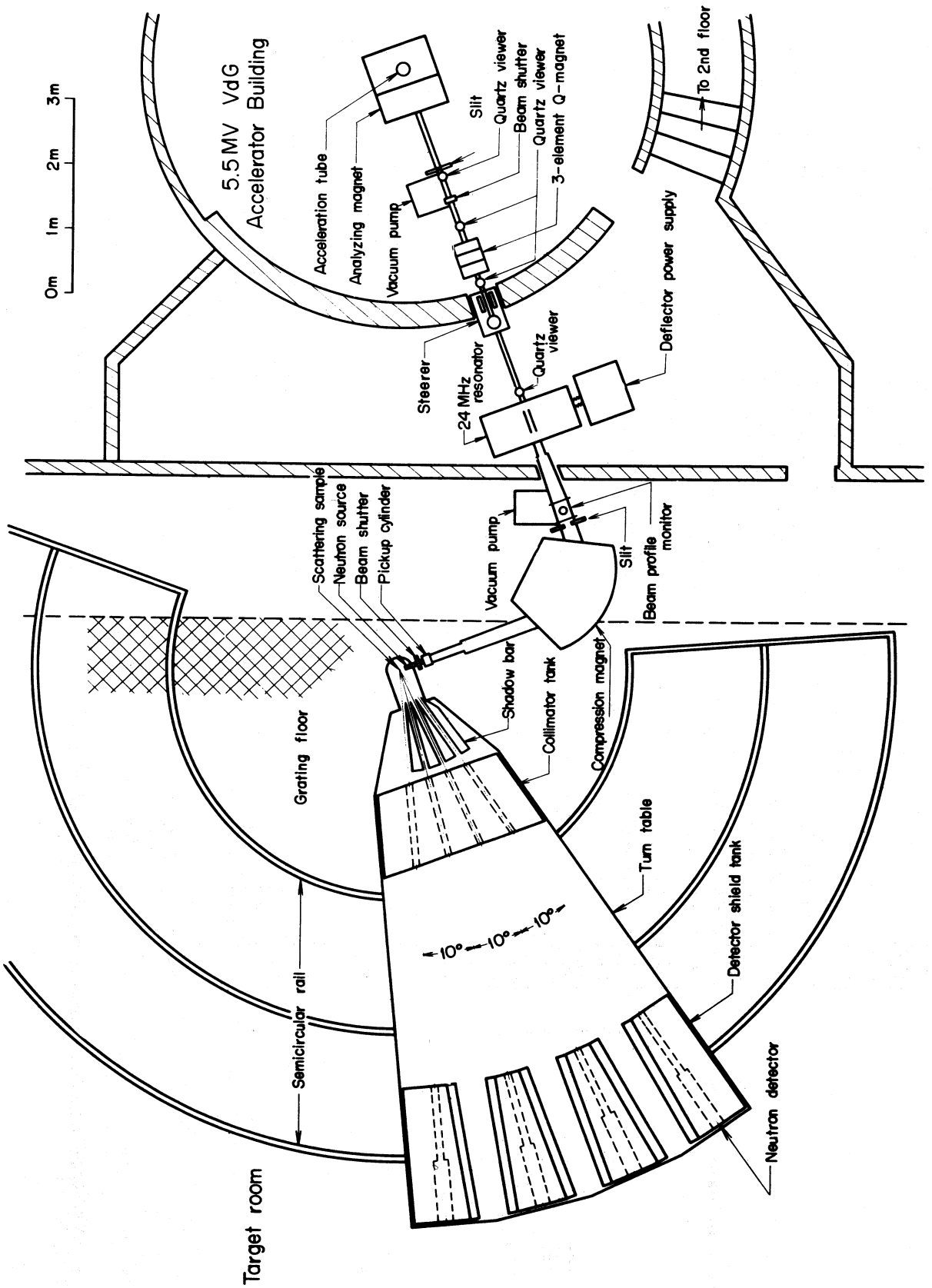
0m 1m 2m 3m
5.5 MV VdG
Accelerator Building
Acceleration tube
Analyzing magnet
Vacuum pump
Slit
Quartz viewer
Beam shutter
Quartz viewer
3-element Q-magnet
To 2nd floor
Steerer
24 MHz resonator
Quartz viewer
Deflector power supply
Scattering sample
Neutron source
Beam shutter
Pickup cylinder
Vacuum pump
Slit
Beam profile monitor
Grating floor
Shadow bar
Collimator tank
Compression magnet
Turn table
Detector shield tank
Semicircular rail
10°
10°
10°
Neutron detector
Target room

Fig. 1

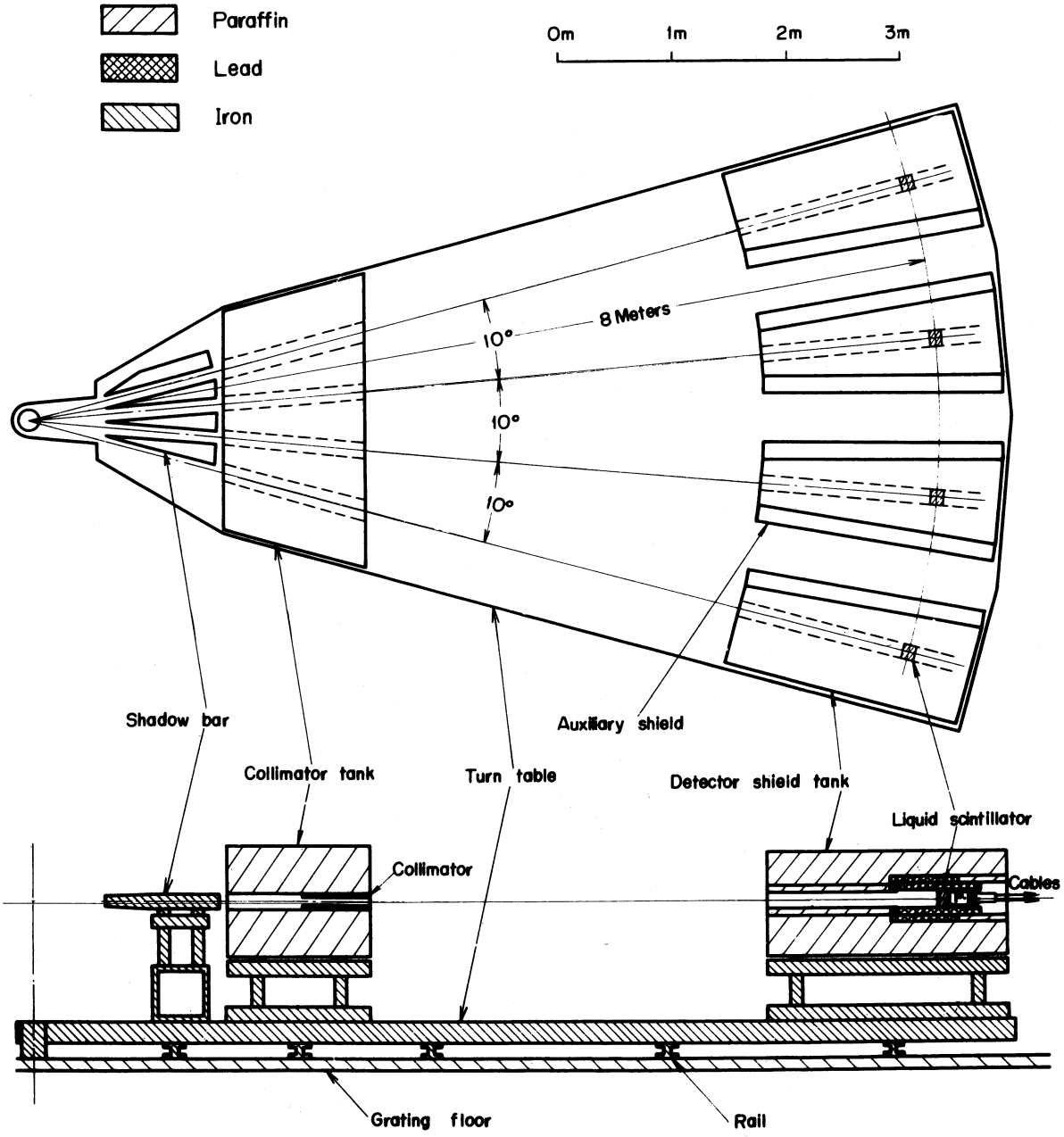
Paraffin
Lead
Iron
0m
1m
2m
3m
10°
8 Meters
10°
10°
Shadow bar
Collimator tank
Turn table
Auxiliary shield
Detector shield tank
Liquid scintillator
Collimator
Cables
Grating floor
Rail

Fig. 2

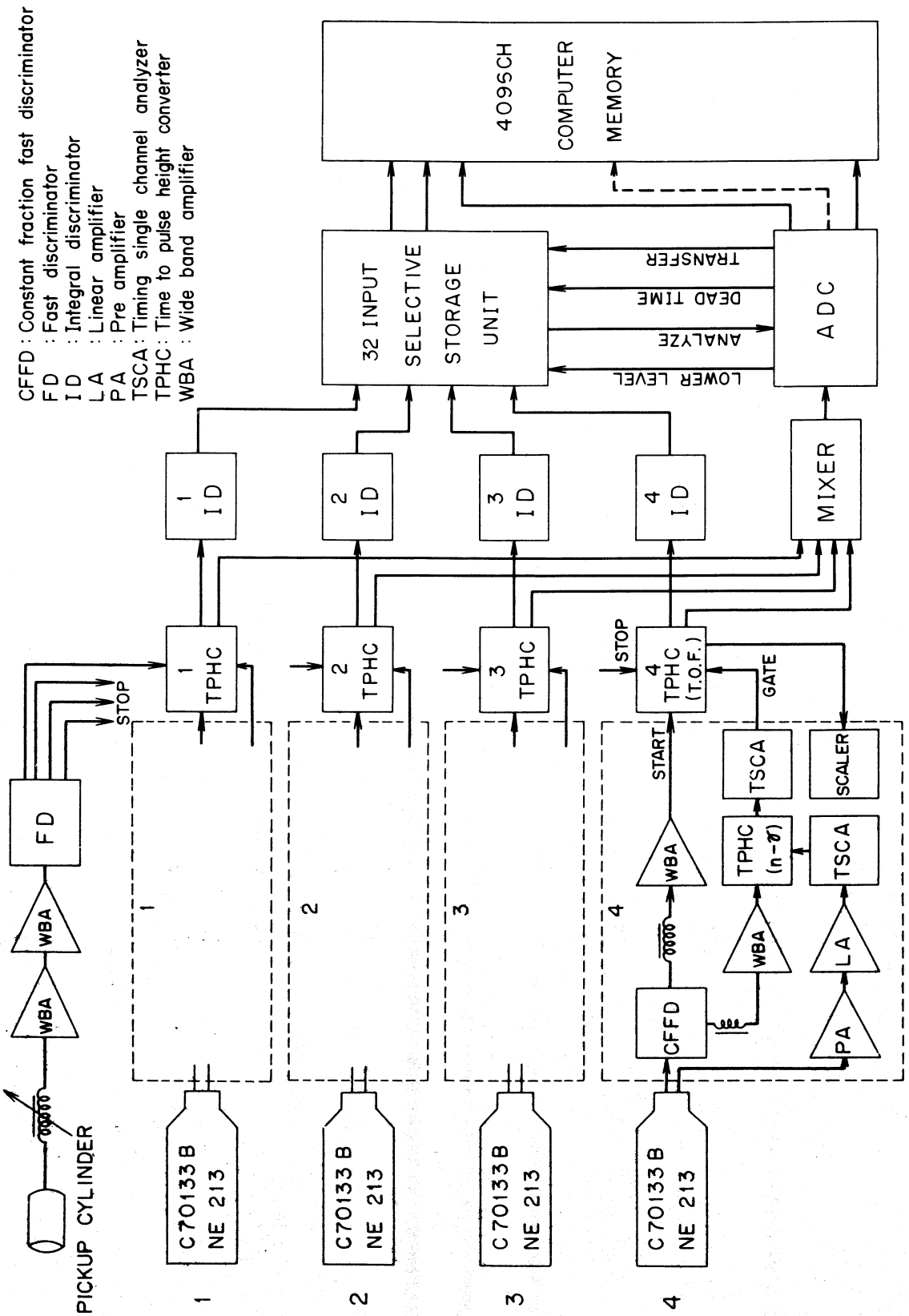
CFFD : Constant fraction fast discriminator
FD : Fast discriminator
ID : Integral discriminator
LA : Linear amplifier
PA : Pre amplifier
TSCA : Timing single channel analyzer
TPHC : Time to pulse height converter
WBA : Wide band amplifier
4096CH
COMPUTER
MEMORY
32 INPUT
SELECTIVE
STORAGE
UNIT
LOWER LEVEL
ANALYZE
DEAD TIME
TRANSFER
ADC
MIXER
1 ID
2 ID
3 ID
4 ID
1 TPHC
2 TPHC
3 TPHC
4 TPHC (T.O.F.)
STOP
START
GATE
FD
WBA
WBA
CFFD
WBA
TPHC (n-σ)
TSCA
LA
PA
TSCA
SCALER
C70133B NE 213
PICKUP CYLINDER
1
2
3
4

Fig. 3

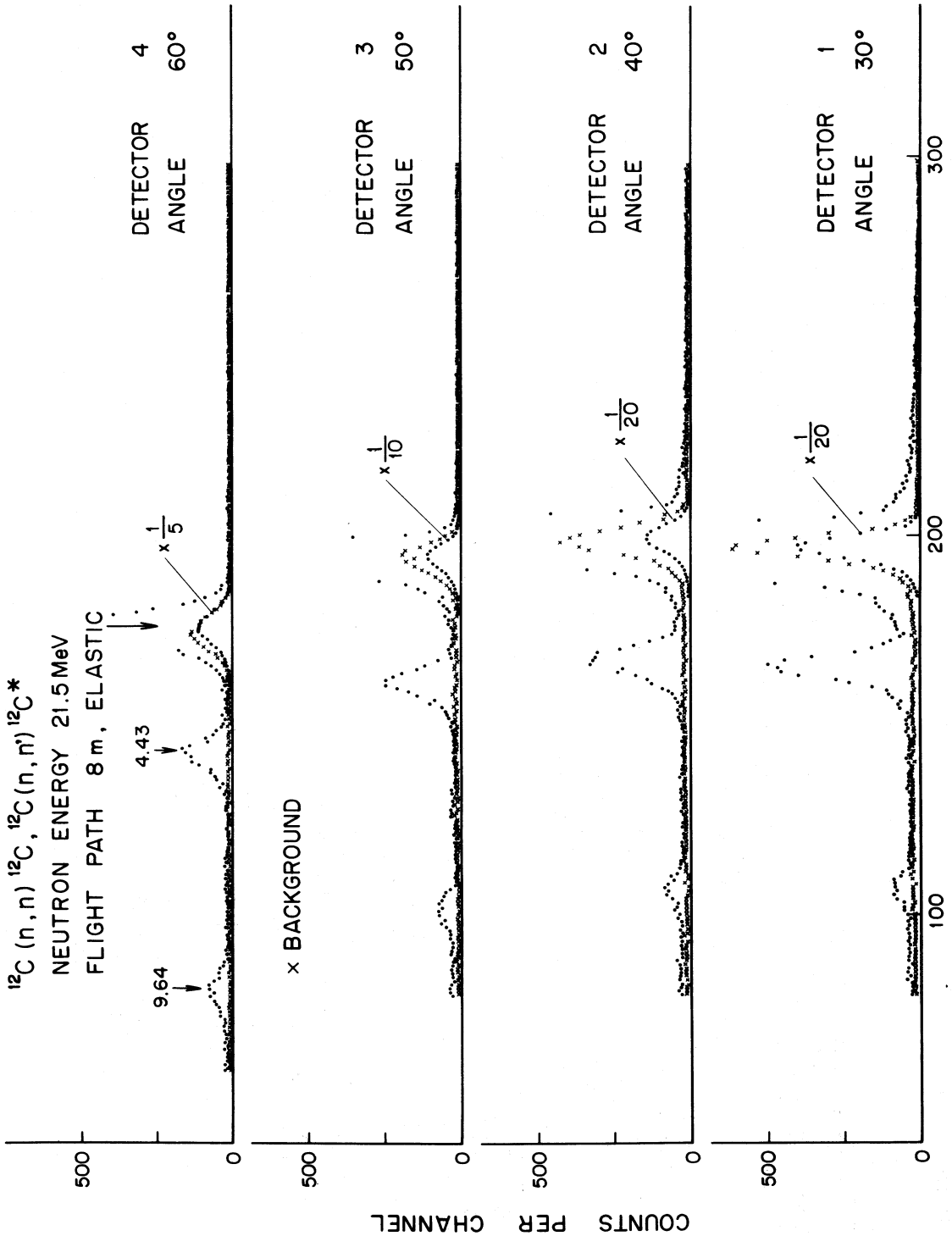
$^{12}C(n,n)^{12}C, ^{12}C(n,n')^{12}C^*$
NEUTRON ENERGY 21.5 MeV
FLIGHT PATH 8 m, ELASTIC
9.64
4.43
DETECTOR 4
ANGLE 60°
× 1/5
× BACKGROUND
DETECTOR 3
ANGLE 50°
× 1/10
DETECTOR 2
ANGLE 40°
× 1/20
DETECTOR 1
ANGLE 30°
× 1/20
500
0
100
200
300
COUNTS PER CHANNEL
CHANNEL NUMBER

Fig. 4

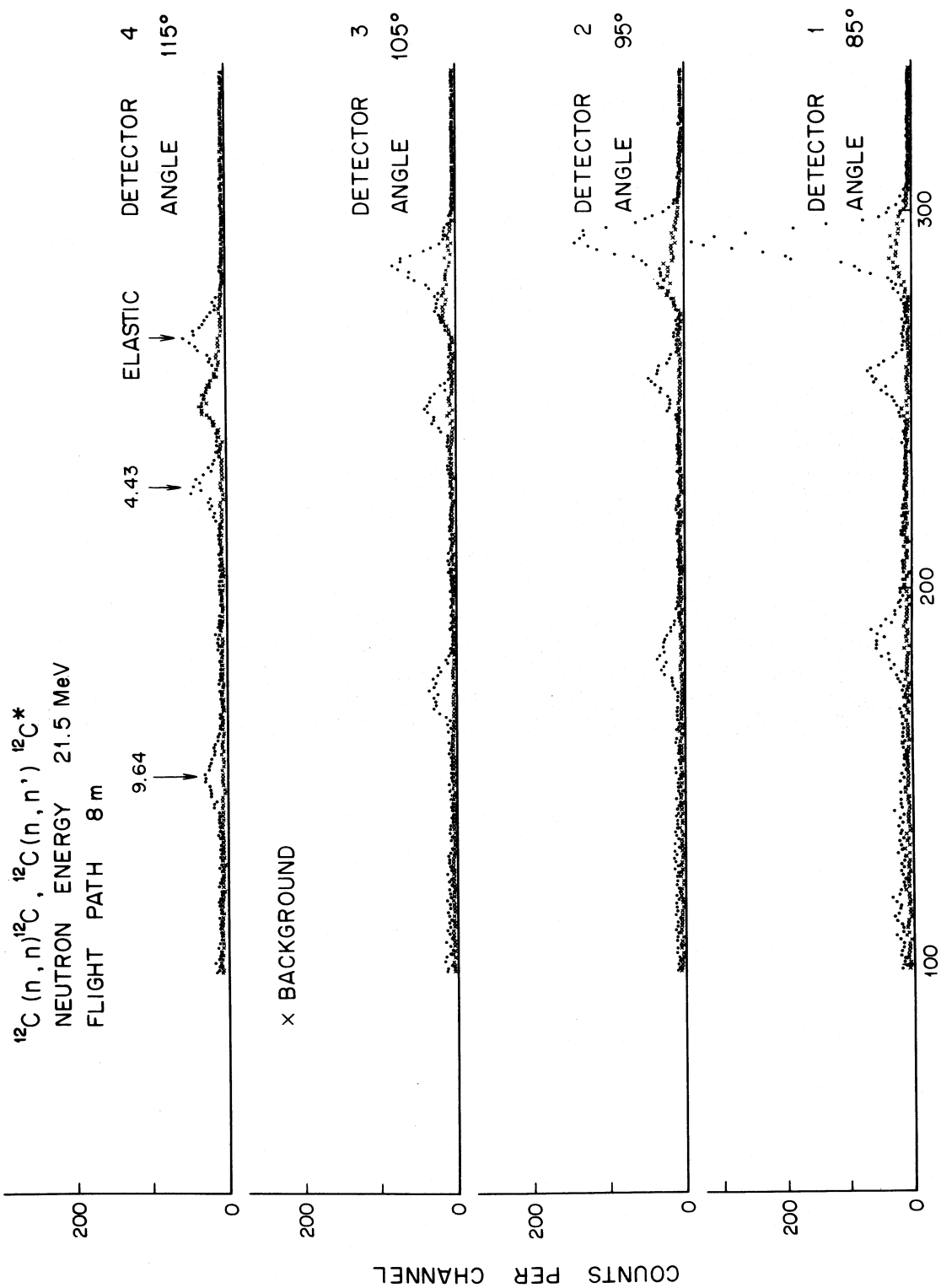
$^{12}C(n,n)^{12}C$, $^{12}C(n,n')^{12}C^*$
NEUTRON ENERGY 21.5 MeV
FLIGHT PATH 8 m
9.64
4.43
ELASTIC
DETECTOR 4
ANGLE 115°
× BACKGROUND
DETECTOR 3
ANGLE 105°
DETECTOR 2
ANGLE 95°
DETECTOR 1
ANGLE 85°
200
0
100
300
COUNTS PER CHANNEL
CHANNEL NUMBER

Fig. 5

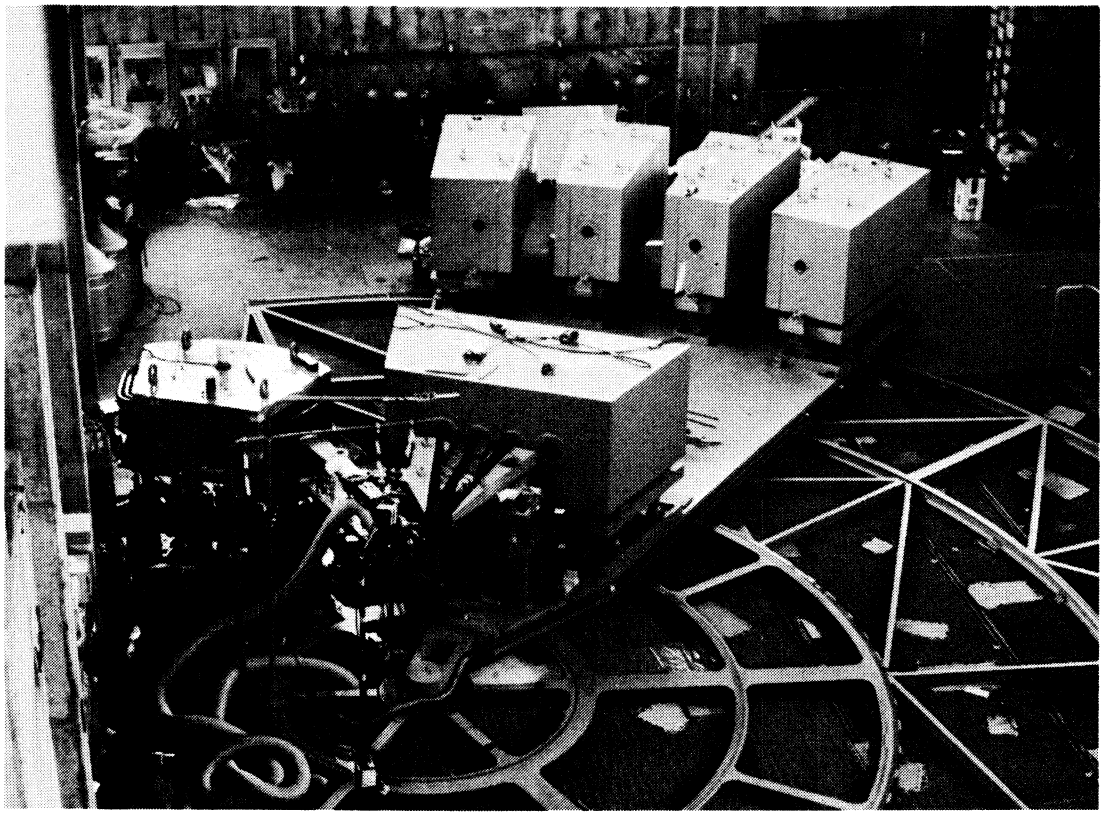

Fig. 6

Cierjacks: What kind of neutron producing reaction is involved for fast neutron scattering experiments ?

reply: 20 MeV neutrons are generated by the $T(d,n)^4He$ reaction, and the $D(d,n)^3He$ reaction. The $T(p,n)^3He$ reaction is used for obtaining several MeV neutrons.

Cierjacks: What is the average neutron source strength of the spectrum, etc. ?

reply: The average neutron flux at the center of scattering sample is about 1.3×10^6 sec^{-1} cm^{-2}.

Cross: What is the lowest energy of a first excited state for which inelastically scattered 20 MeV neutrons can be resolved ?

reply: At present the lowest energy of a first excited state to be resolved is about 1.4 MeV by means of the peeling off method.

Condé: What elements are you going to study at first ?

reply: Elastic and inelastic angular distributions of neutrons scattered from carbon and sulphur were measured at first. Measurements on silicon will be studied next.

Divatia: What is the average current available from the accelerator ?

reply: The average current available from the accelerator is about 5 micro amperes.

This is a blank page

This is a blank page

This is a blank page

Inelastic Scattering of Neutrons from U-238

B.H. Armitage, J.L. Rose and W. Spencer

Measurements of the entire secondary neutron spectrum at 90 degrees have been made at seven neutron energies between 1.13 and 2.37 Mev. The results have been compared with calculations due to Prince which take into account direct excitation of rotational levels in addition to the dominant contribution due to compound nuclear formation.

This is a blank page

INELASTIC NEUTRON SCATTERING FROM ^{238}U

Although a number of measurements of the ^{238}U inelastic neutron scattering cross sections have been made up to 1.5 MeV, the only recent measurements reported above this energy are those of Knitter [1] and Batchelor [2]. The present measurements, which have been made between 1.13 MeV and 2.37 MeV, are in the vicinity of the ^{238}U fission threshold and consequently cover an important energy region for fast reactor nuclear data purposes. Furthermore this energy region is one where direct interaction contribution may be just significant and where the total inelastic cross section is less likely to be dominated by threshold effects which pose difficulties for calculations of the Hauser-Feshbach type.

The measurements were made by neutron time-of-flight techniques using 1 ns pulses of protons from the Harwell IBIS electrostatic accelerator. The neutrons which were produced by the $^{7}Li(p,n)^{7}Be$ and the $^{3}H(p,n)^{3}He$ reactions, had an average energy spread of 25 keV. The ^{238}U sample, which consisted of a 5 cm long hollow cylinder 2.5 cm diam. with 0.3 cm wall thickness, was placed about 13 cm from the target. Flight paths between 1.7 and 2.6 m were used and the scattered neutrons were detected in a 5 cm diameter 3.8 cm thick NE 102A phosphor with an RCA 31000D photomultiplier. The detector was protected from direct target neutrons by a Heavy Alloy Shield and a pulse shape discrimination system was used to reduce the gamma-ray yield.

The energy dependence of the detector efficiency was measured by Rose [3] and the normalization of the cross section data was carried out by a method described by Barnard [5].

Time-of-flight spectra were obtained alternately with the ^{238}U sample in position and with the sample removed. The secondary neutron spectrum was then obtained by subtracting the 'sample out' spectrum from the 'sample in' spectrum. Natural activity and induced activity following fission produced a uniform background in the secondary neutron spectrum which was estimated from the intensity of the low energy region of the spectrum where the detector bias eliminated time dependent neutrons from the sample. The contribution due to fission was then subtracted on the supposition that the ^{238}U fission neutron spectrum was identical in shape to that obtained from ^{235}U with 130 keV neutrons [3] : normalization was made to the region of the fission spectrum with energy greater than the elastic. Separation of the ^{238}U elastic peak from the inelastic distribution above 0.05 MeV excitation energy was made with the aid of peak shapes obtained with Bi and C samples.

The present measurements have been made at an observation angle of 90° and it is assumed that the integral cross section can be obtained by multiplying the differential cross sections by 4π. Although significant departures from isotropy have been observed by Knitter [1] other measurements made by Smith [4] and by Barnard [5] at energies up to 1.5 MeV suggest that the error introduced by this procedure is unlikely to exceed 10%.

In the figure preliminary values for the measured cross sections which it must be emphasized may be subject to later revision, are compared with calculations due to Prince [6]. The compound nuclear cross section, $\sigma_{nn'}$(compound), was obtained with a combination of an optical model and Hauser-Feshbach using the width fluctuation correction. The compound nucleus cross section is also divided into a $\sigma_{nn'}$(discrete) component, using existing level data and a $\sigma_{nn'}$ (continuum) component. The direct component $\sigma_{nn'}$(rot.) was obtained using a deformed optical potential and by coupling the first three excited states to the ground state.

References

(1) H.H. Knitter, M. Coppola, N. Ahmed and B. Jay, Z. Physik 244 (1971) 358.

(2) R. Batchelor, W.B. Gilboy and J.H. Towle, Nucl.Phys.65 (1965) 236.

(3) J.L. Rose, Ph.D Thesis, Polytechnic of the South Bank, London; to be submitted.

(4) A.B. Smith, reported by W.P. Poenitz, Proceedings of Conference on Nuclear Data for Reactors, Helsinki (1970).

(5) E. Barnard, J.A.M. Villiers and D. Reitmann, Proceedings of Helsinki Conference (1970).

(6) A. Prince, Proceedings of Helsinki Conference (1970).

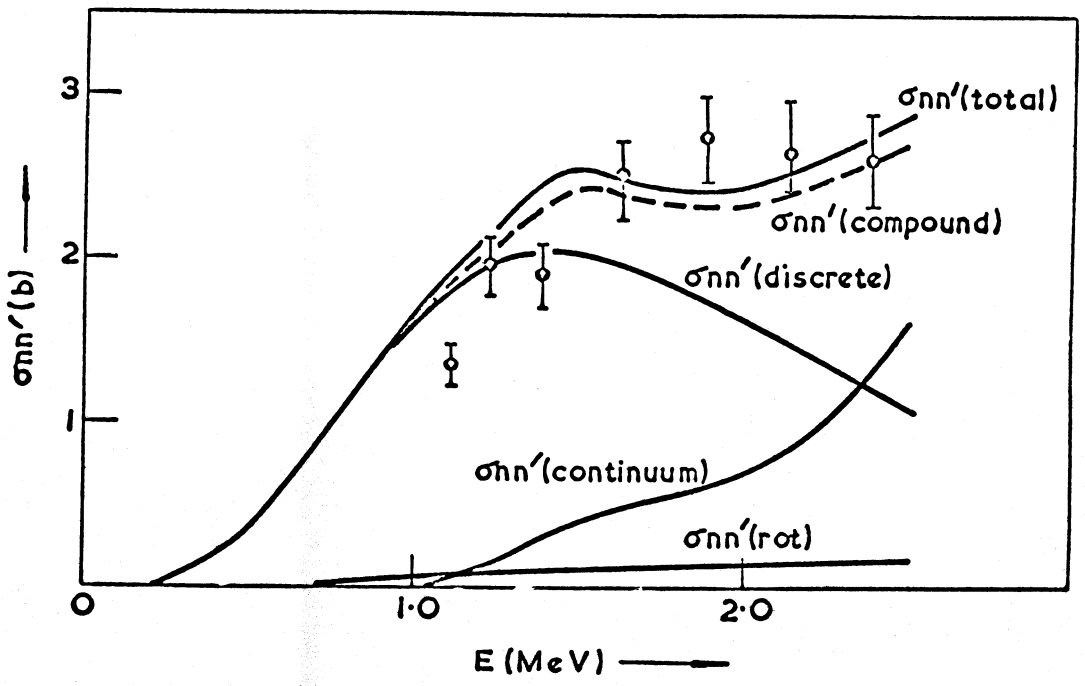

Fig. Total (nn') cross section for all levels above 0.045 MeV

Cierjacks: Are you able to deduce the inelastic excitation functions for separated levels either ?

reply: It will be possible to deduce the excitation functions of the separate levels, but this has not been done yet.

Cierjacks: Has this portion for separated levels been compared with previous results for the first few low-lying levels, e.g. the data of Reitmann from Pelindaba ?

reply: Not yet.

Joly: Up to which energy do you think you are able to extend your measurements ? I think the subtraction of fission neutrons will become more and more uncertain when the energy of the incident neutrons will be increased.

reply: The upper energy will be limited, by the maximum accelerator voltage of 3.7 MeV, to about $2\frac{1}{2}$ MeV.

Yankov: Are you surprised that a "hump" in the calculated $\sigma_{in}(U^{238})$ in the region $\sim$1.5 MeV exists ?

reply: I do not know whether to be surprised or not.

Ribon: Have you analyzed the spectrum of secondary neutrons ?

reply: Not yet.

This is a blank page

"Remarks on the U-238 Inelastic Scattering Cross-Sections"(*)

V. Benzi and E. Menapace

CNEN - Bologna (Italy)

ABSTRACT

The direct collective and single-particle contributions to the neutron inelastic scattering by U-238 are estimated by using the generalized optical model and the Brown-Muirhead model. The possible influence of these effects on the neutron energy spectrum in bulk Uranium is discussed.

(*) Contribution to the Fifth INDC Meeting topical discussion on "Inelastic Scattering of Fast Neutrons"

This is a blank page

REMARKS ON U-238 INELASTIC SCATTERING CROSS-SECTIONS

V. Benzi, E. Menapace

Centro di Calcolo del C.N.E.N., Bologna, Italia

Some preliminary results which have been obtained in Bologna concerning the interpretation of neutron spectra measurements in massive blocks of depleted uranium will be referred here as an example of the role that the collective scattering might play in the field of nuclear reactor physics.

Fig. 1 shows, qualitatively, the shape of the experimental spectrum in the "equilibrium" region, together with the results which are generally obtained from one-dimensional, multigroup calculations.

Large differences are found below 100 keV (where the measured spectrum lies about 30-40% below the calculated spectrum), and above 700 keV where the curve of the ratio of the calculated-to-measured spectrum falls off rapidly to a value of about 0.4 at ~1.5 MeV neutron energy. Then, the ratio increases again, even if it remains somewhat below the unity.

It has been tentatively suggested by various authors that these discrepancies might be due to an underestimate of the capture cross-section of U-238 in the lower energy range and to an overestimate of the total inelastic scattering in the higher energy range. In fact, a quantitative agreement in the high energy region can be obtained by reducing the total inelastic scattering by about 10÷15% or more, a reduction which seems well beyond the uncertainties in the experimental cross-section data. For this reason, we are exploring the effects of different splittings of the total inelastic scattering cross-section in its various components. Up to now, we have compared the results obtained using KEDAK with those given by a different file, in which direct processes are taken into account. To obtain such a file, we have carried out some theoretical calculations above 2 MeV of the direct excitation of the first and second excited level (for which experimental data exist up to ~1 MeV), using the generalized optical model in adiabatic approximation. The parameters of the optical potential were fixed by fitting the experimental total cross-section and the measured angular distributions of the elastic scattering. The theoretical total

cross-section was in good agreement with the one evaluated by Schmidt, the differences being within the experimental errors.

Rather high values of the first 2^+ and 4^+ inelastic scattering cross-sections were obtained. These calculated cross-sections were smoothly joined with the Schmidt evaluation up to 1 MeV, as is shown in Fig. 2.

Then, a nuclear data file was prepared, in which all the KEDAK data are kept up to 1 MeV.

Above this energy, the following modifications have been introduced:

i) The total cross-section above 2 MeV has been slightly modified in accordance with the theoretical calculations.

ii) The total inelastic scattering cross-section has been increased above 8 MeV to take into account the existence of the 2^+ and 4^+ direct components.

iii) The values of the excitation functions of all the excited levels above the second one have been renormalized in the range 1÷2 MeV, in order to reproduce the KEDAK total inelastic cross-section.

iv) The KEDAK σ_f ,σ_γ and σ_{2n} have been kept unchanged.

v) The total elastic cross-section above 2 MeV has been obtained as a difference between the adopted total and non-elastic cross-sections.

In the KEDAK file, 24 separate excitation functions are given up to 2 MeV. Above this energy, only the total inelastic cross-section is given, so that the inelastic slowing down kernel has to be calculated on the basis of the compound nucleus evaporation process. However, as it was shown several years ago by Brown and Muirhead [1], the compound nucleus process is not the unique process possible in the continuum. In fact, at some MeV impinging neutron energy the possibility exists for neutrons to be emitted directly since the first collision. This "direct process" is obviously different from the direct excitation of collective states calculated by the generalized optical model, which does not involve single particle interactions.

---

(1) G. Brown and H. Muirhead: Phil. Mag. 2 , 473, (1957)

Using the Brown-Muirhead theory, we have estimated the cross--section at various energies and the energy distribution of the directly emitted neutrons.

Fig. 3 shows the theoretical spectrum of the emitted neutrons at 7 MeV. Such a spectrum is obtained by adding the compound and direct spectra weighted on the basis of the respective calculated cross-sections. By accident, the theoretical spectrum is in good agreement with the measurements by Batchelor et al. On the basis of these results, the total inelastic cross-section above 2 MeV was splitted into the following components:

i) the 2^+ and 4^+ first excited level cross-sections calculated by means of the generalized optical model;

ii) the direct component calculated on the basis of the Brown and Muirhead model;

iii) the compound nucleus evaporation component.

The next step in our work was the calculation of the equilibrium energy spectrum. If one assumes an infinite block of pure U-238 with a uniform source of fission neutrons, the situation at equilibrium can be represented by a Volterra equation which can be solved by iterating on the fission neutron source.

A computer programme which reads the pointwise cross-sections directly from the file was written to solve the Volterra equation. It was found that above 0.6 MeV the solution converges very well in a reasonable computer time.

Fig. 4 shows the energy spectra obtained by using the original KEDAK and the modified version. The ratio of the two curves is also shown. Such a ratio is in qualitative agreement with the experimental results. The calculated ratio at about 1.5 MeV, however, was smaller than the observed one.

In addition, both theoretical energy spectra show a dip at 1.5 MeV which is not shown by the measurements. This might be due to the drastic change in the representation of the inelastic scattering process at 2 MeV, from which the evaporation spectrum is used instead of the various excitation functions. To explore such a possibility, a third file was built, in which the evaporation process is assumed to start at 1.7 MeV, but no sig-

nificant changes in the calculated spectrum were observed.

We have also explored the effect of a much harder fission neutron spectrum, using the Grundl spectrum instead of the Cranberg one, which was adopted in KEDAK.

The effect of such a change was found to be negligible. The last change we tried was to remove the "Phrygian cap" between 1.6 and 2 MeV in the cross-section, as shown in Fig. 5. The excitation functions of all levels above the second one and the total elastic scattering cross--sections were changed accordingly.

In this case, the dip in the energy spectrum disappears and the ratio of the two spectra approaches the experimental results (see Fig. 4).

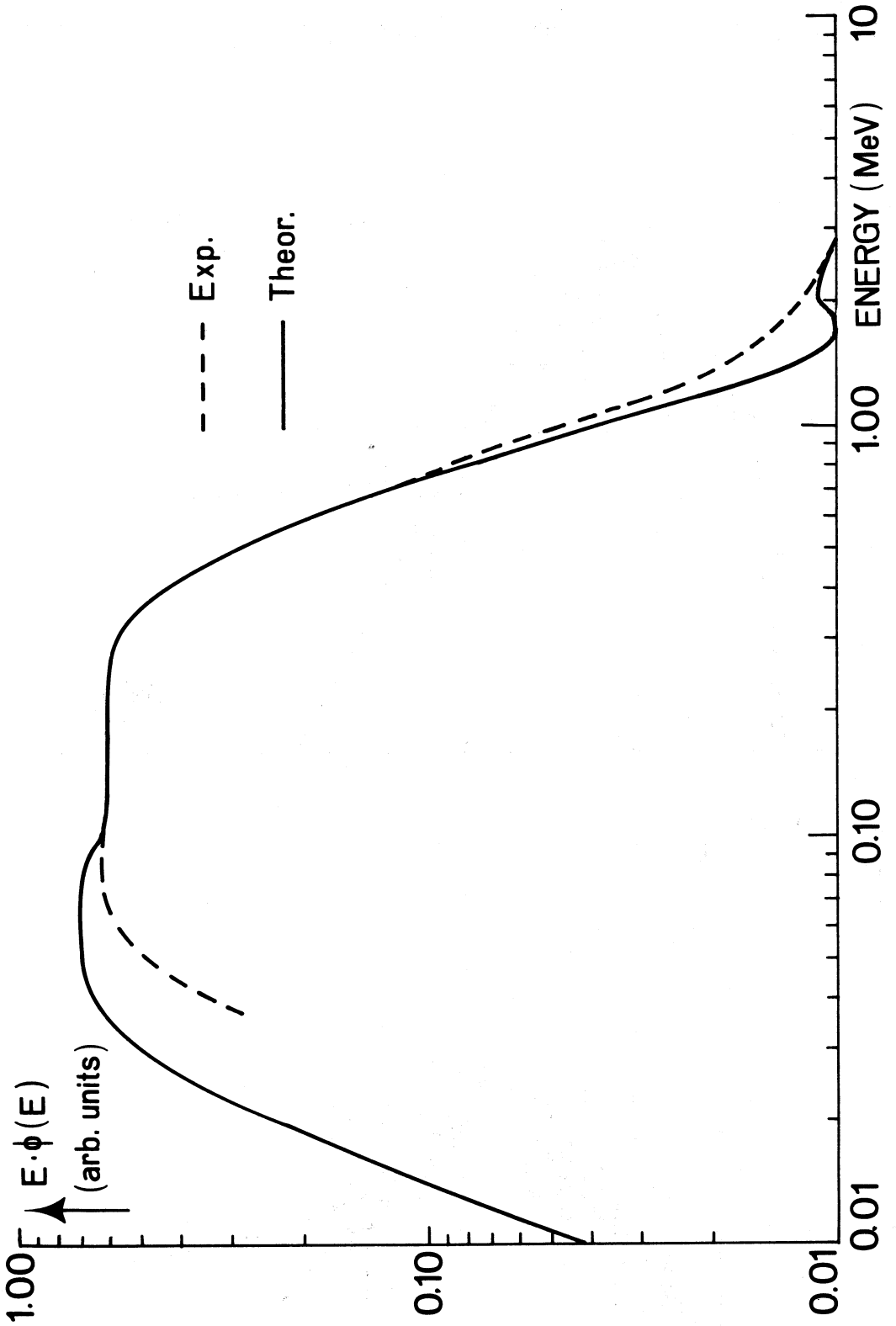

Fig. 1

INELASTIC EXCITATION CROSS SECTION FOR U^{238}

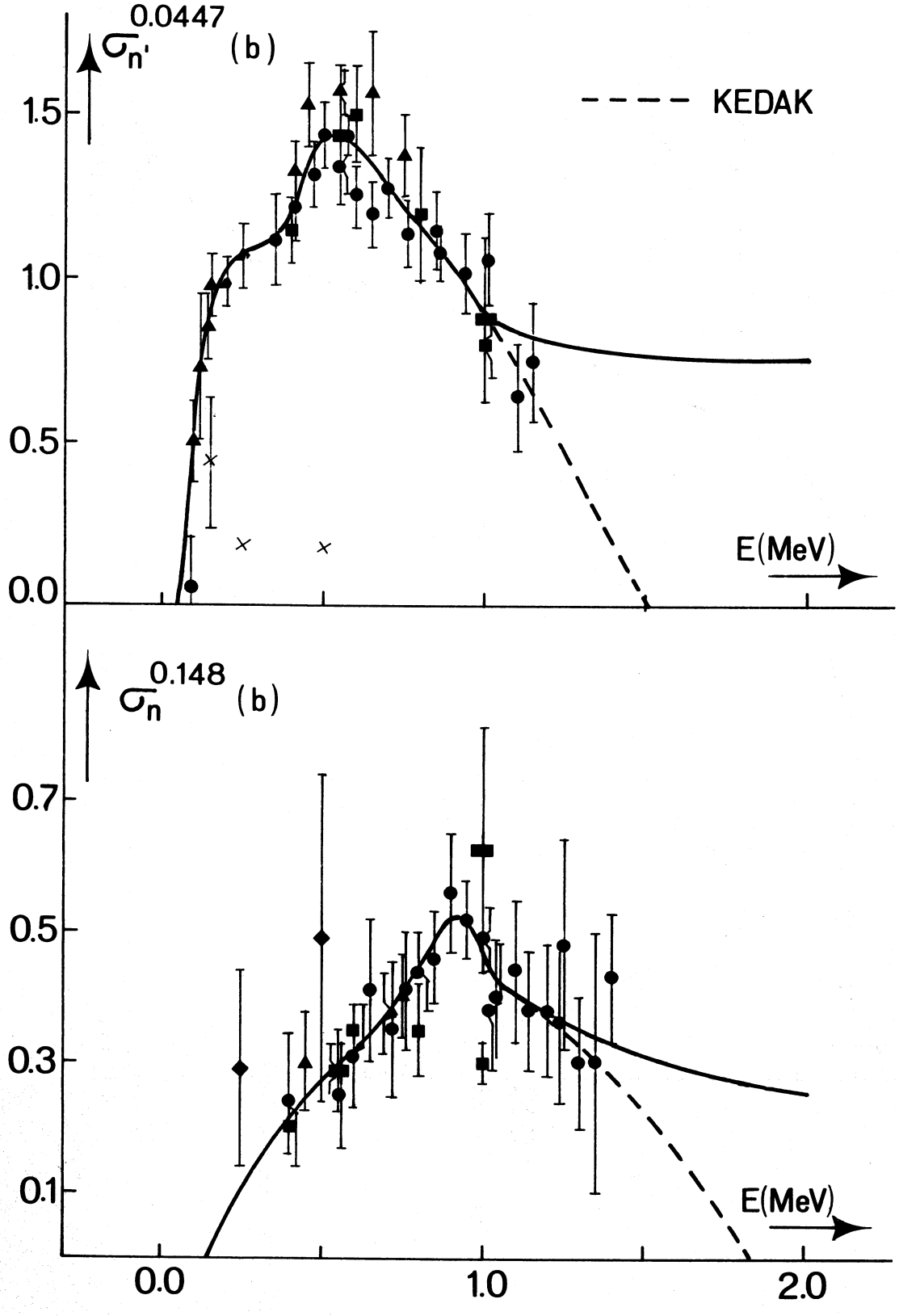

Fig. 2

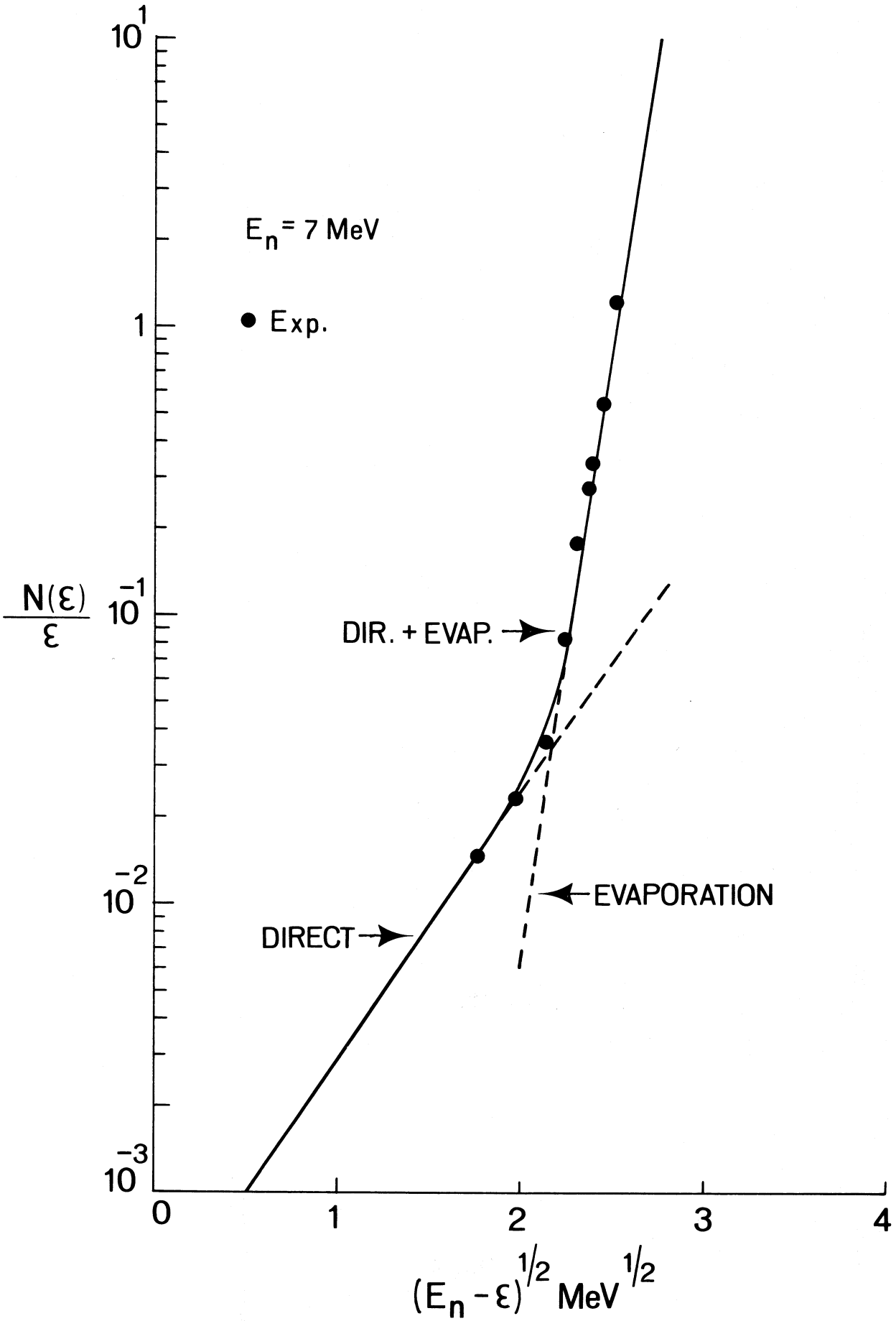
10^{1}
E_n = 7 MeV
● Exp.
1
$\frac{N(\varepsilon)}{\varepsilon}$
10^{-1}
DIR. + EVAP.
EVAPORATION
10^{-2}
DIRECT
10^{-3}
0
1
2
3
4
$(E_n - \varepsilon)^{1/2}$ MeV$^{1/2}$

Fig. 3

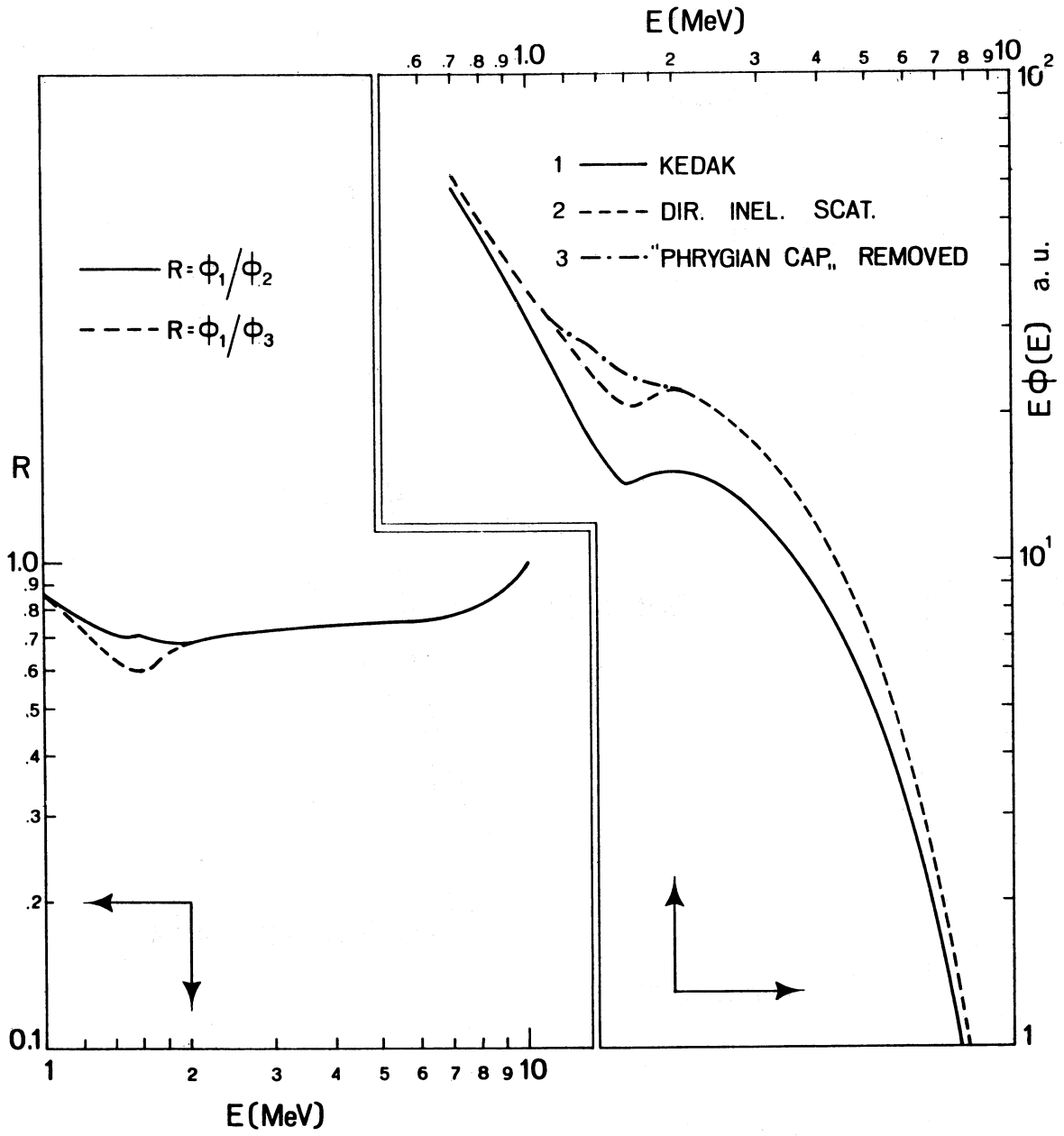
E(MeV)
.6 .7 .8 .9 1.0 2 3 4 5 6 7 8 9 10
1 —— KEDAK
2 ---- DIR. INEL. SCAT.
3 —·—·"PHRYGIAN CAP„ REMOVED
—— R=Φ1/Φ2
---- R=Φ1/Φ3
R
1.0
.9
.8
.7
.6
.5
.4
.3
.2
0.1
1 2 3 4 5 6 7 8 9 10
E(MeV)
10^2
10^1
1
EΦ(E) a.u.

Fig. 4

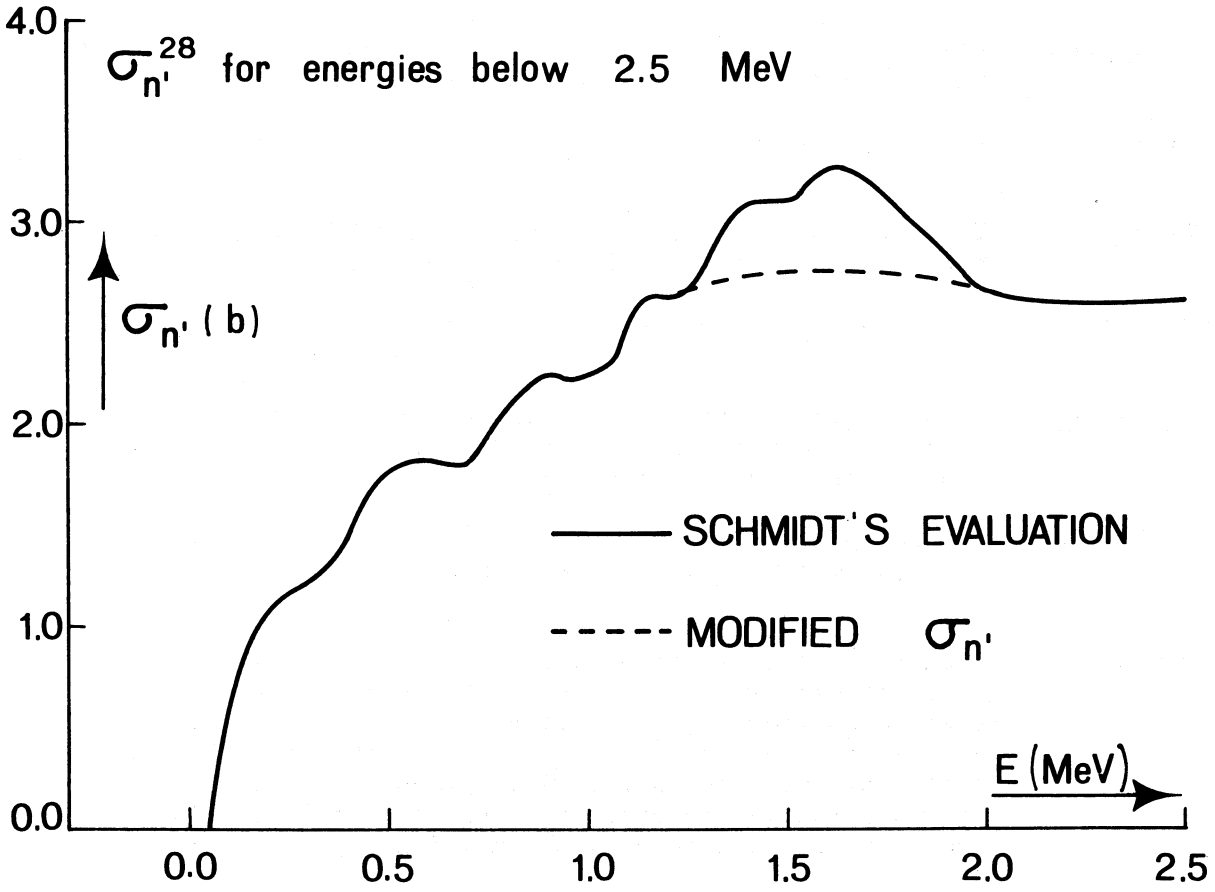
4.0
3.0
2.0
1.0
0.0
$\sigma_{n'}^{28}$ for energies below 2.5 MeV
$\sigma_{n'}$ (b)
SCHMIDT'S EVALUATION
MODIFIED $\sigma_{n'}$
E (MeV)
0.0
0.5
1.0
1.5
2.0
2.5

Fig. 5

Yankov: Have you made inelastic scattering cross section calculations for 0.0447 MeV and 0.148 MeV levels only or also for higher levels ?

reply: The adiabatic approximation we have used allows for the simultaneous calculation of all levels belonging to the fundamental band. However, the direct excitation cross-section of levels above the second one seems to be negligible at energies below $\sim$15 MeV.

Nishimura: How much did you decrease the cross sections you obtained in the energy range 1.2 to 2.0 MeV ?

reply: About 15% at maximum.

Cross: In comparing your results with the KEDAK calculations how were the two sets of results normalized ?

reply: To the same neutron source intensity.

Rowlands: Is it necessary to take account of the anisotropy of the direct collective and single-particle contributions to the inelastic scattering ?

reply: It does not seem so, because this anisotropy is (very likely) small at few MeV neutron energy.

Rowlands: When these contributions are added to the KEDAK evaluation is it necessary to revise both the total inelastic and elastic scattering, and the angular distributions for elastic scattering to take account of the fact that the evaluator may have included the direct collective and single-particle contributions in the elastic scattering (because the measurements did not distinguish them) ?

reply: In principle, I agree with you. But the aim of our work was to explore the effects of different decompositions of the total inelastic cross-section, so that we have maintained the same values of KEDAK, except for minor changes. As far as the angular distribution of the elastic scattering cross-section is concerned, it can be easily demonstrated that its shape is absolutely irrelevant in determining the shape of the neutron equilibrium spectrum at high energies for a material so heavy as U-238. Last point: the spectrum of the single-particle direct inelastic scattering is a rather hard one. The knocked-out neutrons do not contribute to the "elastic" peak.

INELASTIC NEUTRON SCATTERING DATA FROM SOME RECENT MEASUREMENTS

by
E. Almén, B. Holmqvist and T. Wiedling
Neutron Physics Laboratory, Studsvik, Nyköping, Sweden

ABSTRACT

During the last three years fast neutron inelastic scattering from twenty elements in the atomic mass region 24 to 209 has been measured with high resolution time-of-flight technique in the energy range 2.0 to 4.5 MeV. These data can give a good background for the proper understanding of the reaction mechanisms and of the usefulness of the nuclear models describing the scattering process.

Neutron inelastic scattering from the studied elements were mostly observed at one scattering angle, i.e. 125^{o}, assuming the angular distributions to be isotropic or symmetric around 90^{o}. The validity of this assumption has been investigated by observing differential inelastic cross sections at several angles for 3.0 MeV incident neutron energy.

Since the inelastic scattering process is mainly characterized by compound nucleus formation in the investigated energy range, the interpretation of the experimental data was made in terms of the Hauser and Feshbach statistical model corrected according to Moldauer for level width fluctuations and resonance-interference effects. The transmission coefficients were calculated using a local optical potential including a spin-orbit interaction term.

For most elements analysed so far good agreement with the experimental data is obtained taking the above mentioned corrections into account and assuming many overlapping levels in the compound nucleus. The pure Hauser-Feshbach model can overestimate the cross sections by as much as a factor of 2 at low primary energies where the statistical assumptions of the compound nucleus are not valid and only a few decay channels are available.

This is a blank page

INELASTIC NEUTRON SCATTERING DATA FROM SOME RECENT MEASUREMENTS

by

E. Almén, B. Holmqvist and T. Wiedling

Neutron Physics Laboratory, Studsvik, Nyköping, Sweden

It has been a tradition in our laboratory that our research programs are concentrated on systematic studies of nuclear reaction processes. Thus, for more than a decade we have been doing neutron elastic scattering experiments. We have also had for some years a program concerning fission neutron spectra studies and another one on systematic investigations of the inelastic neutron scattering process.

Systematic investigations are of great value to test theoretical models and thus form a sound and reliable basis for further theoretical calculations of cross sections for reactor physics purposes.

We made neutron inelastic scattering measurements a decade ago but we began planning a more complete program three years ago.

Neutron scattering experiments, elastic as well as inelastic, demand large amounts of material in the scattering sample to get a large enough neutron yield. Without any supply of enriched isotopes our measuring program has to be designed with regard to elements with natural isotopic abundances. These circumstances have limited our research goal in some respects. The investigations must usually be limited to elements which have only a few isotopes. Otherwise elements with many isotopes with a large number of levels will give several overlapping neutron transitions which are impossible to resolve with presently available neutron time-of-flight or other neutron detection techniques. Of course, some of these difficulties may be overcome by use of high resolution Ge(Li) gamma detectors, but these are less suitable for absolute cross section measurements than for instance the proton recoil scintillation detector.

Measurements have been made on the following twentyone elements: Mg, Al, S, Ti, V, Cr, Mn, Fe, Co, Ni, Cu, Zn, Ga, Y, Nb, In, Pr, Ta, Pb, Pb_r and Bi (Pb_r stands for radiogenic lead).

Several neutron inelastic scattering measurements have already been reported on these elements. Cranberg et al. (1) have measured at only one energy, i.e. 2.45 MeV. Cranberg et al. (2) also reported measurements on Pb and Bi in the energy

region of 2 to 8 MeV. Towle et al. (3-5) have observed inelastic scattering from Al, V and Fe in the energy range 1 to 4 MeV. Scattering from V has also been investigated by Holmqvist et al. (6), Smith (7) and Barrows et al. (8). Boschung et al. (9) have measured scattering from Fe and Ni at 4 to 5.6 MeV primary neutron energy. Results on inelastic scattering from Mn in the energy region of 1 to 3 MeV have been reported by Barrows et al. (8) and on Nb from 0.45 to 1.79 MeV by Rogers et al. (10). In spite of these measurements there is still a lack of a more homogeneous experimental material.

In this report results will be given for some of the elements already mentioned. These are Al, V, Mn, Fe, Ni, Pb and Pb_r. Excitation functions were measured for each 0.25 MeV in the energy interval 2.0 to 4.5 MeV at an angle of 125°. Angular distributions were measured at 3.0 MeV primary neutron energy at five angles, i.e. 30°, 60°, 90°, 125° and 150°, relative to the neutron beam. All cross sections were determined relative to the n-p scattering cross sections.

The present experimental data sets have been compared with those calculated using the Hauser-Feshbach theory (11) corrected for level width fluctuations and resonance-interference effects according to Moldauer (12). This formalism is considered valid since the inelastic scattering process is mainly described by the formation of compound nuclei in the investigated energy region. Optical model parameters evaluated by Holmqvist et al. (13) have been used to calculate the transmission coefficients necessary for the H.F. calculations.

EXPERIMENTAL DETAILS

Without going into any details it should be mentioned that the measurements were performed with a time-of-flight spectrometer in connection with a 6 MV Van de Graaff accelerator. This machine has a klystron bunching system, and the experiments were mostly run with a pulse width of about 2 ns.

Neutrons were produced with the $T(p,n)^3He$ reaction by using a gas target which gave a total energy spread of about $\pm$50 keV.

The scattering samples of the investigated elements consisted of hollow cylinders with a length of 5 cm, an outer diameter of 2.5 cm and an inner diameter of 0.95 cm.

DATA ANALYSES AND CORRECTIONS

The resolution in the time spectra was not sufficient to enable individual levels in the residual nucleus to be resolved at all incident neutron energies. Therefore in those cases cross sections were determined for groups of levels.

The inelastic cross sections have been corrected for the neutron source anisotropy, attenuation of neutron flux in the scatterer, as well as for finite geometrical effects, using Monte Carlo technique. Multiple scattering corrections have also been performed for the contribution to the inelastic peak from elastic-inelastic scattering and the reduction of the inelastic peak because of inelastic-inelastic events. The contribution to the inelastic peak due to elastic-elastic-inelastic scattering is negligible.

ESTIMATION OF ERRORS

There are two main sources of error in an experimental inelastic scattering cross section: the one related to the uncertainty of the determination of the relative intensity of a neutron group in the time-of-flight spectrum and the uncertainty in the cross section correction calculation for neutron attenuation and multiple scattering in the sample. The error due to the intensity measurement is about 10 per cent in the worst case. The uncertainty in the correction is also about 10 per cent and is mainly due to uncertainties in the neutron total and elastic scattering cross sections applied at the calculations. The total errors are thus in most cases of the order of 15 per cent or better.

THEORETICAL ANALYSES

1. Hauser and Feshbach Calculations

The elastic and inelastic scattering processes are mainly characterized by compound nucleus formation at low neutron energies. Using the Hauser and Feshbach (H.F.) (11) formalism the angular distributions and the total scattering cross sections can be calculated for the compound elastic as well as inelastic scattering processes. Thus the total cross section for scattering to a certain level is given by the expression

$$\sigma(J_i,J_f;E,E') = \pi\lambda^2 \sum_{\ell_i\ell_f j_i j_f} \frac{T_{\ell_i}^{j_i}(E)}{2(2J_i+1)} \sum_J \frac{(2J+1)\, T_{\ell_f}^{j_f}(E')}{\sum_P T_{\ell_p}^{j_p}(E'_p)}$$

where E is the neutron energy, ℓ_i is the orbital angular momentum and j_i is the total angular momentum of the incoming neutron, and E', ℓ_f and j_f ($\bar{j} = \bar{\ell} + \bar{s}$) are the corresponding numbers of the outgoing neutron. The initial and final spins of the nucleus are J_i and J_f, respectively. The transmission coefficients $T_{\ell i}$ and $T_{\ell f}$ are related to a two-body optical potential of the type discussed below. The Hauser-Feshbach analysis is thus closely connected to a knowledge of the proper nuclear potential.

According to Moldauer (12) the H.F. cross section formula is not valid when few levels are excited at low neutron energies. The reason is the compound-nucleus level width fluctuations and resonance-interference effects which are ignored in the H.F. formalism.

A more general expression than that of Hauser-Feshbach for the inelastic cross section is

$$\sigma_{\alpha\alpha'} = \pi\lambda^2 \{ < \frac{\theta_{\mu\alpha}\, \theta_{\mu\alpha'}}{\theta_\mu} >_\mu - M_{\alpha\alpha'} \}.$$

This expression consists of an average resonance term $< \frac{\theta_{\mu\alpha}\, \theta_{\mu\alpha'}}{\theta_\mu} >$ and of a resonance interference term $M_{\alpha\alpha'}$, ($M_{\alpha\alpha'} = \frac{1}{4}\, \delta_{\alpha\alpha'}\, Q_\alpha < \theta_{\mu\alpha} >^2$). The transmission coefficients have been replaced by averagies over the resonance parameters, $\theta_{\mu\alpha}$

$$<\theta_{\mu\alpha}> = T_\alpha^{comp} + \frac{1}{Q_\alpha} \left[1-(1-Q_\alpha T_\alpha^{comp})^{1/2}\right]^2$$

(μ denotes a resonance).

The compound-nucleus transmission coefficient, T_α^{comp}, is equal to the optical-model transmission coefficient, T_α, apart from that portion of the transmitted flux which induces direct reaction processes. Usually T_α^{comp} is equal to T_α.

The parameter Q_α is dependent on the properties of the compound nucleus. In the limit of infinitely many overlapping resonances the numerical value of Q_α goes to zero while in the case of isolated resonances Q_α approaches one.

2. Nuclear Optical Model Potential

A local spherical potential of the form

$$-V(r) = Uf(r) + iWg(r) + U_{SO} \left(\frac{\hbar}{\mu_\pi c}\right)^2 \frac{1}{r} \frac{d}{dr} |f(r)|\, \bar{\sigma} \cdot \bar{\ell}$$

was chosen to describe the interaction between the incoming neutron and the target nucleus. The real and imaginary parts of the potential are described by Uf(r) and Wg(r) with the functions f(r) and g(r) expressing the radial variations. A spin-orbit interaction term is also included with the potential depth U_{SO}, the Pauli spin and angular momentum operators $\bar{\sigma}$ and $\bar{\ell}$, respectively, and the pion mass μ_π. The radial shapes of the real and imaginary parts of the potential are described by the Saxon-Woods and derivative Saxon-Woods form factors

$$f(r) = \left[1 + \exp\left(r - R_U\right)/a\right]^{-1}$$

and

$$g(r) = 4\left[1 + \exp\left(r-R_W\right)/b\right]^{-2} \exp\left[\left(r-R_W\right)/b\right]$$

where $R_U = r_{oU}A^{1/3}$ and $R_W = r_{oW}A^{1/3}$ are the radii, and a and b are the diffuseness parameters.

RESULTS

In the following the studied elements will be discussed one by one in the order of increasing atomic number.

The calculations have been made with the Abacus-Nearrex computer program. This program has a limitation in the number of levels included, i.e. the maximum number of levels is 17.

Aluminium

Fig. 1 shows the excitation functions for transitions to levels up to 3.0 MeV. The Hauser-Feshbach calculations are also shown. The pure H.F.-formalism (the solid lines) gives systematically too large cross sections as does also the calculations with $Q_\alpha = 1$ (the dashed pointed lines), i.e. the case with isolated resonances. The best descriptions of the experimental excitation functions are obtained for $Q_\alpha = 0$ (the dashed lines). This would mean that the number of overlapping resonances is large.

The angular distribution functions are isotropic or only slightly anisotropic and symmetric around 90° (Fig. 2).

Vanadium

Vanadium is a very suitable element for neutron scattering investigation. It has many well separated levels giving easily resolvable neutron groups up to several MeV incident neutron energy. Fig. 3 shows the experimental results and the calculated excitation functions. The same trend as was seen for the previous elements is apparent here.

Manganese

The manganese results are shown in Fig. 4. The pure H.F. calculations describe the experimental data well above about 2.5 MeV, but the correction term has to be applied below that energy. The discrepancy between theory and experiment for the five level excitation at 2.2 to 2.3 MeV may be due to uncertain spin values of the states. This has to be investigated further.

The angular distributions are mainly isotropic (Fig. 5).

Iron and Nickel

The results for iron and nickel are shown in Fig. 6, 7, 8 and 9. They are similar to those for previous elements.

Lead

Fig. 10 shows the results for lead for levels up to 2.61 MeV. The agreements between experiments and calculations are good except for the 1.47 and 1.51 MeV levels. The reason for this is probably related to the lack of knowledge of level spin properties. The angular distributions (Fig. 11) have the common compound nucleus behaviour.

These are only a few examples of the results which have been obtained in the neutron inelastic cross section field at our laboratory. Agreement of similar quality has been obtained for the other elements studied. The general conclusion is that the experimental neutron inelastic scattering cross sections for the elements investigated so far can in general be adequately described in terms of the H.F. model properly corrected according to Moldauer and by using transmission coefficients calculated from the generalized spherical optical model.

REFERENCES

1. Cranberg, L. and Levin, J.S.
Phys. Rev. 103(1956)343.

2. Cranberg, L., Oliphant, T.A., Levin, J. and Zafiratos, C.D.,
Phys. Rev. 159(1967)969.

3. Towle, J.H. and Gilboy, W.B.,
Nucl. Phys. 39(1962)300.

4. Towle, J.H.,
Nucl. Phys. A117(1968)657.

5. Gilboy, W.B. and Towle, J.H.,
Nucl. Phys. 64(1965)130.

6. Holmqvist, B., Johansson, S.G., Lodin, G. and Wiedling, T.,
Nucl. Phys. A146(1970)321.

7. Smith, A.B., Whalen, J.F. and Takeuchi, K.,
Phys. Rev. C1(1970)581.

8. Barrows, A.W., Lamb, R.C., Velkley, D. and McEllistrem, M.T.,
Nucl. Phys. A107(1968)153.

9. Boschung, P., Lindow, J.T. and Schrader, E.F.,
Nucl. Phys. A161(1971)593.

10. Rogers, V.C., Beghian, L.E., Clikeman, F.M., Hofman, F. and Wilensky, S.,
Nucl. Phys. A142(1970)100.

11. Hauser, W. and Feshbach, H.,
Phys. Rev. 87(1952)366.

12. Moldauer, P.A.,
Phys. Rev. 135B(1964)642.

13. Holmqvist, B. and Wiedling, T.,
AE-430 (1971).

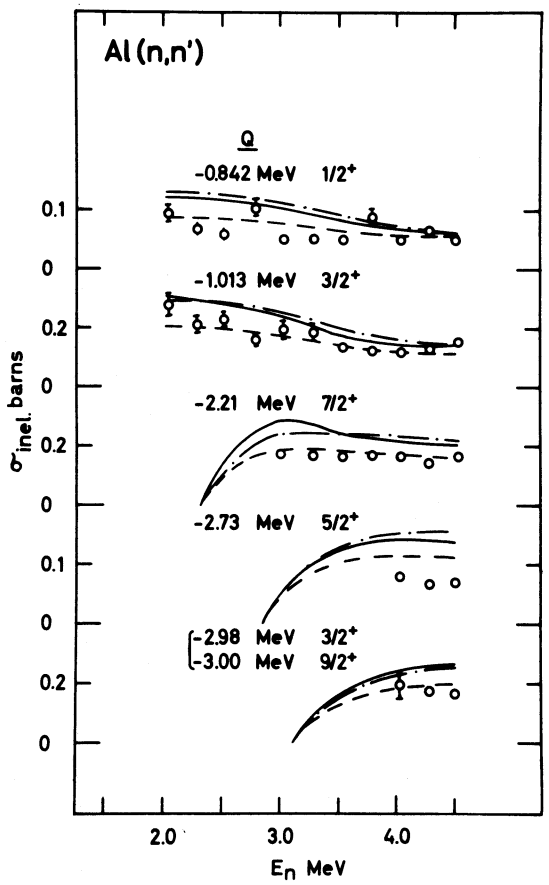

Fig. 1. Excitation functions for inelastic scattering from Al. H.F. calculations (solid lines). Moldauer calculations with Q_α= 0 (dashed lines) and with Q_α=1 (dashed pointed lines).

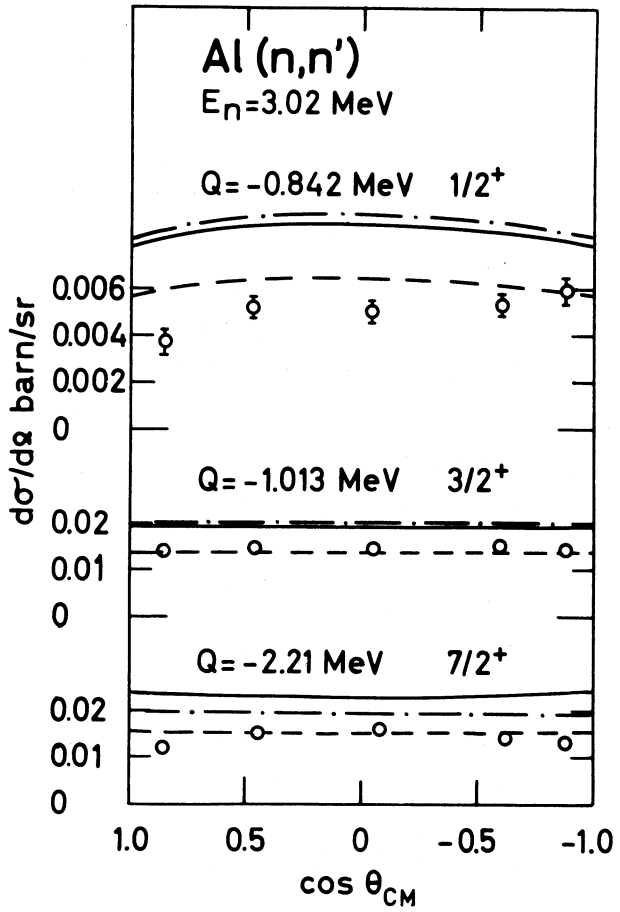

Fig. 2. Angular distributions of the inelastic scattering cross sections for Al at 3.0 MeV incident neutron energy. The notations are the same as in Fig. 1.

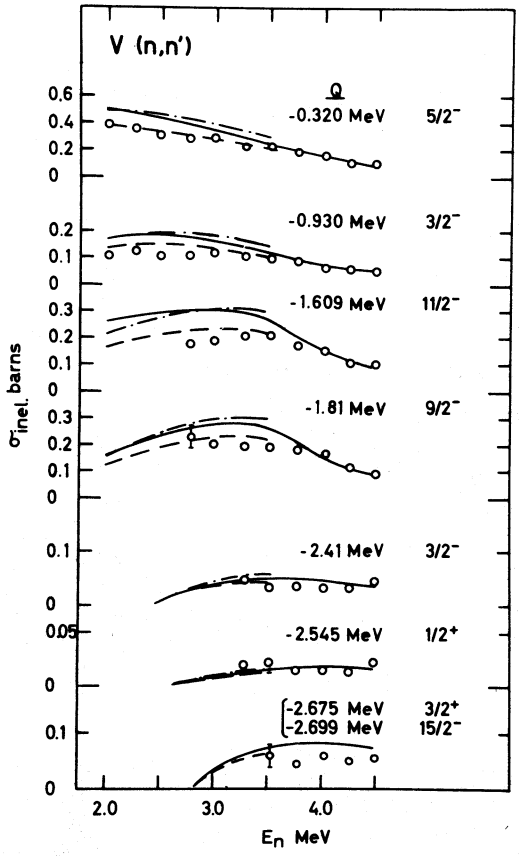

Fig. 3. Excitation functions for inelastic scattering from V. The notations are the same as in Fig. 1.

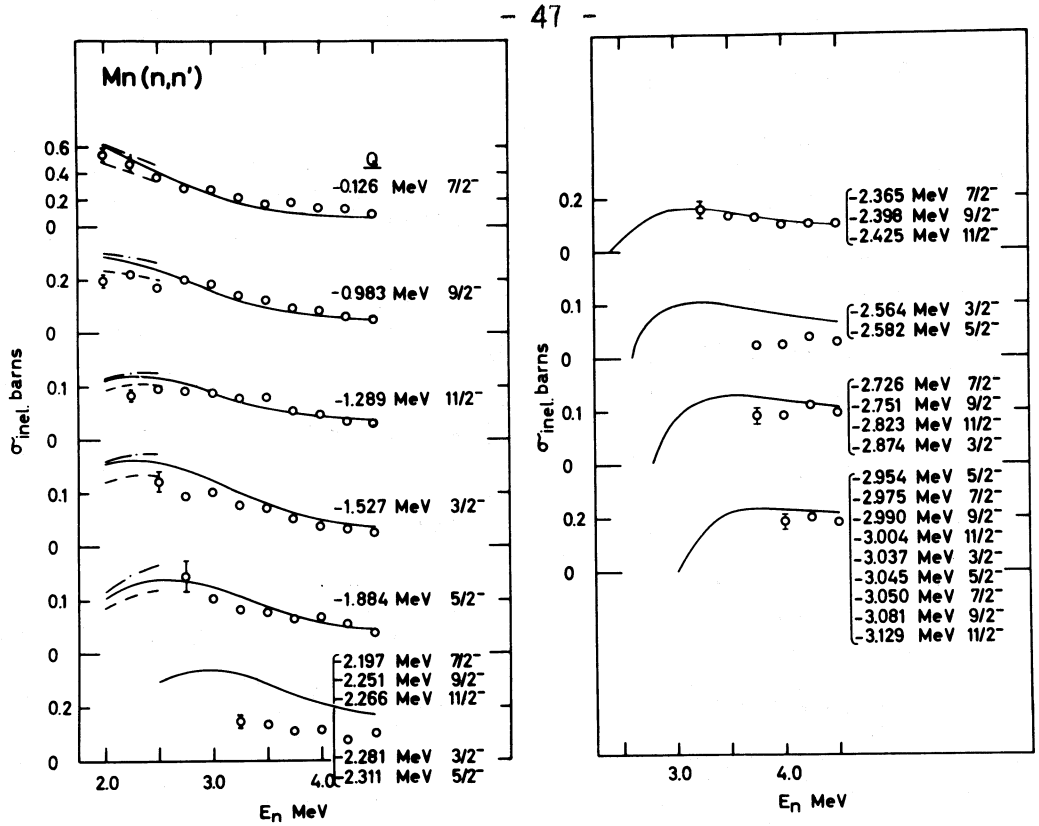

Fig. 4. Excitation functions for inelastic scattering from Mn. The notations are the same as in Fig. 1.

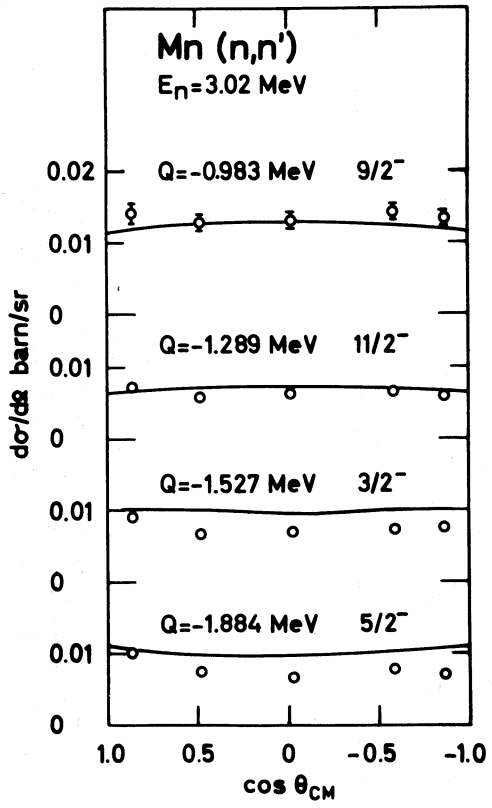

Fig. 5. Angular distributions of the inelastic scattering cross sections for Mn at 3.0 MeV incident neutron energy. The notations are the same as in Fig. 1.

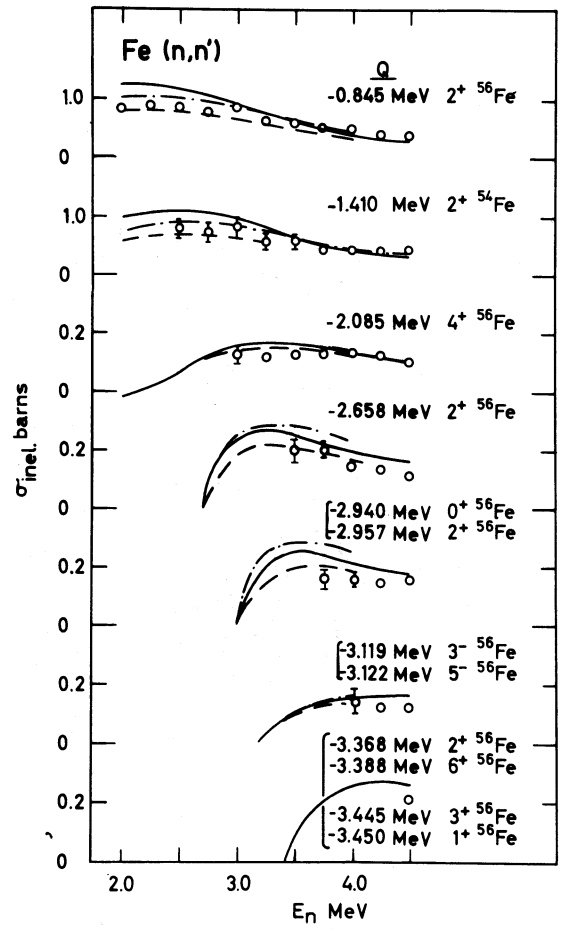

Fig. 6. Excitation functions for inelastic scattering from Fe. The notations are the same as in Fig. 1.

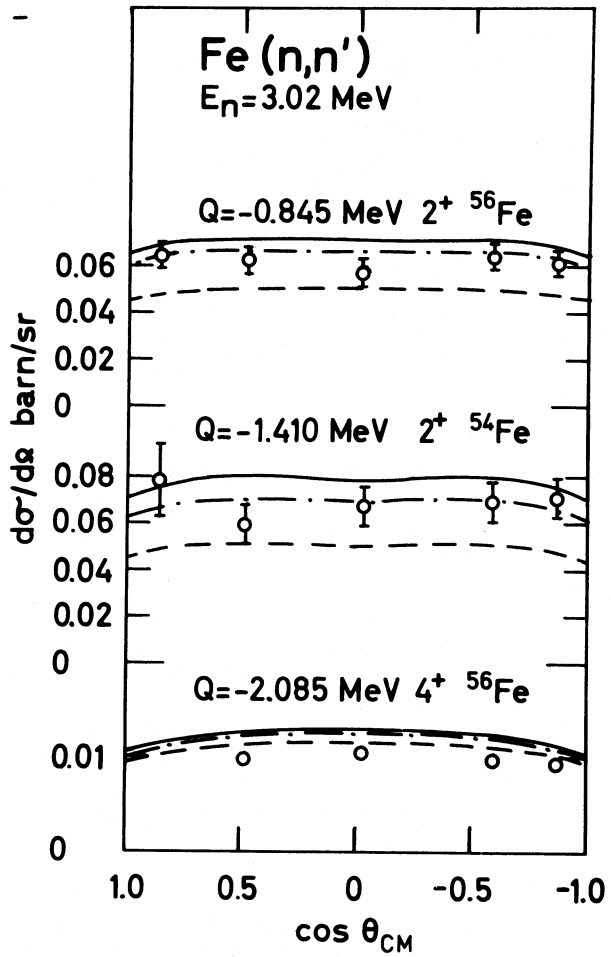

Fig. 7. Angular distributions of the inelastic scattering cross sections for Fe at 3.0 MeV incident neutron energy. The notations are the same as in Fig. 1.

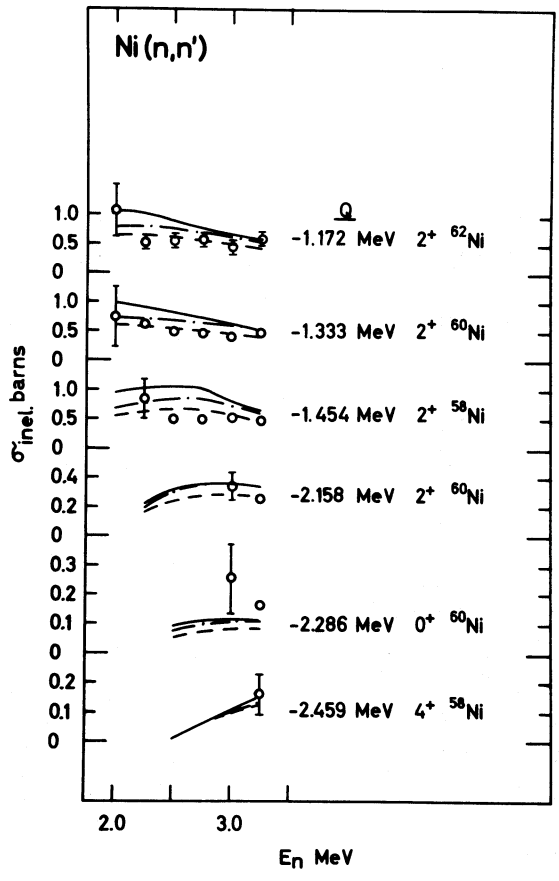

Fig. 8. Excitation functions for inelastic scattering from Ni. The notations are the same as in Fig. 1.

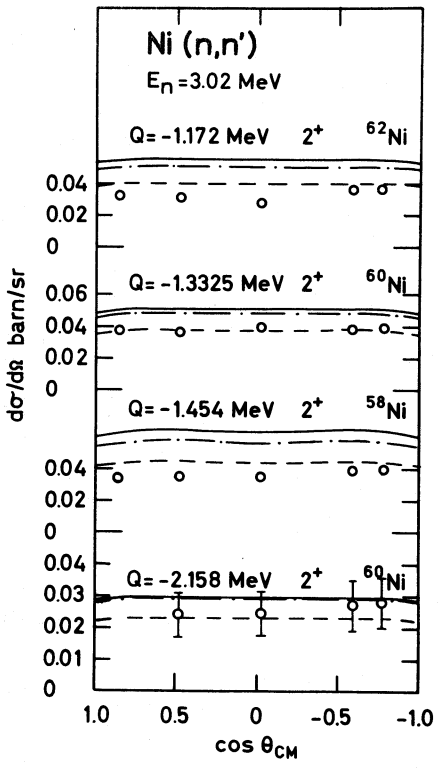

Fig. 9. Angular distributions of the inelastic scattering cross sections for Ni at 3.0 MeV incident neutron energy. The notations are the same as in Fig. 1.

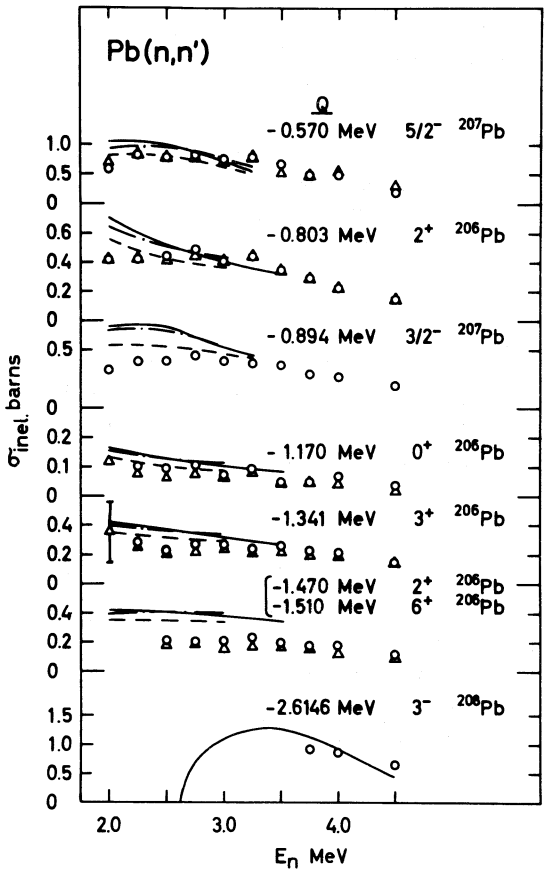

Fig. 10. Excitation functions for inelastic scattering from Pb. Experimental results are obtained both with a Pb scatterer (circles) and a Pb_r scatterer (triangles). The other notations are the same as in Fig. 1.

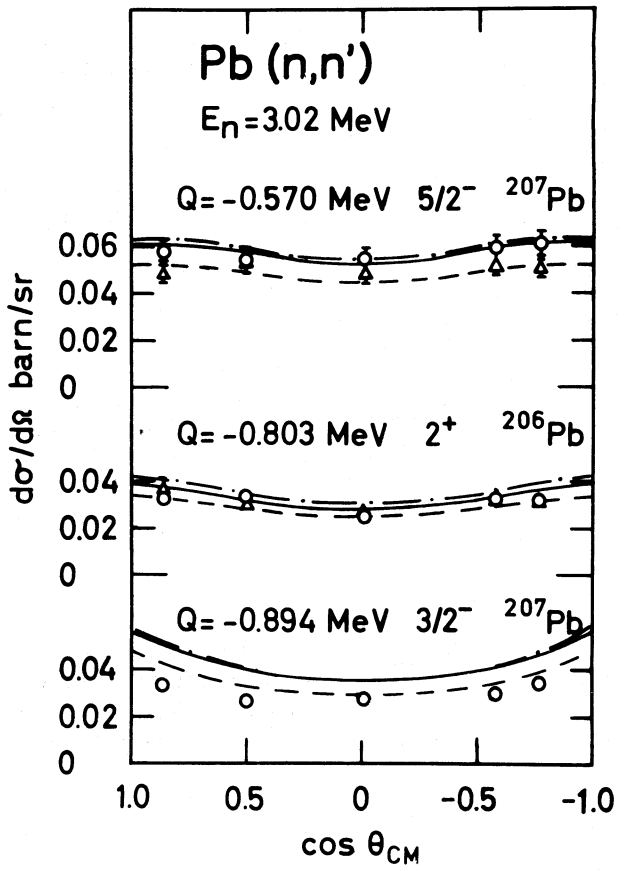

Fig. 11. Angular distributions of the inelastic scattering cross sections for Pb at 3.0 MeV incident neutron energy. The notations are the same as in Figs. 1 and 10.

Joly: All your slides show 3 calculated curves for comparison with your experimental data; you have mentioned that the solid curve corresponds to a Hauser-Feshbach calculation and the dashed curve takes into account Moldauer correction. What is the third curve representing ?

reply: The third curve represents a Moldauer calculation with $Q_\alpha = 1$, i.e. isolated resonances in the compound nucleus.

Benzi: May I ask you if the optical model parameters used for the theoretical analysis fluctuate with the energy ?

reply: No.

Cierjacks: How much contributes the uncertainty in multiple scattering calculation to the total uncertainty of the absolute cross section ? You have used fairly large samples.

reply: I do not have any figure at present.

Dunford: I noted the increased agreement of calculations and experimental values when Moldauer's "Q" is not zero. Kerman (MIT) has been able to derive the Hauser-Feshbach theory without introducing a "Q" parameter.

Analysis of Fast Neutron Scattering Using the Coupled-Channels Theory

S. Tanaka

The angular distributions of elastically and inelastically scattered neutrons were calculated using the spherical optical model, the statistical theory for the compound nuclei and the coupled-channels theory, and the results were compared with our experimental data. The calculations were made for Fe, Ni, Zn, ^{120}Sn, ^{139}La, ^{141}Pr, Gd, Er and ^{209}Bi in the energy range of about 1.4 to 3.5 MeV, except for Zn. In this case, the calculations were performed up to 8 MeV.

All the calculations were based on an optical potential with one set of parameter values, which had been obtained from a comparison of calculation and experimental data for the elastic cross sections of ^{209}Bi.

For the elastic angular distribuitons of Fe, Ni, Zn, ^{120}Sn, ^{139}La and ^{141}Pr, which were assumed to be vibrational, the results calculated with the coupled channels theory fit the experimental data far better than those calculated with the straightforward spherical optical potential. The inelastic cross sections for some low-lying levels of these nuclei were also better fitted by adding the results of the coupled-channels calculations to those of the Moldauer calculations.

For Gd and Er, which have large deformation parameters, the results of elastic scattering calculated with the coupled-channels theory gave better results than the spherical optical-model calculations, although there were still disagreements between the experimental data and the coupled-channels calculations. The inelastic data for these nuclei have rather large error. Accordingly, it is difficult to deduce clear results.

This is a blank page

Analysis of Fast Neutron Scattering Using the Coupled-Channels Theory

Shigeya Tanaka

Japan Atomic Energy Research Institute, Tokai-mura, Ibaraki-ken, Japan

1. Introduction

Recently it has been demonstrated[1] that the angular distributions of elastic neutrons for rare-earth nuclei such as ^{139}La, ^{141}Pr, Er calculated with the coupled-channels theory[2] fit the experimental data better than those calculated with the spherical optical model. Analysis using the coupled-channels theory has been extended to other nuclei. This paper reports the analysis for neutron scattering by Fe, Ni, Zn, ^{120}Sn and Gd.

In this kind of analysis, choice of the parameter values of an optical potential is very important. In the previous report[1], we determined a set of potential parameters from comparison of calculations based on the spherical optical model with the measured values for neutron scattering by ^{209}Bi. This procedure was adequate, because the coupling between the ground and excited levels in ^{209}Bi was expected to be weak, and it was proved that the spherical optical model is applicable to this nucleus. All the calculations in this report, therefore, are based on an optical potential with this set of parameter values, although changes in the parameter values are made within small quantities in some cases.

2. Analysis and Discussions

In the coupled-channels calculations the following potential was used:

$$V(r,\theta,\varphi) = -V\frac{1}{1+\exp[(r-R)/a]} - 4iW\frac{\exp[(r-R)/b]}{\{1+\exp[(r-R)/b]\}^2}$$

$$- V_{so}(\sigma\ell)\lambda_\pi^2 \frac{1}{ar} \frac{\exp[(r-R_o)/a]}{\{1+\exp[(r-R_o)/a]\}^2}, \qquad (1)$$

where $\lambda\!\!\!^{-}$ is π-meson Compton wave length, and radius R depends on angles as follows:

$$R = R_0 \{ 1+\beta\, Y_{20}(\theta') \} ,$$
$$Y_{20}(\theta') = \Sigma_\mu\, D_{\mu 0}^{2}(\theta_i) Y_{2\mu}(\theta,\varphi), \qquad (2)$$

for the rotational model, and

$$R = R_0 \{ 1+\Sigma_\mu \alpha_\mu \quad Y_{2\mu}(\theta',\varphi) \}, \qquad (3)$$

for the vibrational model, where $R_0 = r_0 A^{1/3}$. The quantities θ and φ are of space-fixed coordinates. In the case of the vibrational model, β is defined as

$$\beta^2 = < 0 | \Sigma_\mu \; | \; \alpha_\mu \; |^2 \; | \; 0 > . \qquad (4)$$

If β=0 in eq.(1), it is reduced to a spherical optical potential.

The coupled-channels calculations were made with the computer code JUPITOR-1[3], and the rest of the calculations with the code STAX2[4].

Table 1 shows the values of the potential parameters and the coupling modes between the ground and excited levels used in the present analysis. In all the cases the couplings were taken to be complex. For comparison, the values for ^{139}La, ^{141}Pr and Er, which have already reported in ref. 1), are shown in the table. As mentioned in section 1, these parameter values are based on the parameters searched with respect to the elastic data of ^{209}Bi, although in some cases small amounts were changed from V = 50.9 - 24(N-Z)/A MeV, W = 4.3 MeV and r_0 = 1.25 fm so as to be better fitted to the experimental values. The rest of the parameter values was fixed. The coupled-channels calculations were performed with the vibrational model for Fe, Ni, Zn and ^{120}Sn and with the rotational model for gadolinium. The values of the defomation parameter β_2 were taken from ref. 5), except for the case of

gadolinium. In this case a value a little smaller than in ref. 5) was taken.

In figs. 1-5 angular distributions of elastic scattering are shown at the left-hand side and the inelastic scattering at the right-hand side. In the figures for elastic cross sections spherical-potential calculations are shown by dashed curves, and the coupled-channels calculations by solid curves. Generally, in the analysis in the present energy region the contributions of the compound process to the elastic scattering are not negligible. They were estimated by using the Moldauer theory[6], and the compound elastic cross sections were added to both the calculated results, when it seemed that they were not negligible. In the figures for inelastic cross sections, the calculations due to the Moldauer theory are shown by the dashed curves. Direct inelastic scattering is added to these results, and the results are shown by solid curves.

Fig. 1 shows the scattering cross sections for iron. In order to estimate the contribution of the compound process, seven excited levels up to an excitation energy 3.12 MeV were taken into account in the Moldauer calculation. The coupled-channels calculations show very good agreement with the experiment. In the case of inelastic scattering for 845 keV level, the solid curves show large deviations from the experimental values at E_n = 1.71, 2.01 and 2.65 MeV. However, intermediate structures with widths of 0.2 MeV have been reported at E_n = 1.6 and 2.05 MeV[7]. The measurement was made with an energy spread of neutrons 0.09 MeV[8]. Therefore, the deviations at these two incident energies are consistent with the existence of the intermediate structures. The deviation at E_n = 2.65 MeV may also be due to the fluctuation in the excitation function.

Fig. 2 shows the cross sections for nickel. The compound elastic and inelastic cross sections were estimated by taking into account six excited levels assumed in a "nucleus" averaged over even-even isotopes of nickel in the Moldauer calculation. The excitation energy of the sixth level assumed was 3.05 MeV. Both the elastic and inelastic results calculated by taking into account the coupling between the ground and first 2^+ levels show better agreements than the case without the coupling.

Fig. 3 is for zinc. Triangles in the figure of elastic scattering are data of Holmqvist and Wiedling.[11] The Moldauer calculation was made for the cross sections at incident neutron energies less than 4.5 MeV. In the calculation six excited levels up to an excitation energy 3.3 MeV were assumed in a "nucleus" averaged over even-even isotopes of zinc. In the case of E_n = 4.48 MeV, however, the results of the Moldauer calculation were normalized to the observed inelastic cross sections for the second 2^+ level. All the elastic cross sections and the inelastic cross sections for the incident energies up to 4.48 MeV, which were calculated by taking the coupling between levels into account, show better agreement with the experimental data. The reason for disagreement in the inelastic cross sections at energies higher than 5.92 MeV is not clear. It might be necessary that the couplings with higher levels are taken into account.

Fig. 4 is for ^{120}Sn. Twenty-one excited levels up to an excitation energy 3.07 MeV were taken into account in the Moldauer calculation. The effect of the coupling on the elastic and inelastic cross sections is not large, but in general the results with the coupled channels show better agreement with the elastic and first 2^+ inelastic data than the case without the coupling.

Calculations for gadolinium were made with respect to a "nucleus" averaged over gadolinium isotopes with a weight of isotopic abundances. The couplings between levels in the ground rotational band up to the 6^+ level were considered with the adiabatic approximation. As the first trial, the following values were taken: r_0 = 1.25 fm and β_2 = 0.34 (ref. 5). As was expected, the coupled-channels calculation for the elastic scattering gave far better results than the spherical optical model calculation. However, there was disagreement between the experimental data and the coupled-channels calculation. This was somewhat improved by changing the parameter values as follows: r_0 = 1.23 fm and β_2 = 0.30, although still there remains some disagreement. Fig. 5 shows the results with these values. Contribution from the compound process was estimated by comparing the backward inelastic cross sections for the 4^+ level with the Moldauer calculation and was taken into account for the calculated results up to E_n = 2.57 MeV. The angular distributions for the elastic data

of gadolinium are i) very similar to those for erbium[1], and differences between the calculated results and the experimental data are of same magnitudes in both cases of gadolinium and erbium. The first 2^+ inelastic data for these nuclei have rather large errors, and, accordingly, it is difficult to deduce clear results.

Comparison is made also for the total cross sections in table 2. Here, $\sigma_{T,sph}$ and $\sigma_{T,c-c}$ denote the cross sections calculated with the spherical optical model and the coupled-channels theory, respectively, and $\sigma_{T,obs}$ are observed data. The values of $\sigma_{T,c-c}$ are closer to $\sigma_{T,obs}$ than the values of $\sigma_{T,sph}$, except for the case of gadolinium.

3. Conclusion

In the previous analysis[1] a parameter set has been obtained from the comparison of theoretical calculations with measured values for ^{209}Bi, and we obtained some results by applying this parameter set to ^{131}La, ^{141}Pr and Er. The further application of this parameter set in the present analysis to the calculations for the other nuclei, combining with the previous results, leads to the following conclusions:

(i) For Fe, Ni, Zn, ^{120}Sn, ^{139}La and ^{141}Pr, the coupled-channels calculations gives better agreement with the experimental elastic data than the spherical optical-model calculations, by using the present parameter set for both the calculations. In the most cases of inelastic scattering, good results are obtained by taking into account the coupling between the ground and excited levels.

(ii) For Gd and Er, the elastic angular distributions calculated with the spherical optical model result in large deviation from the measured values, and the coupled-channels calculaitons lead to far better results by using the present parameter set. But there remain certain disagreements, whose magnitutes are larger than supposed experimental errors.

References

1) S. Tanaka, Y. Tomita, K. Ideno and S. Kikuchi, Nucl. Phys. A179 (1972) 513

2) T. Tamura, Rev. Mod. Phys. 37 (1965) 679

3) M. Wakai, S. Igarasi, O. Mikoshiba and S. Yamaji, JAERI memo 3833, 1969

4) Y. Tomita, JAERI 1191, 1970

5) P. H. Stelson and L. Grodzins, Nucl. Data Sect. A1 (1965) 21

6) P. A. Moldauer, Phys. Rev. 135 (1964) B642

7) Y. Tomita, K. Tsukada, M. Maruyama and S. Tanaka, Nuclear Data for Reactors, Vol. II, Helsinki, (1970) 301

8) K. Tsukada, S. Tanaka, Y. Tomita and M. Maruyama, Nucl. Phys. A125 (1969) 641

9) K. Tsukada, Y. Tomita, S. Tanaka and M. Maruyama, Nuclear Data for Reactors, Vol. II, Helsinki (1970) 305

10) S. Tanaka, K. Tsukada, M. Maruyama and Y. Tomita, Nuclear Data for Reactors, Vol. II, Helsinki (1970) 317

11) B. Holmqvist and T. Wiedling, AE-337 (1968)

12) S. Tanaka, Y. Tomita, Y. Yamanouti and K. Ideno, submitted to Conf. on Nucl. Structure with Neutrons, Budapest, (1972)

TABLE 1

Potential Parameters and Coupling Modes

	V	a W b V_{so}	r_o	β_2	Coupling
Fe	$51.8-24\frac{N-Z}{A}$ $= 50.0$	0.65 5.0 0.48 7.0	1.23	0.23	$0^+ - 2^+$ for ^{56}Fe
Ni	$51.1-24\frac{N-Z}{A}$ $= 50.0$	0.65 5.0 0.48 7.0	1.23	0.194	$0^+ - 2^+$ for ^{e-e}Ni
Zn	$51.6-0.3E$ $-24\frac{N-Z}{A}$	0.65 5.0 0.48 7.0	1.23	0.234	$0^+ - 2^+$ for ^{e-e}Zn
^{120}Sn	$50.0-24\frac{N-Z}{A}$ $=46.0$	0.65 4.3 0.48 7.0	1.25	0.112	$0^+ - 2^+$
^{139}La	$49.9-24\frac{N-Z}{A}$ $= 46.0$	0.65 4.3 0.48 7.0	1.25	0.12	$0^+ - 2^+$ for ^{138}Ba core
^{141}Pr	$50.3-24\frac{N-Z}{A}$ $= 46.0$	0.65 4.3 0.48 7.0	1.25	0.104	$0^+ - 2^+$ for ^{140}Ce core
Gd	$50.4-24\frac{N-Z}{A}$ $=46.0$	0.65 4.3 0.48 7.0	1.23	0.30	$0^+-2^+-4^+-6^+$ rot. for ^{e-e}Gd
Er	$51.1-24\frac{N-Z}{A}$ $= 46.0$	0.65 4.3 0.48 7.0	1.25	0.34	$0^+-2^+-4^+-6^+$ rot. for ^{e-e}Er
^{209}Bi	$50.9-24\frac{N-Z}{A}$ $= 46.0$	0.65 4.3 0.48 7.0	1.25	β_3 $=0.10$	0^+-3^- for ^{208}Pb core

* Weak coupling between the core and a proton was assumed.

TABLE 2

Total Cross Sections

	E_n (MeV)	$\sigma_{T,sph}$	$\sigma_{T,c-c}$	$\sigma_{T,obs}$ [a]
Fe	1.37	3.66	3.57	2.7
	1.71	3.91	3.54	2.9
	2.01	3.86	3.53	3.1
	2.65	3.82	3.51	3.1
	3.26	3.58	3.52	3.2
Ni	2.01	3.43	3.40	3.2
	2.65	3.36	3.35	3.2
	3.26	3.41	3.40	3.3
Zn	1.71	3.28	3.24	3.2
	2.24	3.15	3.19	3.2
	3.00	3.25	3.32	3.4
	4.08	3.77	3.73	3.74
	5.92	4.02	3.82	3.84
	6.97	4.00	3.75	3.79
	7.99	3.85	3.63	3.70
^{120}Sn	1.52	6.52	6.15	6.00 [b]
	2.05	5.53	5.35	5.45 [b]
	2.57	4.75	4.74	4.88 [b]
	3.08	4.24	4.35	4.52 [b]
	3.60	4.02	4.15	4.27 [b]
Gd	1.52	7.44	6.78	7.05
	2.05	7.33	6.38	6.85
	2.57	6.83	6.01	6.53
	3.08	6.25	5.68	6.17
	3.60	5.72	5.36	5.85

a) The values are taken from BNL 325 and BNL 325 2nd Ed.

b) Data for natural tin.

Figure Captions

Fig. 1. Differential cross sections for elastic (left-hand side) and inelastic (right-hand side) scattering by iron. The closed points are our experimental data[8]. The dashed and solid curves for the elastic scattering are cross sections calculated with the spherical optical potential and with the coupled-channels theory, respectively. The compound elastic cross sections calculated with the Moldauer theory were added to both the calculated results. The dashed curves for the inelastic scattering are cross sections calculated with the Moldauer theory. The solid curves represent the results of the coupled-channels calculation plus those of the Moldauer theory.

Fig. 2. Differential cross sections for elastic and inelastic scattering by nickel. The points[8] and curves have the same meaning as in fig. 1.

Fig. 3. Differential cross sections for elastic and inelastic scattering by zinc. The closed points are our experimental data[9,10]. The open triangles are data of Holmqvist and Wiedling[11] The curves have the same meaning as in Fig. 1. The compound processes are neglected for the case of incident neutron energies higher than 5 MeV.

Fig. 4. Differential cross sections for elastic and inelastic scattering by ^{120}Sn. The points[12] and curves have the same meaning as in Fig. 1.

Fig. 5. Differential cross sections for elastic and inelastic scattering by gadolinium. The points are our experimental data[12]. The open circles indicate the elastic plus the inelastic cross sections for the first 2^+ levels in gadolinium isotopes. Accordingly, the direct inelastic cross sections for these levels calculated with the coupled-channels theory were added to the elastic cross sections calculated with this theory. Excluding this case, the solid and dashed curves have the same meaning as in fig. 1. In order to show the contribution of the compound process, the results due only to the coupled-channels calculation are shown by dotted curves in the figure of left-hand side.

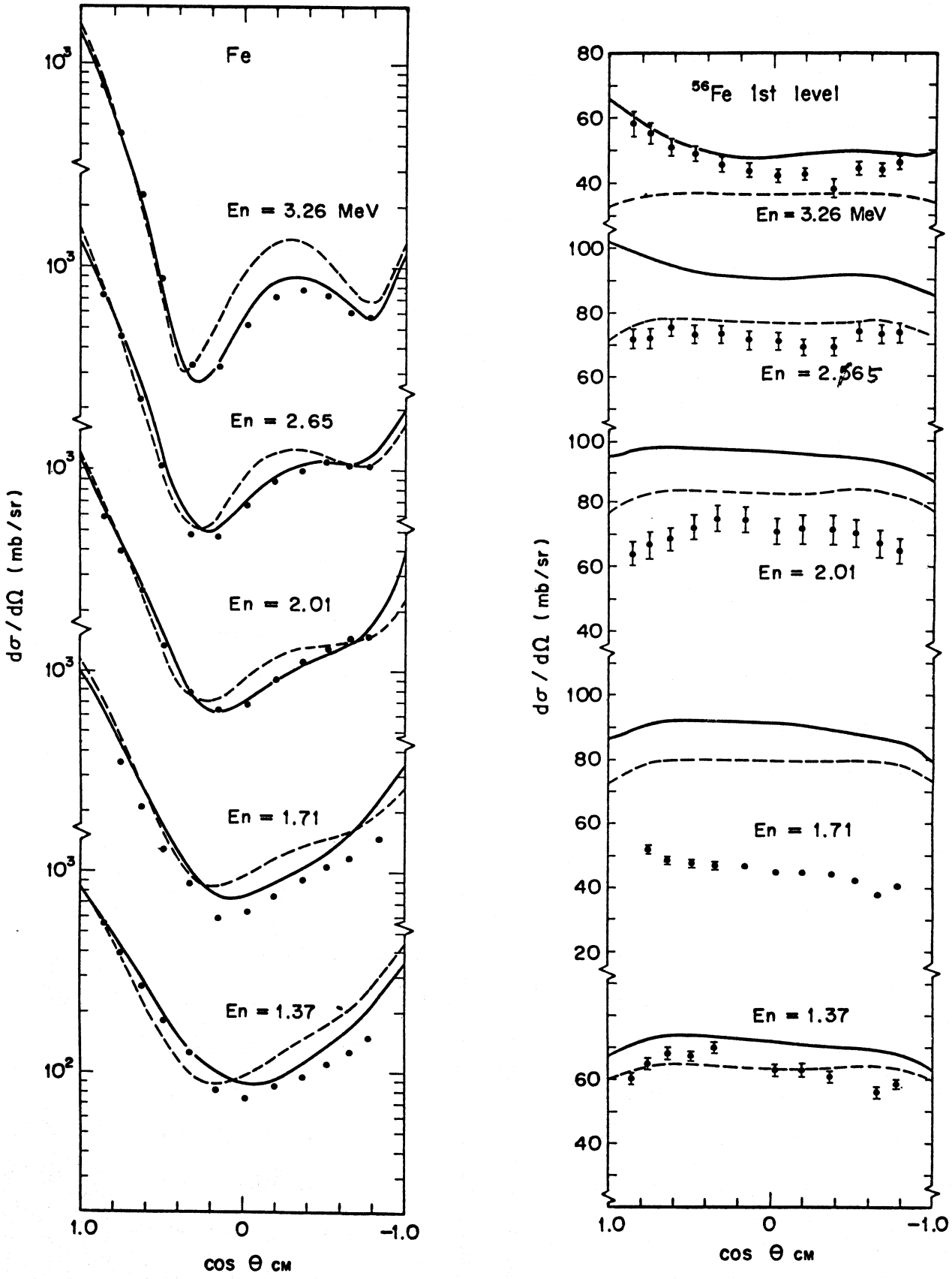
Fe
En = 3.26 MeV
En = 2.65
En = 2.01
En = 1.71
En = 1.37
dσ / dΩ (mb / sr)
cos Θ cm
56Fe 1st level
En = 3.26 MeV
En = 2.565
En = 2.01
En = 1.71
En = 1.37
dσ / dΩ (mb / sr)
cos Θ cm

Fig. 1

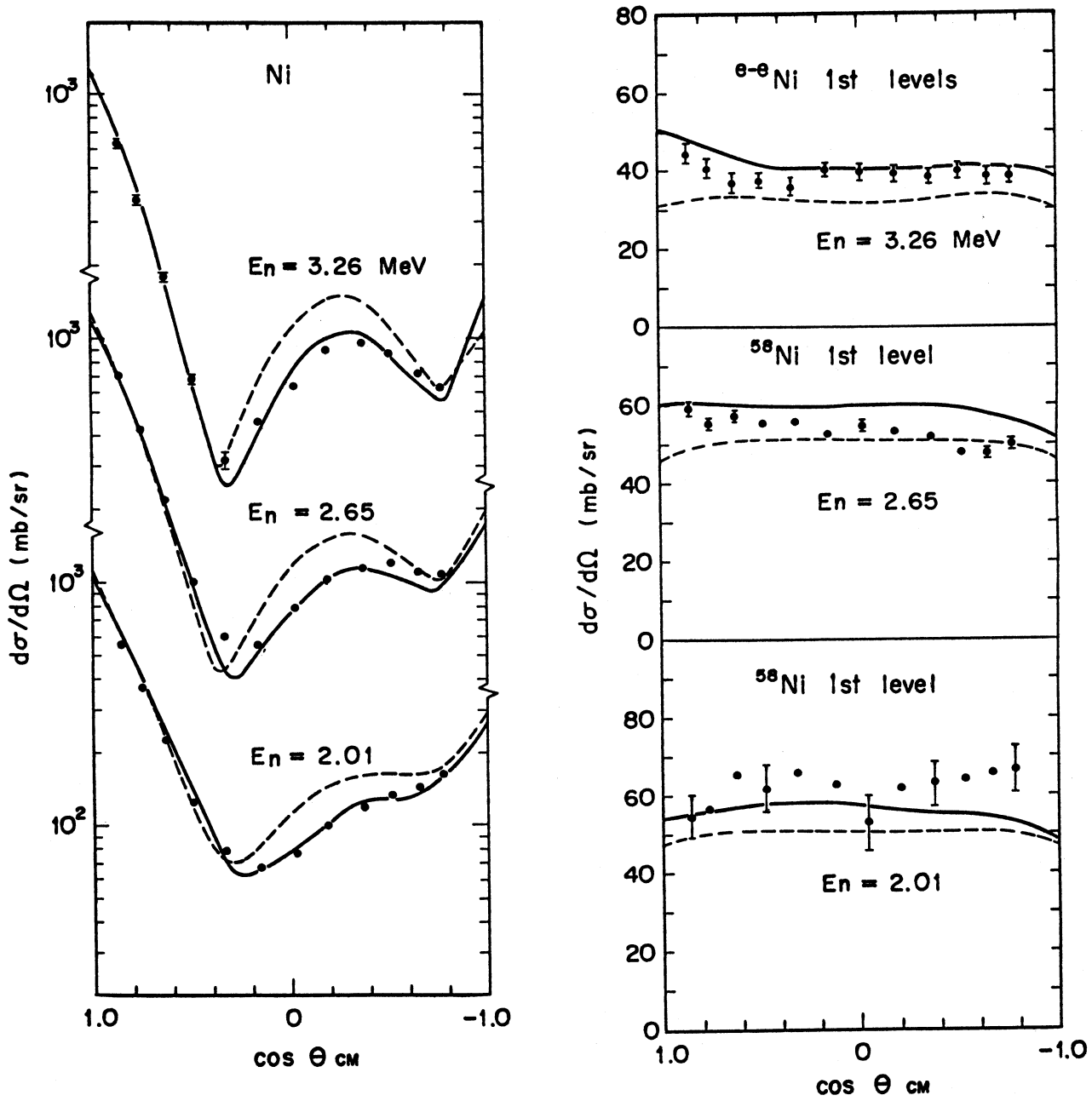
Ni
En = 3.26 MeV
En = 2.65
En = 2.01
dσ/dΩ (mb/sr)
cos θ cm
e-e Ni 1st levels
En = 3.26 MeV
58Ni 1st level
En = 2.65
58Ni 1st level
En = 2.01
dσ/dΩ (mb/sr)
cos θ cm

Fig. 2

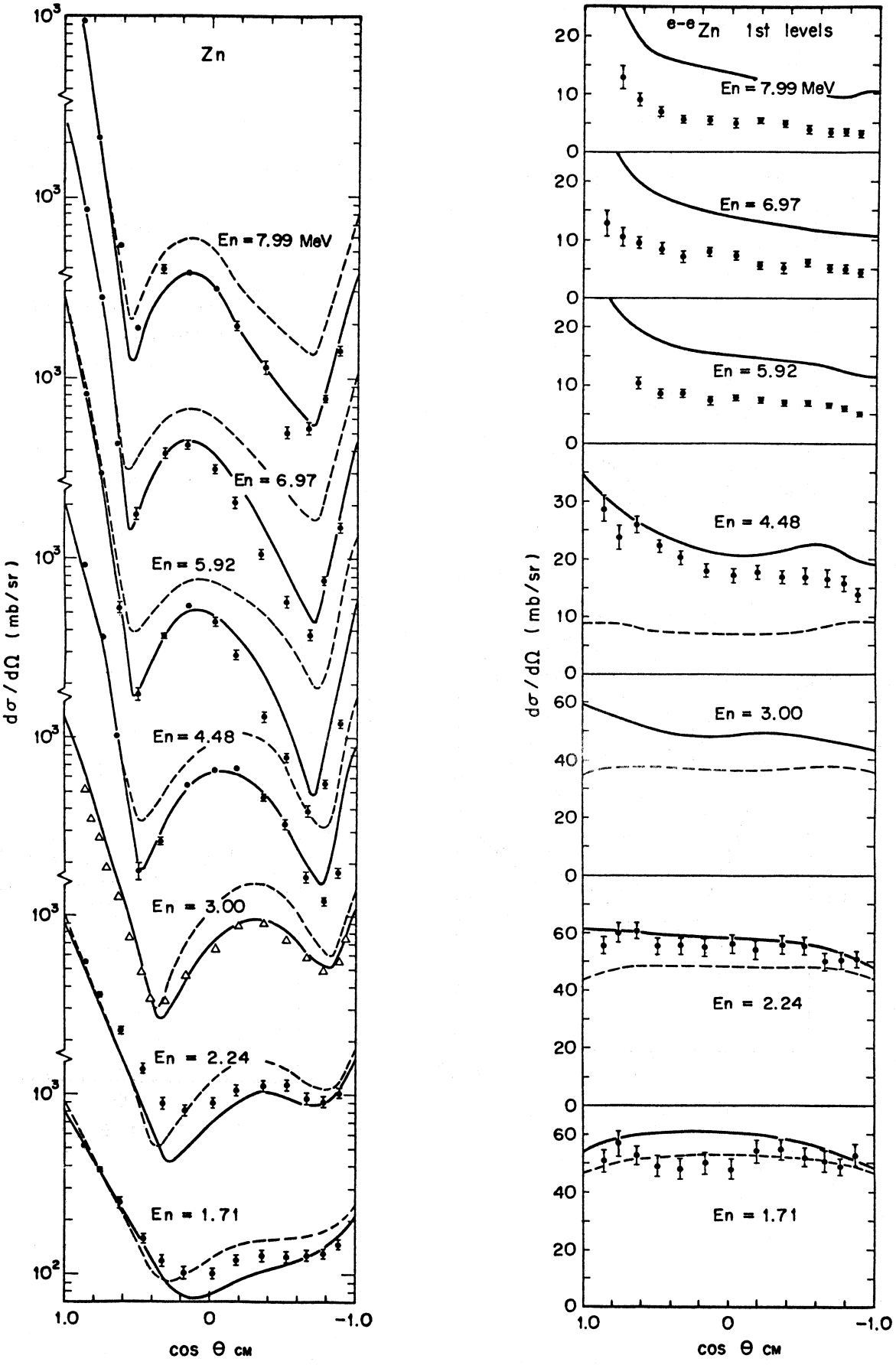
Zn
En = 7.99 MeV
En = 6.97
En = 5.92
En = 4.48
En = 3.00
En = 2.24
En = 1.71
dσ/dΩ (mb/sr)
cos θ cm
e-e Zn 1st levels
En = 7.99 MeV
En = 6.97
En = 5.92
En = 4.48
En = 3.00
En = 2.24
En = 1.71
dσ/dΩ (mb/sr)
cos θ cm

Fig. 3

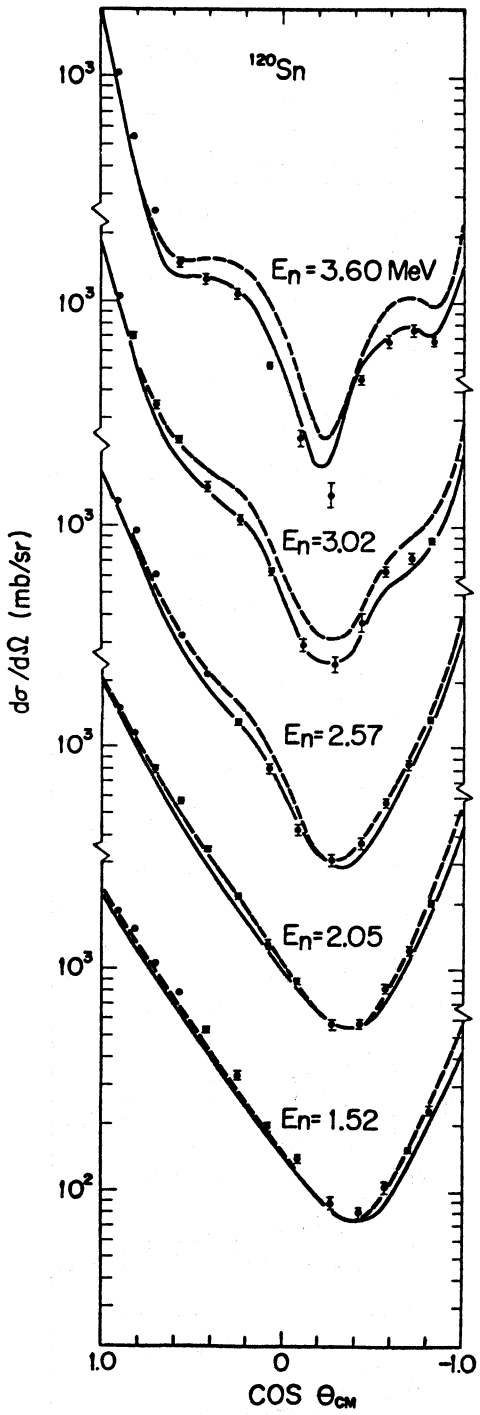
^{120}Sn
E_n = 3.60 MeV
E_n = 3.02
E_n = 2.57
E_n = 2.05
E_n = 1.52
$d\sigma/d\Omega$ (mb/sr)
COS θ_{CM}

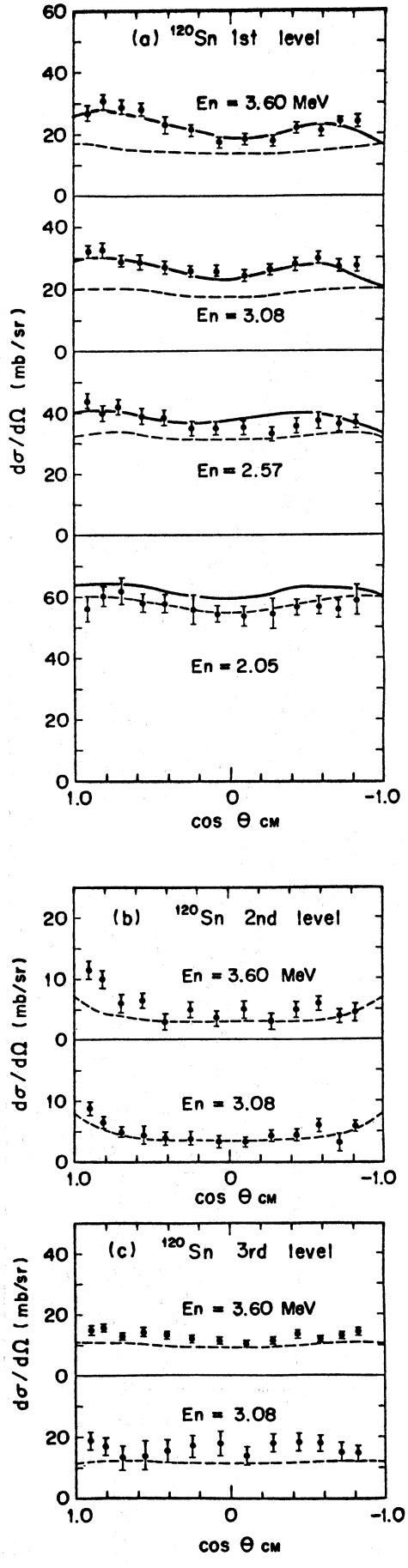
(a) ^{120}Sn 1st level
En = 3.60 MeV
En = 3.08
En = 2.57
En = 2.05
(b) ^{120}Sn 2nd level
En = 3.60 MeV
En = 3.08
(c) ^{120}Sn 3rd level
En = 3.60 MeV
En = 3.08
$d\sigma/d\Omega$ (mb/sr)
cos θ cm

Fig. 4

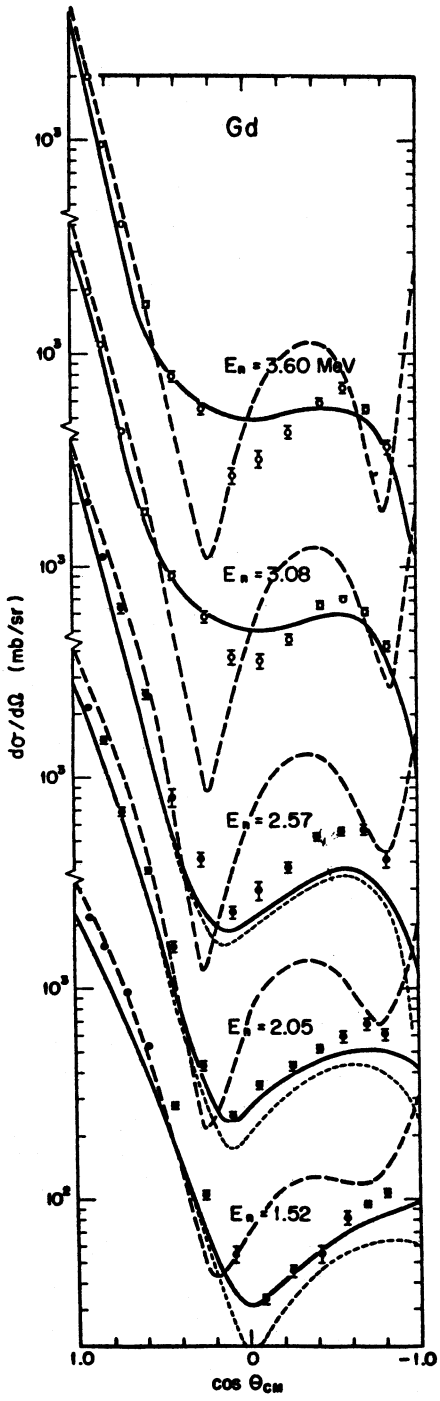
Gd
E_n = 3.60 MeV
E_n = 3.08
E_n = 2.57
E_n = 2.05
E_n = 1.52
dσ/dΩ (mb/sr)
cos θ_{cm}
1.0
0
-1.0

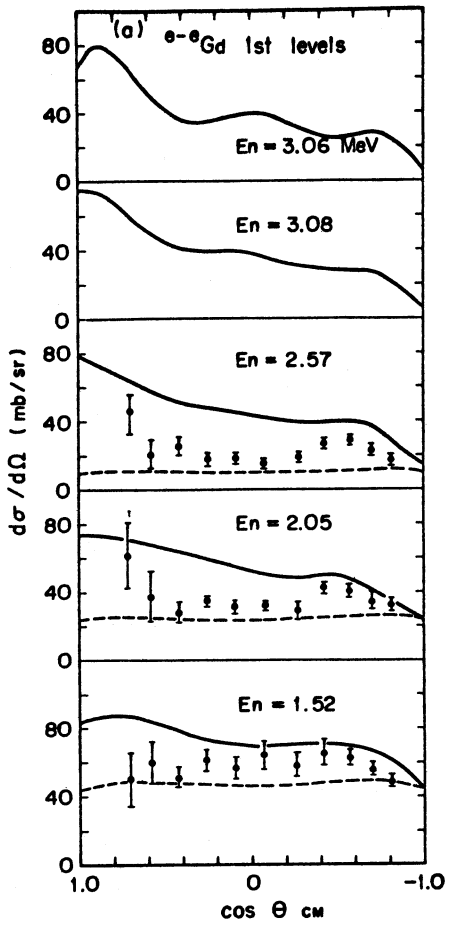
(a) $^{e-e}$Gd 1st levels
En = 3.06 MeV
En = 3.08
En = 2.57
En = 2.05
En = 1.52
dσ/dΩ (mb/sr)
cos θ cm
1.0
0
-1.0

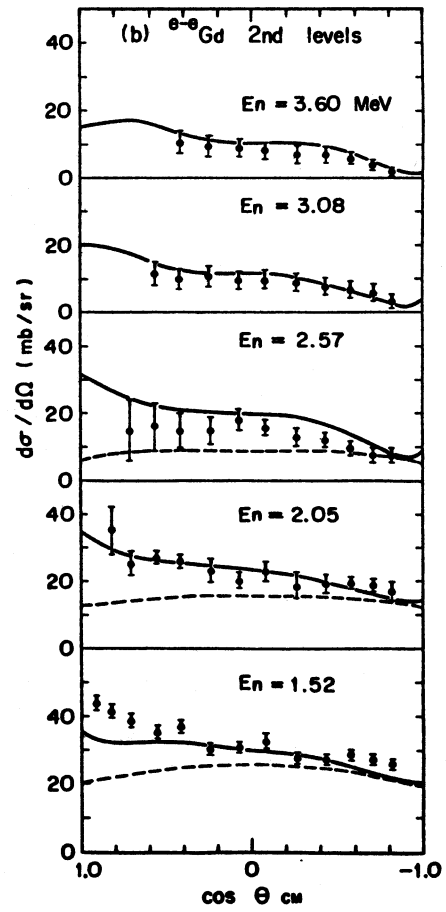
(b) $^{e-e}$Gd 2nd levels
En = 3.60 MeV
En = 3.08
En = 2.57
En = 2.05
En = 1.52
dσ/dΩ (mb/sr)
cos θ cm
1.0
0
-1.0

Fig. 5

Benzi: Which computer code was used to carry out the optical model calculations ? In particular, how were the compound nucleus cross-sections calculated ?

reply: STAX2 code (Y. Tomita, JAERI 1191, 1970) was used to carry out the spherical optical model calculations and Moldauer calculations to estimate the compound nucleus cross sections. This means that the compound nucleus cross sections were calculated on the basis of the spherical optical model, not on the basis of the generalized optical model in which the coupling between levels is taken into account. Such calculations were made for convenience sake.

Cierjacks: For the inelastic scattering you have used only - if I understood correctly - the coupling between ground state and first excited state. Have the authors also tried to include more than two states?

reply: We considered only the coupling between ground state and first 2^+ (3^- state for ^{209}Bi) state in the vibrational-model calculations. For Gd and Er, the ground rotational bands up to 6^+ states were considered. We are going to try further calculations including more than two states for vibrational nuclei.

Usachev: How many parameters did you use when fitting the experimental points by the theoretical curves ?

reply: Seven parameters were used. They are V, a, W, b, V_{so}, r_o and β_2 or β_3. But in the present analysis, only V and W were searched so as to be fitted to the experimental data of ^{209}Bi. Other parameters, a, b, V_{so} and r_o were fixed, and β_3 was taken from a bibliography. Then, nearly the same optical parameter values were used for the rest of nuclei.

Ribon: Was the β_2 parameter adjusted or deduced from bibliographic informations ?

reply: Most β_2 parameters used in the present analysis were taken from a bibliographic information, i.e. P.H. Stelson and L. Grodzins, Nucl. Data Sect. A1 (1965) 21. The β_2 value for gadolinium was adjusted from $\beta_2 = 0.34$ to 0.30.

This is a blank page

Study of Energy Levels of ^{120}Sn through the (n,n'γ) Reaction

S. Kikuchi and Y. Sugiyama

The energy levels of ^{120}Sn were studied by means of the (n,n'γ) reaction in the energy range 2.0 ∿ 3.1 MeV. A 20 cc Ge(Li) detector, associated with a pulsed-beam time-of-flight spectrometer, was used to detect γ-rays. From the threshold energies of γ-ray production cross sections, the energies of levels were determined. For the purpose of obtaining informations about spins and parities of these levels, the γ-ray angular distributions were measured at E_n=2.3, 2.7 and 3.1 MeV. Detailed analysis is now in progress.

This is a blank page

Study of Energy Levels of ^{120}Sn Through the (n,n'γ) Reaction

S. Kikuchi and Y. Sugiyama

The energy levels of ^{120}Sn were studied by means of the (n,n'γ) reaction in the energy range 2.0 ∿ 3.1 MeV. A 20 cc Ge(Li) detector, associated with a pulsed-beam time-of-flight spectrometer, was used to detect γ-rays.

The production cross sections of the observed γ-rays are shown in Fig. 1. From the threshold energies of those cross sections, the energy of level associated with each γ-ray was determined and is shown in Fig. 2. The 412 keV γ-ray cannot be assigned to any transition between levels obtained in the present study.

For the purpose of obtaining informations about spin values of the levels, the γ-ray angular distributions were measured at En = 2.3, 2.7 and 3.1 MeV. Estimated spin values of the levels are also shown in Fig. 2.

Typical results of the γ-ray angular distribution (E_γ = 1183.7 keV) is shown in Fig. 3. From this figure, the 1184 keV transition is not definitely determined whether it is $3^- \rightarrow 2^+$ or $2^+ \rightarrow 2^+$ transition. However, it is clearly determined as a $2^+ \rightarrow 2^+$ transition by using a δ-ellipse representation as shown in Fig. 4. The figures indicated on the ellipse are multipole mixing ratio δ and the hatched box represents the error limit of the observed coefficients a_2 and a_4 of Legendre Polynomials fitted to the observed angular distribution. In this case, the multipole mixing ratio is determined to be $\delta = 3.39 \pm 0.15$.

Detailed analysis and theoretical interpretation is now in progress.

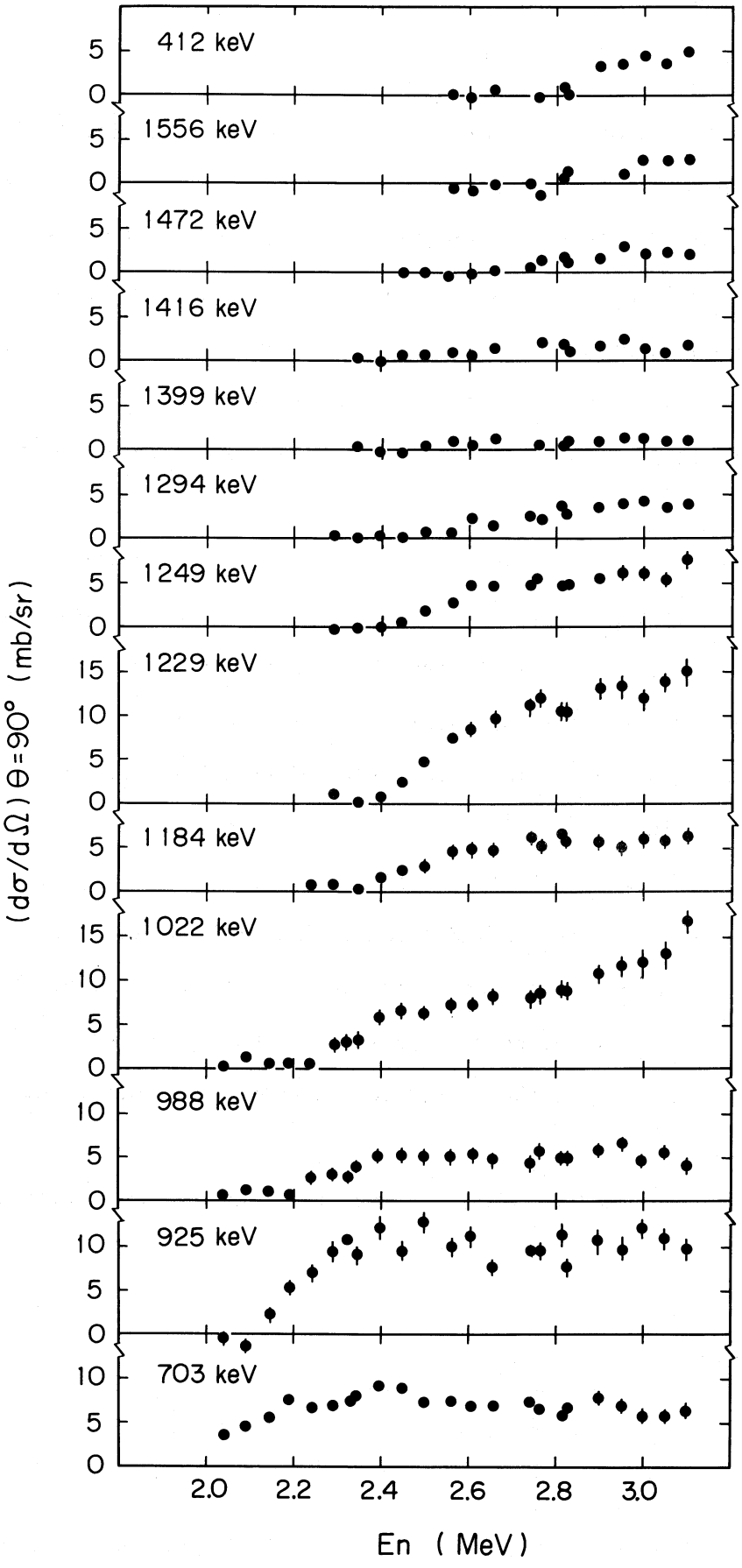
412 keV
1556 keV
1472 keV
1416 keV
1399 keV
1294 keV
1249 keV
1229 keV
1184 keV
1022 keV
988 keV
925 keV
703 keV
(dσ/dΩ) Θ=90° (mb/sr)
En (MeV)
2.0
2.2
2.4
2.6
2.8
3.0

Fig. 1

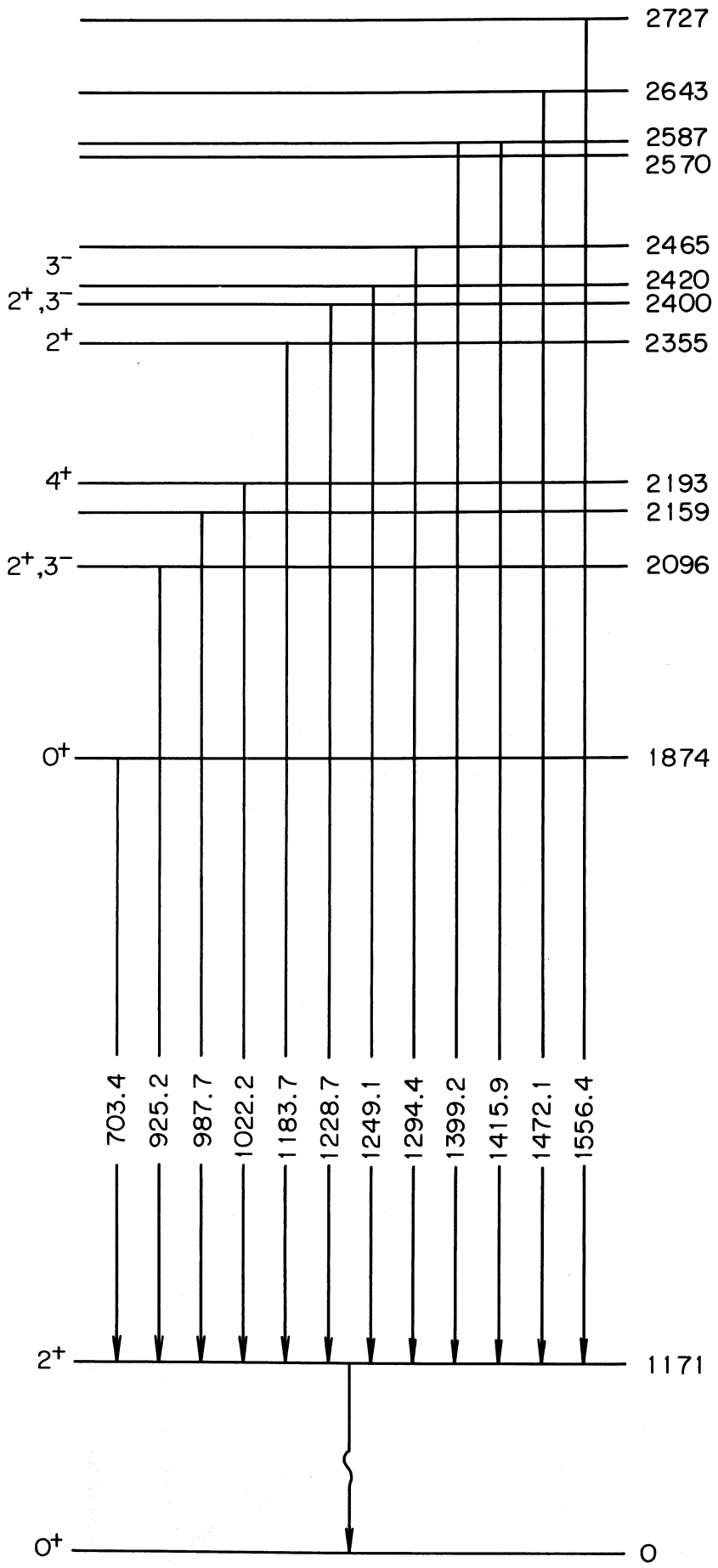
2727
2643
2587
2570
2465
3⁻
2420
2⁺,3⁻
2400
2⁺
2355
4⁺
2193
2159
2⁺,3⁻
2096
0⁺
1874
703.4
925.2
987.7
1022.2
1183.7
1228.7
1249.1
1294.4
1399.2
1415.9
1472.1
1556.4
2⁺
1171
0⁺
0

Fig. 2

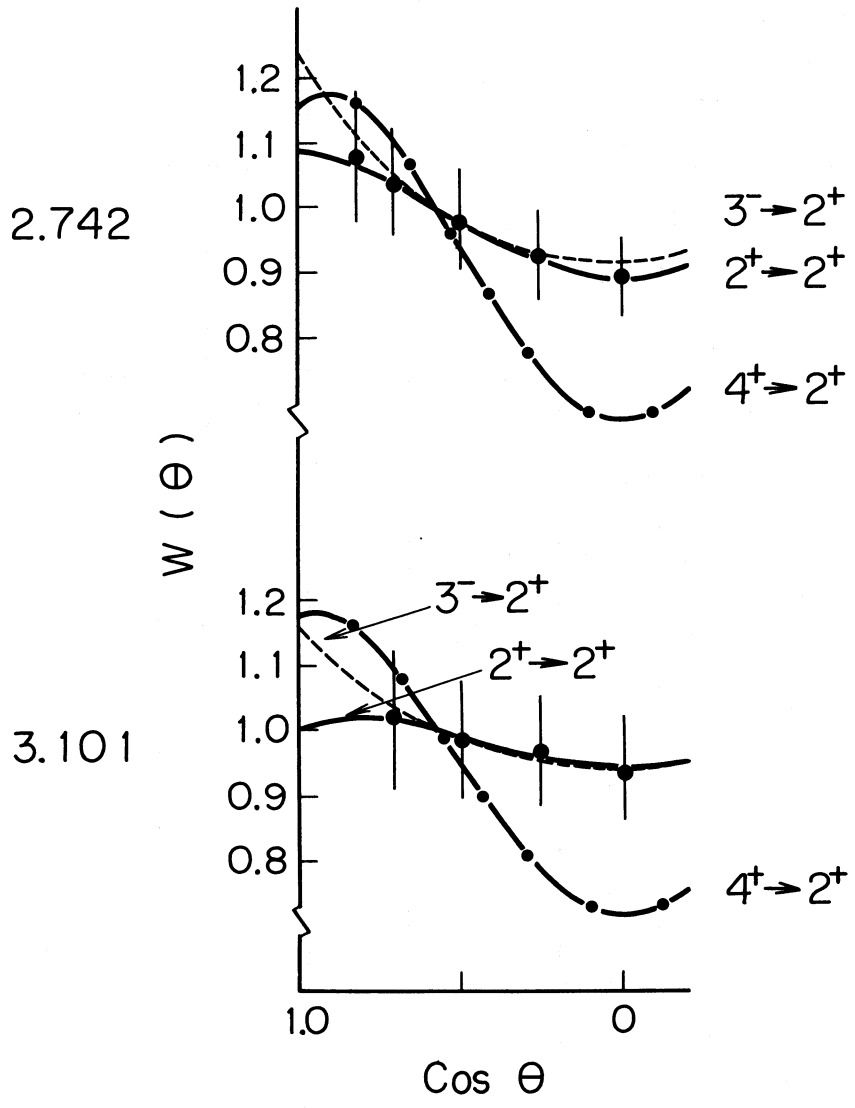

Fig. 3

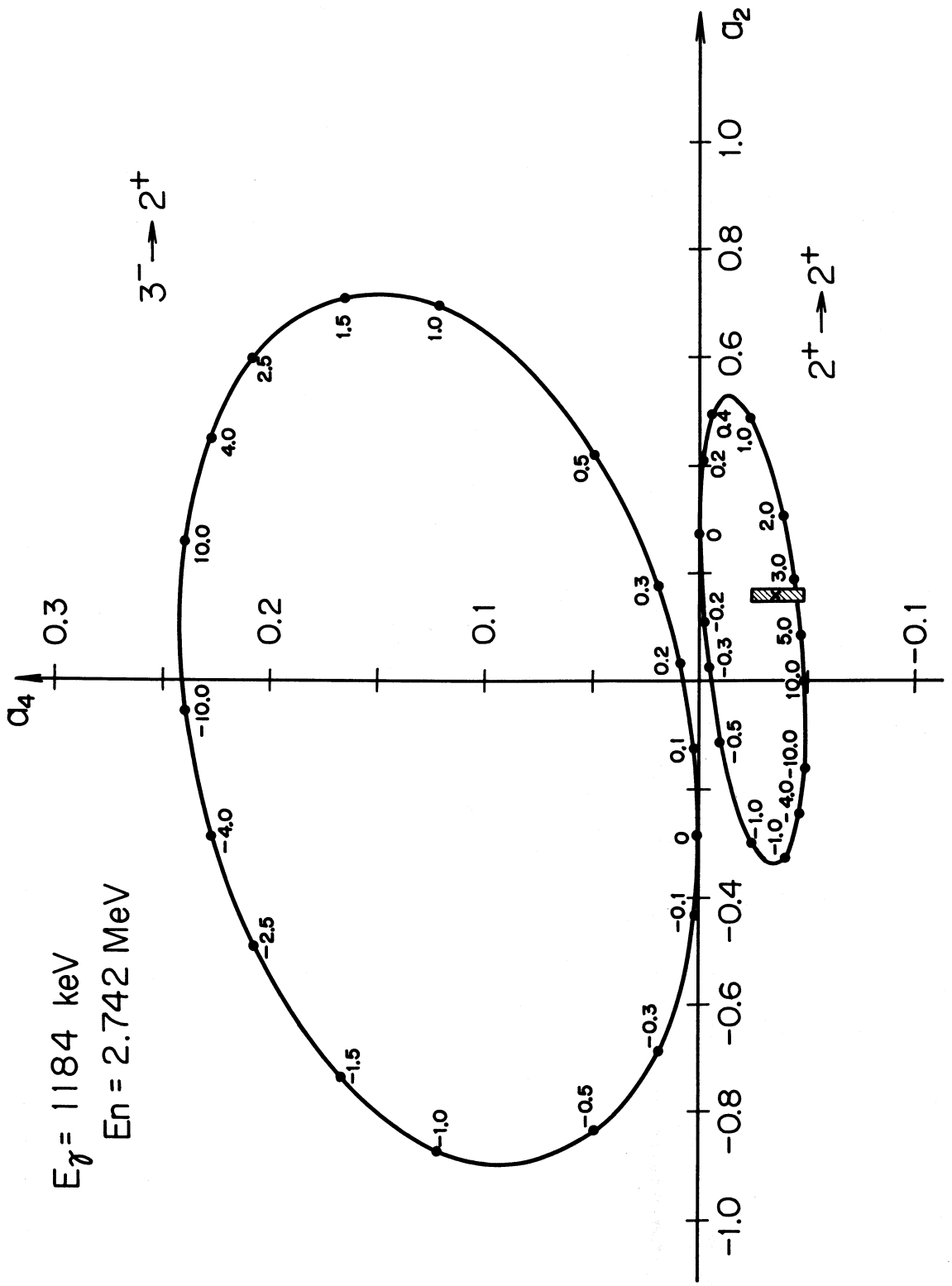
a_2
a_4
$3^- \rightarrow 2^+$
$2^+ \rightarrow 2^+$
E_γ= 1184 keV
En = 2.742 MeV
1.0
0.8
0.6
-0.4
-0.6
-0.8
-1.0
0.3
0.2
0.1
-0.1

Fig. 4

This is a blank page

Use of spectrum measurements in fast media to get information on cross sections

M^me P. Corcuera, P. Govaerts, J.P. L'Heriteau

The neutron spectrum of an uranium assembly is measured with protron recoil detectors; the experimental spectrum is compared to the theoretical one.

The discrepancies are mainly due to the neutron inelastic scattering, and can be reduced by adjusting the cross sections. The influence of the spectrum of inelastic scattered neutrons is not so clear, and will be studied systematically.

This is a blank page

ON THE VALIDITY OF THE TEMPERATURE LAW

INDC Topical Discussion

(Vienne - 17/21 Juillet 1972)

J.P. L'Hériteau and P. Ribon

Département de Physique Nucléaire

C.E.N. Saclay, BP n° 2, 91190 Gif sur Yvette (France)

The energy distribution of inelastically scattered neutrons is usually described by a temperature law :

$$p(E)\ dE' = \frac{E'}{T^2}\ e^{-\frac{E'}{T}}\ dE' \qquad (1)$$

This law is valid only when many levels contribute to the scattering - i.e. in the continuum. It cannot be used to describe the spectrum of secondary neutrons when only a few levels are involved ; but there should be a continuity between this resolved level energy range and the continuum.

Furthermore, this law assumes many approximations which are more or less fulfilled even in the continuum. At first, we shall remind these assumptions, and then examine the continuity between these two energy ranges in the case of ^{238}U.

I - THE DERIVATION OF THE TEMPERATURE LAW.

Basic assumption : the statistical model is valid and there is no direct interaction.

We shall use the following notations :

i : spin of the particle α

I : spin of the target nucleus

j : channel spin $\vec{j} = \vec{i} + \vec{I}$

ℓ : angular momentum

J : total momentum $\vec{J} = \vec{\ell} + \vec{j}$

The quantities (E', α',i',j',I',ℓ') refer to an exit channel. The energy E' is such that :

$$\varepsilon' = E - Q - \delta - E'$$

where Q is the threshold value for the (α,α') reaction. The correction δ is generally interpreted as a pairing energy ; more rigorously, it represents the "Rosenzweig effect" and depends explicitely on the details of the structure and ground state occupation of the simple particle energy level scheme [1].

The (α,α') cross-section can be written as follows :

$$\sigma_{\alpha,\alpha'}(E,E')dE' = \pi\lambda^2 \sum_{J j \ell} \frac{2J+1}{(2i+1)\ (2I+1)}\ T^J_{\alpha j \ell}(E)\ \frac{\sum_{I'\ell'j'} T^J_{\alpha'j'\ell'}(E')\ \omega_{\alpha'}(I',\varepsilon')dE'}{\sum_{\substack{\alpha''j''\ell'' \\ I''}} \int_0^{E-Q} T^J_{\alpha''j''\ell''}(E'')\omega_{\alpha''}(I'',\varepsilon'')dE''} \qquad (2)$$

Assumption I. $T^J_{\alpha j \ell}(E) \equiv T_{\alpha\ell}(E)$

The probabilities are independent on J and j ; this implies that the spin orbit potential is small, that the fission probabilities does not depend on j, which is certainly wrong, a.s.o.

Assumption II. $\omega(I',\varepsilon') = (2I'+1)\ \omega(\varepsilon')$

It is well known that, in the Fermi gas model, the variation of the level density as a function of the spin is described by

$$\omega(I,\varepsilon) \propto \omega(\varepsilon)\left(e^{-\frac{I^2}{2\sigma^2}} - e^{-\frac{(I+1)^2}{2\sigma^2}} \right) \qquad (3\ a)$$

$$\# \ \omega(\varepsilon)\ \frac{2I+1}{2\sigma^2}\ e^{-\frac{(I+1/2)^2}{2\sigma^2}} \qquad (3\ b)$$

where σ is the spin cut off factor.

The expression (3 b) is a very good approximation of (3 a) as soon as

$$2\sigma^2 > I + 1/2 \ .$$

This is always verified in practice ; but the assumption II requires that the exponential term may be neglected in (3 b), which is possible only for :

$$\begin{cases} 2\sigma^2 >> (I+1/2)^2 \\ I < \sigma\sqrt{2} - 1 \end{cases}$$

It is obvious that assumption II is a rather crude one

Under these assumptions, the expression (2) may be written :

$$\sigma_{\alpha,\alpha'}(E,E')dE' = \pi\lambda^2 \sum_{Jj\ell} \frac{2J+1}{(2i+1)(2I+1)}\ T_{\alpha\ell}(E)\ \frac{\sum_{I'\ell'j'} T_{\alpha'\ell'}(E')\ (2I'+1)\ \omega(\varepsilon')dE'}{\sum_{\substack{\alpha''j''\ell'' \\ I''}} \int_0^{E-Q} (2I''+1)\ T_{\alpha''\ell''}(E'')\omega_{\alpha''}(\varepsilon'')dE''} \qquad (4)$$

This expression can be transformed by utilizing relations deduced from the angular momentum algebra such as :

$$\sum_{I'}(2I'+1) = (2j'+1)\ (2i'+1)$$

$$\sum_{j'}(2j'+1) = (2J+1)\ (2\ell'+1)$$

We obtain :

$$\sigma_{\alpha,\alpha'}(E,E')dE' = \pi\lambda\!\!\!^{-2} \sum_{\ell}(2\ell+1)\ T_{\alpha\ell}(E)\ \frac{(2i'+1)\sum_{\ell'}(2\ell'+1)T_{\alpha'\ell'}(E')\omega(\epsilon')dE'}{\sum_{\alpha''}(2i''+1)\int_0^{E-Q}\sum_{\ell''}(2\ell''+1)\ T_{\alpha''\ell''}(E'')\ \omega(\epsilon'')dE''} \qquad (5)$$

The total compound cross-section for entrance channel α is given by :

$$\sigma_{\alpha}(E) = \pi\lambda\!\!\!^{-2} \sum_{\ell}(2\ell+1)T_{\alpha\ell}(E) = \frac{k}{E}\sum_{\ell}(2\ell+1)T_{\alpha\ell}(E)$$

Then, by eliminating all the T from (5), we obtain

$$\sigma_{\alpha,\alpha'}(E,E')dE' = \sigma_{\alpha}(E)\ \frac{(2i'+1)E'\ \sigma_{\alpha'}(E')\omega_{\alpha'}(\epsilon')dE'}{\sum_{\alpha''}(2i''+1)\int_0^{E-Q}E''\sigma_{\alpha''}(E'')\omega_{\alpha''}(\epsilon'')dE''} \qquad (6)$$

Now if we are just interested by the energy spectrum of particles α' we may deep the denominator of (6) :

$$p(E,E')dE' = \frac{\sigma_{\alpha,\alpha'}(E,E')dE'}{\int\sigma_{\alpha,\alpha'}(E,E')dE'} \propto E'\sigma_{\alpha'}(E')\omega_{\alpha'}(E')dE' \qquad (7)$$

Assumption III $\qquad \sigma_{\alpha'}(E') = \text{constant}$

This assumes that the total compound cross-section for the inverse reaction (incoming α' particles) is independent of energy ; this may be approximately true when E' is great, but is certainly false for small values of E'. Then :

$$p(E,E')dE' \propto E' \, \omega_{\alpha'}(\varepsilon')dE' \tag{8}$$

with

$$\varepsilon' = E-Q-\delta-E' = \mathcal{E}-E' \tag{8 a}$$

$$\omega_{\alpha'}(\varepsilon') \sim \frac{e^{2\sqrt{a\varepsilon'}}}{(\varepsilon')^p} \tag{8 b}$$

According the assumptions on the model, p may vary around 2.

Assumption IV $\qquad E' << \mathcal{E} = E-Q-\delta$

Then $(\varepsilon')^p = (\mathcal{E} - E')^p$ is approximatively constant, and the exponential term of (8 b) can be written :

$$e^{2\sqrt{a(\mathcal{E}-E')}} = e^{2\sqrt{a\mathcal{E}}\,(1-\frac{1E'}{2\mathcal{E}})} = \text{constant} \times e^{-\sqrt{\frac{a}{\mathcal{E}}}E'}$$

and by noting :

$$T = \sqrt{\frac{\mathcal{E}}{a}} = \sqrt{\frac{E-Q-\delta}{a}} \tag{9 a}$$

we obtain the temperature law :

$$p(E,E')dE' \propto E' \, e^{-\frac{E'}{T}} \, dE' \tag{9 b}$$

II - COMPARISONS IN THE CASE OF INELASTIC SCATTERING OF NEUTRONS BY ^{238}U

1 - *Value of the temperature in the continuum.*

The temperature T can be calculated from formulae (9 a), or adjusted to describe the experimental data. In table 1 we compare the corresponding values.

Table 1 - VALUES OF THE TEMPERATURE T

Energy of incoming neutrons (MeV)	Temperature used to describe the spectrum according Batchelor et al [2]	Temperature used to describe the spectrum recommanded by ENDF - 3 [3]	Temperature calculated by (9-a) δ=1.5 MeV a=20 MeV^{-1}	Temperature calculated by (9-a) δ=0 a=25 MeV^{-1} [2]
2		0. 35	0. 158	0. 28
3	0. 35 ± 0. 04	0. 39	0. 274	0. 35
4	0. 44 ± 0. 04	0. 445	0. 354	0. 40
7	0. 55 ± 0. 02	0. 552	0. 525	0. 53

It is clear that, for small values of E, the formulae (9 a) gives smaller values of T than can be deduced from experimental spectrum ; this discrepancy may be corrected, as did Batchelor et al, by setting $\delta = 0$ (last column of table 1).

Formulae used to describe the experimental results

A formula as (8) would be expected to give a better description than a formula as (9 b). However if we look to the experimental results of Batchelor [2] the agreement obtained with formula (8) is quite as satisfactory as the agreement given by (9 b).

The figure 1 shows the comparison between the two formulae for incoming neutron energy of 3 MeV ; it appears that, in the energy range of experimental results, the difference between the two curves is really two meaningless to obtain a significant improvement when using formula (8) instead of formula (9 b).

2 - Continuity of the energy spectrum of scattered neutrons between the continuum energy range and the resolved level energy.

The knowledge of the energy levels of ^{238}U is good below 1 MeV. Above the evaluation [4] reports some levels experimentally determined. Our aim was to see if we can provide a good description of energy spectrum of scattered neutrons between this range and the continuum energy range.

The figure 2 was built from ENDF/B version 3 data for ^{238}U. The three following quantities are calculated and fitted (figure 2) versus the energy of incoming neutron without taking into account the direct interaction process.

$$\bar{E}' = \frac{\int E' \, p(E \to E') \, dE'}{\int p(E \to E') \, dE'}$$

$$\sigma^2 = \frac{\int (E' - \bar{E}')^2 \, p(E \to E') \, dE'}{\int p(E \to E') \, dE'}$$

$$M^{(3)} = \frac{\int (E' - \bar{E}')^3 \, p(E \to E') \, dE'}{\int p(E \to E') \, dE'}$$

Values of equivalent temperature are deduced and plotted on figure 3 all together with $\sqrt{\frac{E}{26}}$ and $\sqrt{\frac{E-1.5}{20}}$ as proposed by Batchelor [2].

The two curves show a lack of continuity between the two energy ranges for the four quantities plotted. The values in the region of resolved energy levels are higher than those deduced from an extrapolation of the suitable laws in the continuum energy region.

3 - Level density

To study the level density of ^{238}U in the continuum the level spacing D_j of ^{237}U + n was evaluated by comparison with ^{239}Pu + n and ^{235}U + n. The thresholds of (n,γ) reactions on ^{238}U, ^{236}U and ^{240}Pu are taken in reference [3]. The following table resumes this evaluation.

Nucleus	n, γ Thresholds	Level spacing
^{236}U	6.55	$D_{observed}$ = 0, 56 eV
^{240}Pu	6.53	$D_{J=0}$ = 9.6 eV
^{238}U	6.14	$D_{J=0}$ = 15 ± 5 eV

The level spacing of excited nuclide ^{238}U was evaluated assuming that the spin cut off factor is lying between 28 and 50 and the parameter a between 15 and 25 MeV^{-1}.

This value is used to draw on figure 4 the quantity $\frac{dN}{dE}$ using formula :

$$\frac{dN}{dE} = K \sum_{j=0}^{20} (2j+1)\, e^{-\frac{(j+\frac{1}{2})^2}{\sigma^2}} \frac{e^{2\sqrt{a(E-\delta)}}}{(E-\delta)^2}$$

$\frac{dN}{dE}$ was evaluated below 1.5 MeV from the levels taken in reference [4] In spite of a loss of levels just near 1.5 MeV, the curve shows a break between the two regions of energy.

Conclusion

The data on inelastic neutron spectrum of ^{238}U shows a discrepancy between the region of resolved levels and the continuum energy region. This discrepancy is connected to the approximation of the temperature law and the lack of knowledge of the nuclear level density between 1 and 3 MeV.

References

[1] R.B. Kahn and N. Rosenzweig, Phys. Rev. 187 (1969) 1193

[2] R. Batchelor et al., Nucl. Phys. 65 (1965) 236

[3] M.J. Howerton, UCRL 50400, Vol. 9 (1970)

[4] Nuclear data sheets, vol. 4 n°6 (1970)

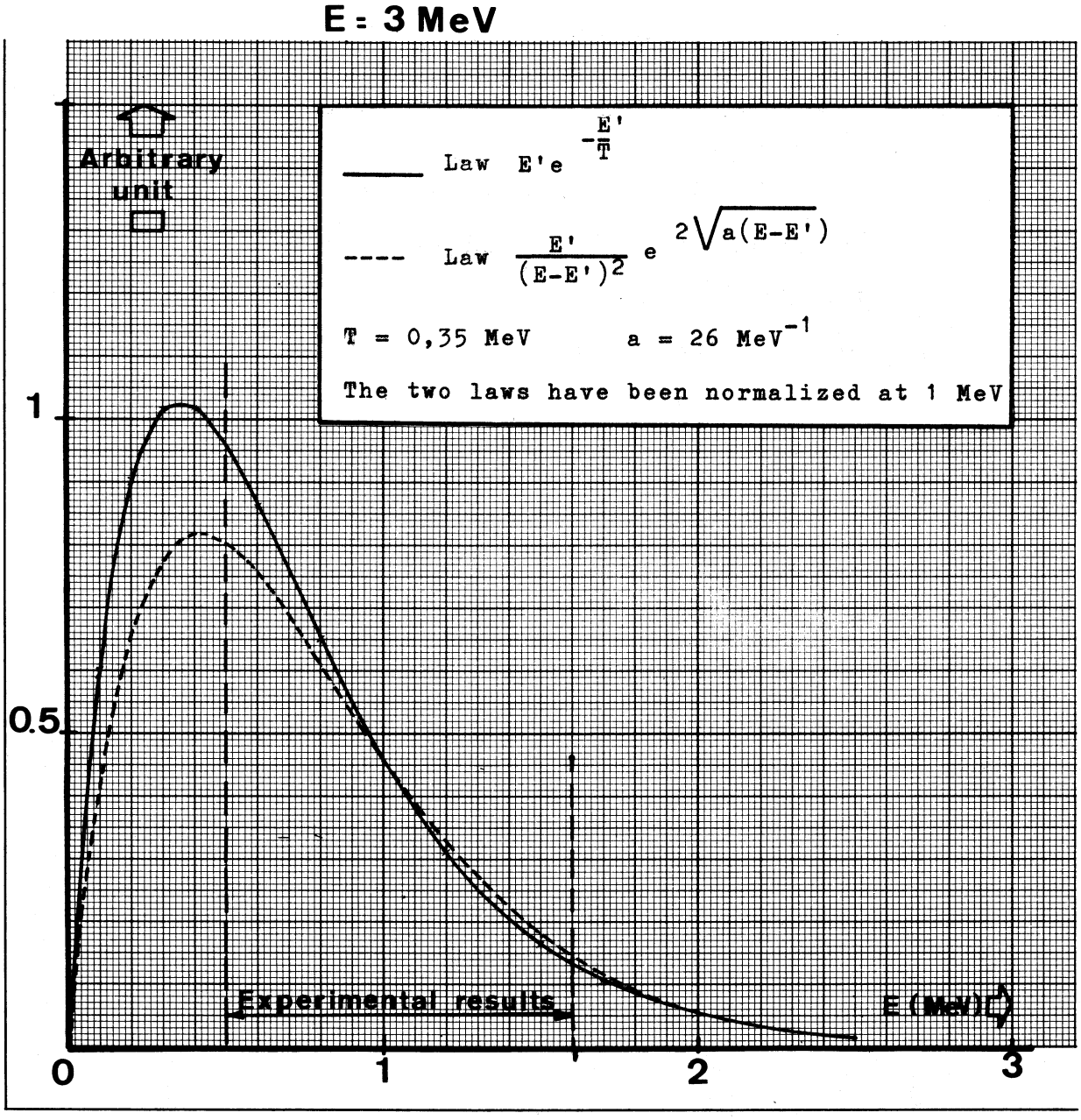
E = 3 MeV
Arbitrary unit
1
0.5
0
1
2
3
E (MeV)
Experimental results
——— Law E'e $^{-\frac{E'}{T}}$
---- Law $\frac{E'}{(E-E')^2}$ e $^{2\sqrt{a(E-E')}}$
T = 0,35 MeV
a = 26 MeV^{-1}
The two laws have been normalized at 1 MeV

Fig. 1

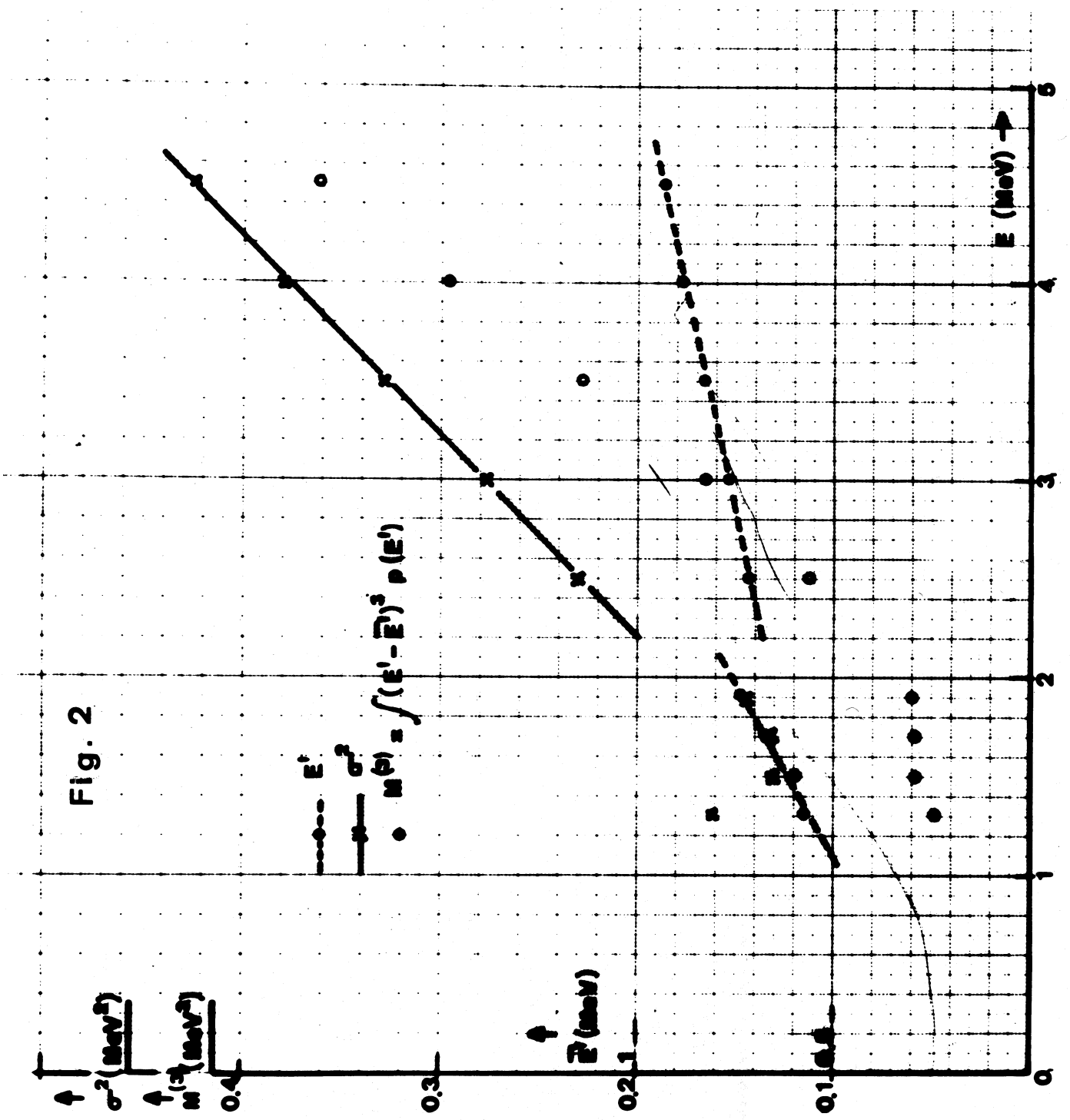
E (MeV)
0
1
2
3
4
5
0.1
0.2
0.3
0.4
σ^2 (MeV^2)
$M^{(3)}$ (MeV^3)
E^2 (MeV^2)
E^2
σ^2
$M^{(3)} = \int (E' - \bar{E})^3 p(E')$

Fig. 2

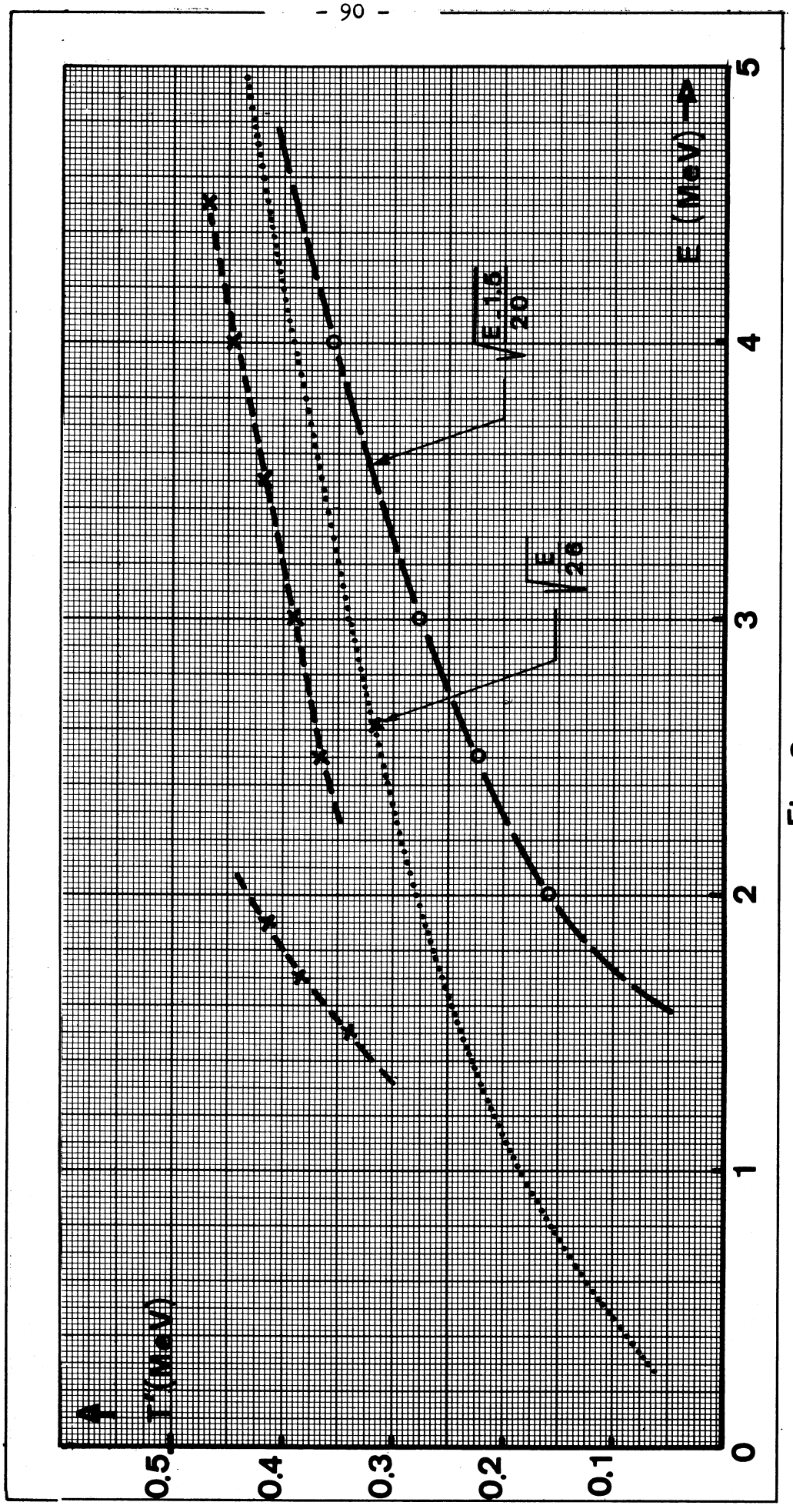

Fig. 3

$$\rho \propto \sum_{j=0}^{j=20} \frac{j+\frac{1}{2}}{\sigma^2} \; \frac{e^{2\sqrt{au} - \frac{\left(j+\frac{1}{2}\right)^2}{2\sigma^2}} \sqrt{\frac{B_n - \Delta}{u}}}{u^2}$$

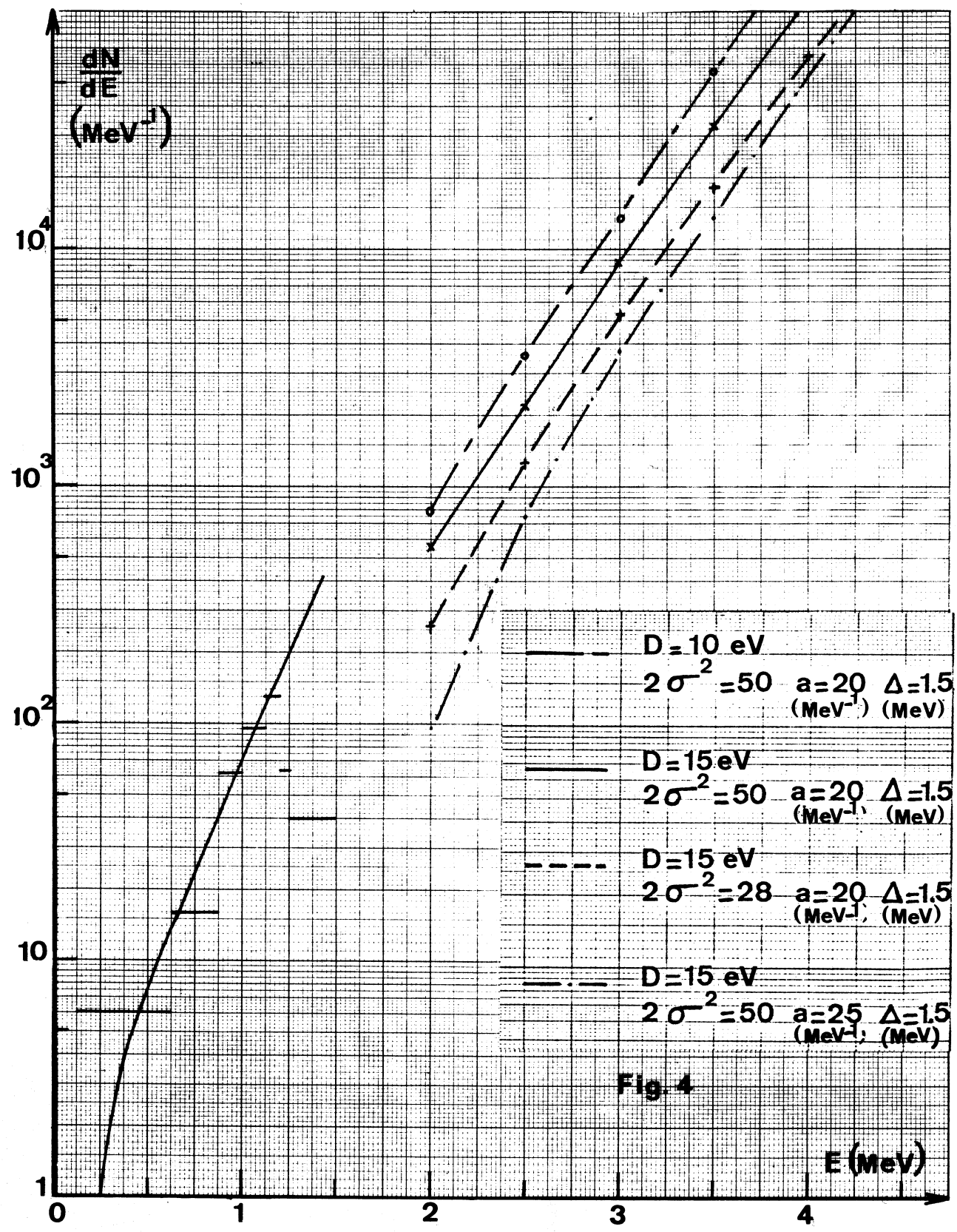

Fig. 4

This is a blank page

Use of spectrum measurements in fast media to get information on cross sections

M^me P. Corcuera, P. Govaerts, J.P. L'Heriteau

The neutron spectrum of an uranium assembly is measured with protron recoil detectors; the experimental spectrum is compared to the theoretical one.

The discrepancies are mainly due to the neutron inelastic scattering, and can be reduced by adjusting the cross sections. The influence of the spectrum of inelastic scattered neutrons is not so clear, and will be studied systematically.

This is a blank page

USE OF SPECTRUM MEASUREMENTS IN FAST MEDIA TO GET INFORMATION ON CROSS SECTIONS

INDC Topical Discussion

(Vienne - 17/21 Juillet 1972)

R. Paviotti Corcuera, P. Govaerts, J. P. L'Hériteau

I - INTRODUCTION -

The information from integral experiments used to help in the evaluation of neutron cross sections has up to now consisted mainly in critical mass, spectral indices and material buckling results. All these quantities are of a very integral nature, being a function of cross sections on the whole energy range (except threshold reactions, which are not of direct interest in reactor calculations, apart $\bar{\sigma}_f$ ^{238}U). The continuous improvement of neutron spectrometry, in particular proton recoil and time of flight methods, has led to the investigation of how these new data could be used to test calculational methods or incorporated in cross section adjustment techniques. Results along these lines have been reported in [1] , where flux ratios are introduced, as well as other integral parameters, in a general least square minimizing program.

A somewhat different line of approach is followed here, where more specific relationships between neutron spectrum and particular cross sections are sought. This stems from the fact that the neutron spectrum is for the most part determined by the total cross section - hence the elastic and inelastic scattering cross sections - while neutron balance is mostly determined by capture and fission events.

As an illustrative example, information is derived here on ^{238}U inelastic scattering from proton recoil neutron spectrum measurements in a $^{235}U/^{238}U$ assembly.

II - DESCRIPTION OF THE EXPERIMENT -

The medium under study is a 6% enriched Uranium assembly with a few % structure elements (cladded fuel platelets held in 2" x 2" cross section stainless steel tubes). In such a composition fission and capture are due exclusively to the fuel, and ^{238}U is responsible for 80 to 90% of the scattering. Sensitivity calculations of the spectrum to cross sections changes are given in section V .

The geometric configuration of the assembly is a parallelepiped (91.5cm x53 cm x 53 cm) fed at its basis by the fast source reactor HARMONIE. The multiplication factor of this experimental column is around 0.8. The neutron spectrum is obtained from a proton recoil counter (outside diameter 25 mm, active length : a few centimeters) located along the vertical axis at about 50 cm from the basis.

Propagation calculations and former experience with experimental assemblies have shown that at this location the spectrum is in equilibrium and very close to the fundamental mode spectrum. Details on the spectrometer and how to derive the neutron spectrum from the measured proton energy distribution are given in [2] . The neutron spectrum extends from 1.35 MeV to around 10 keV ; the high energy limitation comes mainly from wall effect corrections, the low energy one from gamma background. The statistical uncertainty is about 3% in most of the energy range. Comparisons of the proton recoil spectrometry with other techniques (time of flight) are being planned or under way in order to assess the accuracy of the measurement on an absolute basis.

III - CALCULATIONAL METHODS -

As said earlier, at the measurement location, transients effects due to the source boundary conditions have died away and the fundamental mode spectrum is reached. This latter spectrum may be calculated with very much detail, taking into account the resonant structure of the cross sections. as in a multigroup scheme with a $\Delta u = \frac{1}{120}$ mesh. (about 2000 groups to cover the energy range 14 MeV - 0.6 eV). In this study however the interest lies more in the macroscopic behavior of the flux

than in its fine structure ; therefore calculations have been performed with the Cadarache 25 group set [3] which is the basic tool for all project calculations. Cross sections used in this set were derived at first from the UKAEA data file through standard averaging procedures [4] , and adjusted afterwards on integral experiments [5] .

Thus with the Cadarache set, one obtains the spectrum in a $\Delta u = 0.5$ mesh between 3.68 MeV and 275 eV and a coarse mesh outside this range. This calculated spectrum is compared on Fig. 1 to the experimental results condensed into the same mesh in lethargy . The differences $\frac{E - C}{C}$ (E = experiment, C = calculations) are expressed in percent, both spectra integrated 1.35 MeV to 9.12 keV being normalized to unity. Discrepancies larger than 8 to 10% are considered as significant, because the experimental statistical uncertainty is of the order of 3 to 4% and systematic errors might be in the 5 to 8 % range. The experimental value in the last group (9.12 keV-15 keV) is less reliable because few neutrons still exist at these energies and the γ -background is large .

It is seen that important discrepancies between experiment and calculations do indeed occur.

A new evaluation [6] of ^{238}U inelastic scattering cross sections based mainly on the work of PRINCE published at the HELSINKI Conference [7] being available, calculations have been made again with this new data for σ_{inel} ^{238}U, all other cross sections remaining the same as before. The differences $\frac{E - C}{C}$ corresponding to this new calculation appear on fig. 2. Significant discrepancies also occur with these cross sections. Therefore it seems difficult to find a priori cross sections which will yield the correct spectrum and a detailed analysis based on sensitivity studies is mandatory.

For the sake of completeness the new evaluation (cross section and transfer probabilities)is given on Table 1 as well as the older values (1 st line : new evaluation ; 2 nd line : older values).

IV - ADJUSTMENT CALCULATIONS -

Prior to the time the new evaluation [6] became available, adjustement calculations had begun , where total inelastic cross sections were adjusted in the range 300 keV- 50 keV. ^{238}U levels are known in this range, thus the transfer probabilities are supposed correct and only the total inelastic cross sections are subject to the adjustment. Cross sections [9] deduced from the available experimental spectrum are as follows (the reference being the Cadarache set) :

group 7 : - 25%	> while the new evaluation gives	- 14 %
group 8 : - 15%		- 20 %
group 9 : - 40%		- 35 %
group 10 : + 60%		+ 100 %

With these new values, the differences between the experimental spectrum and the calculated one are reduced, as shown on fig. 3. It should be pointed out that the adjusted cross sections are close to the values given in the new evaluation based on more recent measurements and made independently of the adjustment calculations. This a posteriori convergence of results increased the confidence in the validity of the adjustment technique. The older values and the new evaluation have comparable transfer probabilities in the range considered, except in the group above the 45 keV level (cross section rising more rapidly in [6]). By adopting the new probabilities it will be possible to further decrease the discrepancy still remaining in the range 25 keV- 65 keV without altering the lower energy spectrum. Calculations are being done in this direction.

As it is difficult to determine at the same time transfer probabilities and cross sections, the transfer probabilities will be carefully reviewed at energies higher than 300 keV and the cross sections adjusted afterwards. These calculations will be done in the near future.

The sensitivity calculations have shown that 20% change in a cross section results in a 18% to 12% change in the flux. Thus from a

an uncertainty of x % on the experimental flux, one can deduce an uncertainty between $\frac{20}{12}$ x and $\frac{20}{18}$ x on the inelastic cross sections. If x lies in the interval 6 to 17 %, this is still better than most differential cross sections measurements.

V - SENSITIVITY STUDIES

A - These studies were divided in two parts: in the first one the inelastic cross sections were changed and in the second one the transfer probabilities were changed.

α - The influence of a 20% increase in the total inelastic cross section of group g and consequently of all the transfer inelastic cross sections from group g to groups of lower energy is to decrease the flux in group g by 18% (when group g is around 1 MeV) to 12% (when group g is around 100 keV) while the fluxes in the other groups are much less affected. The physical reason is that above 100 keV for the composition considered the inelastic cross section contributes the most to the total cross section, but the inelastic sources to lower energy groups do not change so much (increase of the cross sections, decrease of the flux, hence smaller variation of their product); moreover other phenomena (fission, elastic slowing down) also contribute to the sources. Below 100 keV, the ^{238}U inelastic cross section decreases sharply and its influence on the spectrum diminishes accordingly. Detailed numerical results are available in [8] .

β - The influence of the transfer probabilities is more difficult to assess, because many more variations may be envisaged. Let us write the balance equation for group g :

$$(D_g B^2 + \sum_g^c + \sum_g^f + \sum_g^{el} + \sum_g^{inel})\phi_g = \chi_g S_f + \sum_{j=1}^{g} \sum_{j \to g}^{el} \phi_j + \sum_{j=1}^{g} \sum_{j \to g}^{inel} \phi_j$$

where $D_g B^2 \phi_g$ is the leakage term and S_f is the fission source.

With group widths equal to or larger than $\Delta u = 0.5$, elastic slowing

down takes place only from group g-1 to group g; thus after simplification by the in group scattering terms appearing in both members of the above equation, one gets

$$(D_g B^2 + \Sigma_g^c + \Sigma_g^f + \sum_{g \to g+1}^{el} + \sum_{k=1}^{NG-g} \sum_{g \to g+k}^{inel}) \phi_g = \chi_g S_f + \sum_{g-1 \to g}^{el} \phi_{g-1} + \sum_{j=1}^{g-1} \sum_{j \to g}^{inel} \phi_j$$

In the left hand side for the composition considered here the first three terms are small, $\sum_{g \to g+1}^{el}$ is small because ^{238}U does nearly not slow down neutrons, the removal inelastic cross section is the predominant term. In the right hand side the relative importance of the source terms depend on the energy.

If the inelastic transition probabilities are changed in group g so that the removal inelastic cross section in group g does not change, ϕ_g will remain the same; there will be a very slight influence on the inelastic sources at lower energy which will be reflected on the lower energy fluxes : this influence is even smaller above 100 keV when the fission source contributes heavily to the total source. On the contrary if $\sum_{k=1}^{NG-g}$ $\sum_{g \to g+k}^{inel}$ changes, there will be a direct influence on ϕ_g, exactly as previously when the cross sections were varied.

Numerical examples are given in Table 2, where different spectra, all normalized to unity on the whole energy range, are compared.
These spectra are :

- the reference spectrum obtained with the standard Cadarache cross section set.
- the spectrum obtained with the new evaluation [6] of ^{238}U inelastic cross section.
- the spectrum obtained with the cross sections given in (6) and the transfer probabilities of the Cadarache set.

One can thus observe the respective influences of cross sections and transfer probabilities changes, referring to Table1 for the appropriate data variations.

In summary, in this multigroup formalism, ϕ_g is affected mainly by changes in the removal inelastic cross section, due to either cross sections or to transfer probabilities changes. When this cross section does not change the influence on the spectrum is much smaller.

The removal inelastic cross section in group g differs from the total inelastic cross section by the self scattering $\overline{\sigma}^{inel}_{g \to g}$. Depending on the group width, this cross section is larger or smaller. When the group width is reduced, $\overline{\sigma}^{inel}_{g \to g}$ decreases, as well as the accuracy on the integrated experimental spectrum; thus it may be interesting to adapt the multigroup structure to the accuracy of the experiment (to get information on the rise of cross sections above threshold for example). Such a work has not been done in this case as the emphasis is more on checking a given calculational scheme.

B - Comments.

α - The experimental value of B^2 is equal to $1.\ 10^{-3}\ m^{-2}$ the value corresponding to the calculations of Fig. 1 is $0.95\ 10^{-3}\ m^{-2}$, the one corresponding to Fig. 2 is $0.80\ 10^{-3}$ and the one to Fig. 3 is $1.\ 10^{-3}$.

It is necessary to point out (réf. 6) that such a low value $0.80\ 10^{-3}$ comes from the increase of about 20% in $\overline{\sigma}_{inel}$ in the range 1 to 3 MeV (groups 2 to 4). It is possible to remove that difference by increasing by about 15% $\overline{\sigma}_{fission}$ ^{238}U, a change which agrees with the last tendencies concerning that section.

Modifications of $\overline{\sigma}_{inel}$ below 800 keV do not influence B^2 (réf. 6).

β - Comparing colums 1 and 2 of table 2 one notices a great difference in the range 1 to 10 keV (groups 14 to 17). This excess of neutrons comes from transfer from group 10.

No experimental values are available by the proton recoil method in this energy range which would be covered by time of flight results. We also point out that, as was shown in Fig. 3, it is easy to correct the spectrum by modifications in the inelastic cross sections, but it is very difficult to do that unambiguously by changing the transfer probabilities.

CONCLUSION -

It has been shown that interesting information on inelastic cross sections could be derived from neutron spectrum measurements performed in specific assemblies. The proposed cross sections adjustments agree with recent evaluation in the range of energies considered. More work is in progress to extend the results to higher energies, and this information should be confirmed by measurements on different assemblies.

The study reported here is not exhaustive and the use of spectrum measurements is not limited to the domain of inelastic cross sections. Other compositions may be considered, where more neutrons are present at lower energies, yielding information on the ratio slowing down / absorption (time of flight spectrum measurements). These results may be interpreted on an absolute basis or relatively to one another. For example recent experimental evidence [10] has shown discrepancies in the low energy spectrum of plutonium-graphite systems with respect to Uranium - graphite systems built with the same graphite matrices. These results might give indications on the ratio $\frac{\sigma_a \, Pu_9}{\sigma_a \, U_5}$ below a few keV.

REFERENCES

[1] C. G. CAMPBELL, J. L. ROWLANDS
The relationship of microscopic and integral data
Nuclear data for reactors Vol. II, p. 391 - AIEA 1970

[2] A. P. SCHMITT and A. LERIDON
Fast reactor spectrum measurement and their interpretation
AIEA 138 - Conference Chicago- Novembre 1970

[3] J. RAVIER and J. M. CHAUMONT
Presentation of multigroup cross sections set prepared at Cadarache
ANL 7320, p. 47, Octobre 1966

[4] P. GOVAERTS
Notes sur la Physique des réacteurs à neutrons rapides
PNR/SETR R. 041

[5] J. Y. BARRE, J. RAVIER
Utilisation d'expériences intégrales pour améliorer le jeu de sections efficaces Cadarache - jeu version 2
PNR/SETR 69 031 (1969)

[6] J. P. L'HERITEAU
Comparaison des sections efficaces inélastiques et du spectre de renvoi du ^{238}U avec le jeu SETR version 2
DPh-N/MF (1972)

[7] A. PRINCE
Analysis of High-Energy neutron cross sections for fissile and fertile isotopes.
Nuclear Data for reactors Vol. II, p. 825 AIEA (1970)

[8] R. PAVIOTTI CORCUERA
Sensibilité du spectre, des taux de réaction et d'autres paramètres. à la matricé inélastique de l'Uranium 238
SECPR- 72/32 (1972)

[9] R. PAVIOTTI CORCUERA
Utilisation de mesures de spectrométrie neutronique
Résultats préliminaires pour le milieu UK5 .
SECPR - 72/35 (1972)

[10] H. DUQUESNE
Communication privée.

TABLE I

Averaged inelastic cross section and $P_{i \rightarrow j}$ by group - The value above is our value - The value under is the SETR version 2 set value.

1	2.38 2.45	3.30 7.83 .27 .59	13.98 7.63 .10 .43	24.14 18.70 .04	25.20 25.09	17.13 17.38	9.14 11.90	4.22 6.22	1.78 2.74	.7 1.49
2	2.358	.15 .42	.04 .26		17.37 20.45	9.28 16.59	4.22 9.66	.80 4.54	.72 2.59	.28 1.07
3	2.2425 2.286	23.55 16.05 .035 .35	33.32 21.96 .28	24.30 21.35	12.13 19.55	4.36 6.78	1.39 4.81	0.57 4.37	.24 3.76	.105 .74
4	2.447 2.011	35.58 51.12 .034 .02	17.63 20.09 .02	32.15 8.6 .005	9.79 11.07 .004	3.77 5.22 .002	.62 2.19	.214 1.09	.121 .45	.06 .15
5	2.0[illegible] 1.9667	49.34 [illegible] .0315 .0005	28.135 27.82 .0235	.225 [illegible]	11.54 .16	8.11 .9	1.72 .106	.54 .014	.225 .0035	.11 .001
6	1.5768 1.5867	75.85 68.998	23.77 29.185	.38 1.435	.25	.09	.03	.009	.003	
7	1.103 1.2832	65.72 56.45	33.96 42.11	.32 .98	.41	.05				
8	.66 .82	45.42 40.30	53.07 57.93	1.51 1.545	.12	.07	.02	.012	.003	
9	.277 .4526	0.0	73.35 69.34	23.72 29.06	2.93 1.60					
10	.035 .02006	0.0	0.0	57.09 80.28	34.41 15.17	5.79 3.20	1.96 .95	.75 .35	.05	

TABLE 2

N°	REFERENCE SPECTRUM	$\frac{M-C}{C}$ in %	$\frac{M'-C}{C}$ in %	
1	0.1381 (-1)	- 9.2	- 6.0	
2	0.2500 (-1)	-17.8	- 7.6	
3	0.3673 (-1)	-22.1	0.5	
4	0.7656 (-1)	-20.2	-11.2	+ 9
5	0.1209 (0)	- 5.7	2.9	+ 8
6	0.1660 (0)	- 1.3	- 3.5	- 2
7	0.1499 (0)	8.2	- 0.4	
8	0.1368 (0)	10.6	+ 6.9	
9	0.1020 (0)	17.4	16.6	
10	0.9754 (-1)	- 3.3	-11.4	
11	0.5050 (-1)	-10.1	-14.1	
12	0.1852 (-1)	0.9	5.8	
13	0.4395 (-2)	33.1	48.0	
14	0.7807 (-3)	44.0	207.8	
15	0.1760 (-3)	46.8	413.0	
16	0.5247 (-4)	19.8	296.9	
17	0.2034 (-4)	-35.6	236.1	
18	0.5572 (-5)	-20.7	97.6	
19	0.8296 (-6)	6.4	4.0	
20	0.7702 (-7)	9.8	- 0.9	
21	0.4712 (-8)	8.6	- 1.0	
22	0.2974 (-9)	8.8	- 1.0	
23	0.7480 (-12)	9.5	- 1.0	
24	0.1911 (-14)	-10.7	- 1.0	
25	0.4839 (-18)	10.8	- 1.0	

C Reference spectrum with version 2 set σ_{inel} and transfer probability

M Calculated spectrum with L'HERITEAU's σ_{inel} and transfer probability

M' Calculated spectrum with L'HERITEAU's σ_{inel} and SETR version 2 transfer probabilities.

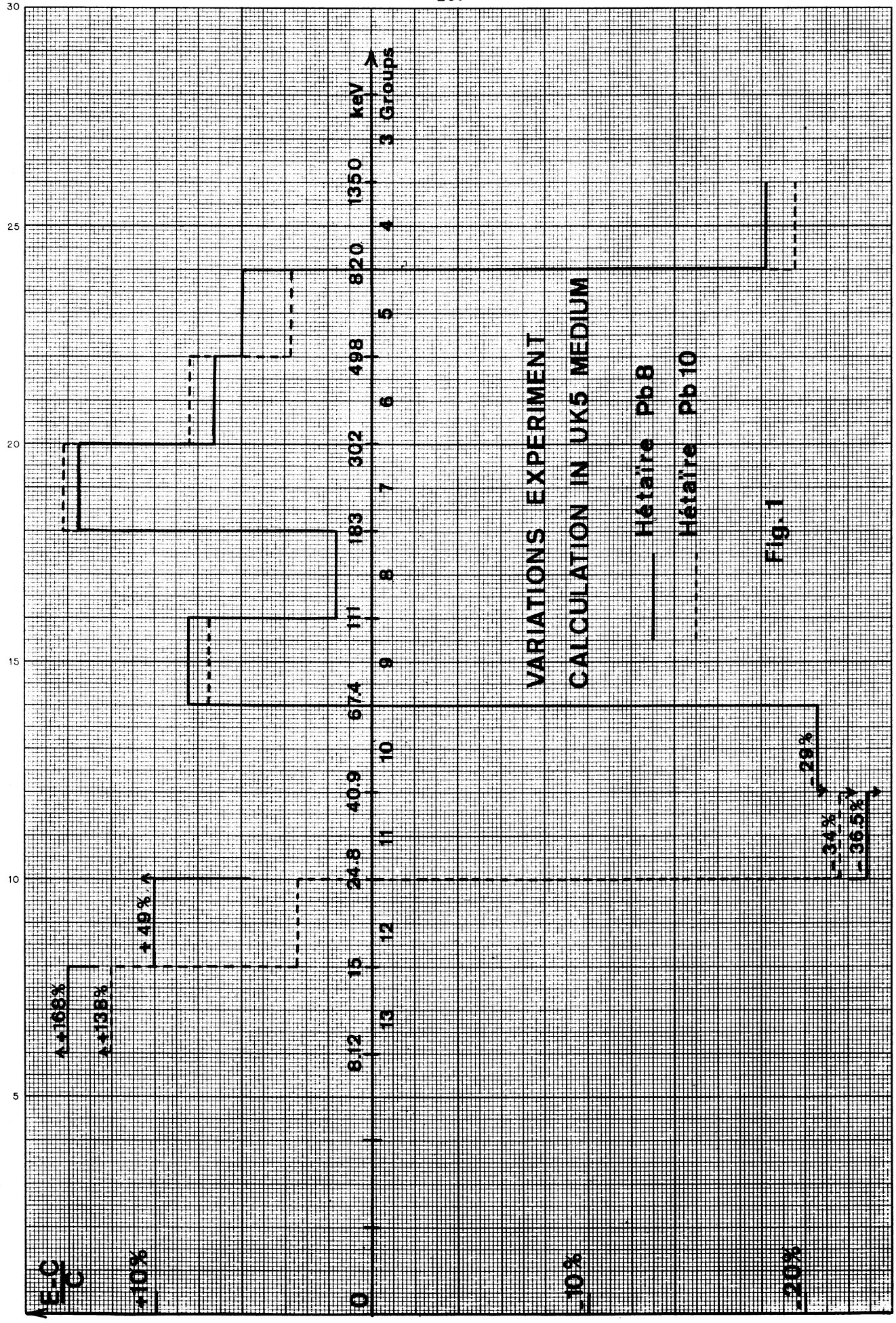

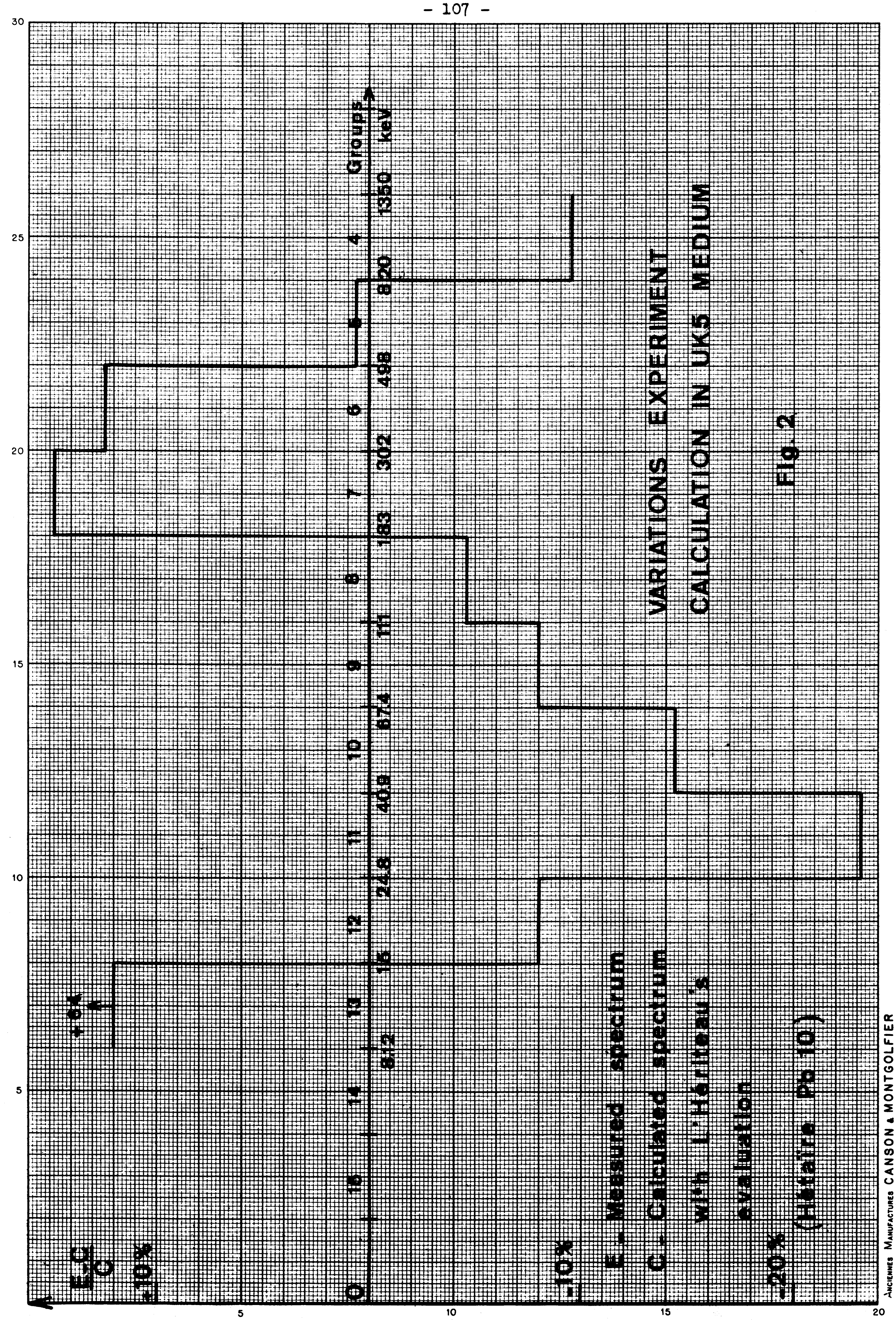
VARIATIONS EXPERIMENT
CALCULATION IN UK5 MEDIUM
E-C / C
+10%
-10%
-20%
E - Measured spectrum
C - Calculated spectrum
with L'Hériteau's
evaluation
(Hétaire Pb 10)
Groups
keV
+84
4 5 6 7 8 9 10 11 12 13 14 15 16
1350 820 498 302 183 111 67.4 40.9 24.8 15 9.12
0
ANCIENNES MANUFACTURES CANSON & MONTGOLFIER

Fig. 2

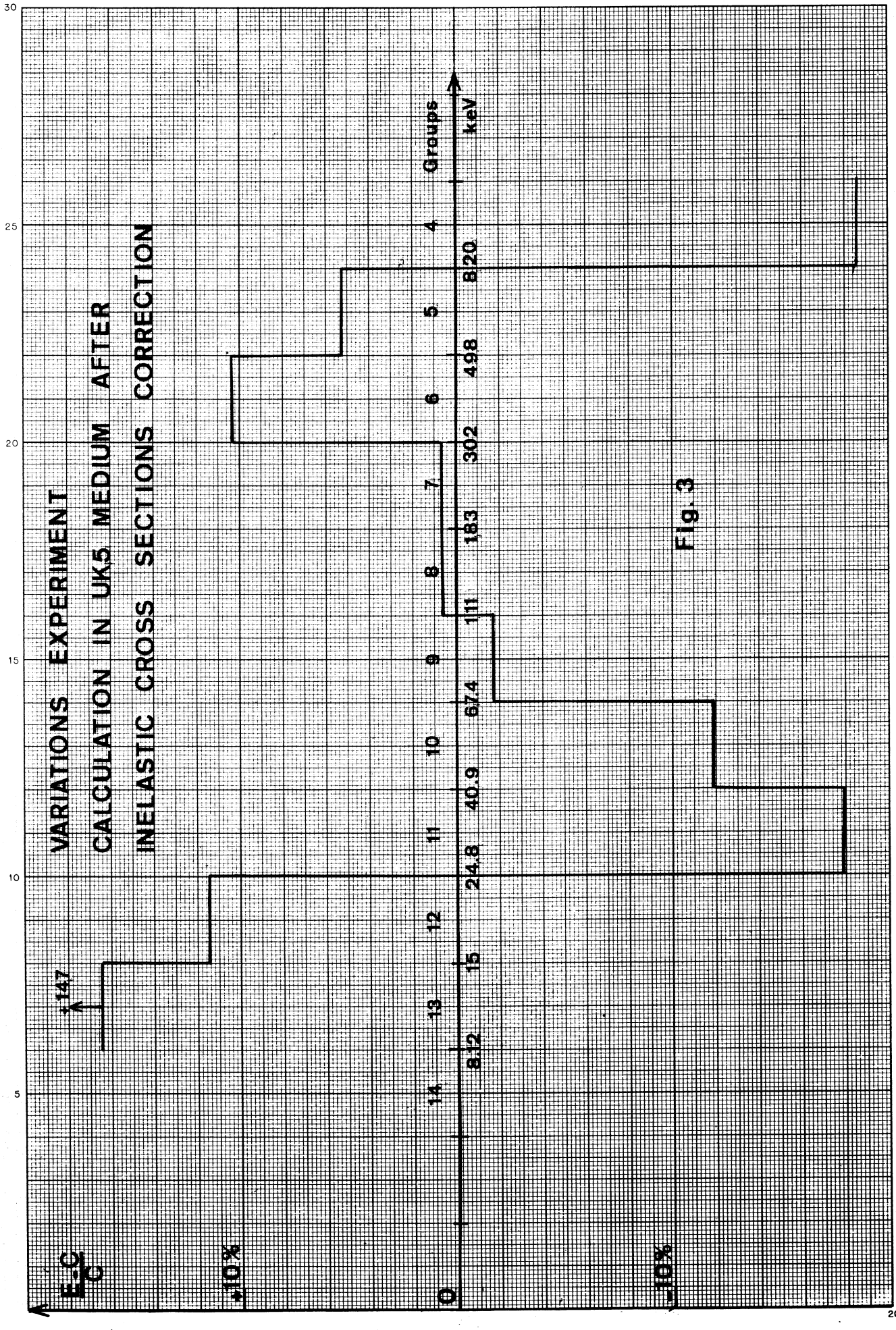
VARIATIONS EXPERIMENT
CALCULATION IN UK5 MEDIUM AFTER
INELASTIC CROSS SECTIONS CORRECTION
E-C
C
+10%
0
-10%
Groups
keV
4
820
5
498
6
302
7
183
8
111
9
67.4
10
40.9
11
24.8
12
15
13
8.12
14
+147
30
25
20
15
10
5
20
Fig. 3
ANCIENNES MANUFACTURES CANSON & MONTGOLFIER

Usachev: Dr. Ribon, have you carried out a systematic investigation of the sensitivity coefficients; do you have the matrix of these coefficients ?

reply: This study was carried out at Cadarache by Mrs. Corcuera and was published in report SECPR-72/32.

Benzi: Could you tell me if the general trend of the observed discrepancy is similar to the one obtained in Karlsruhe ?

reply: Up to now we have no results above 1.3 MeV; but we observe the same general trend, between 20 keV and 1 MeV, as seen at Karlsruhe.

Rowlands: I would like to make a comment about the value of spectrum measurements and the results of UK cross-section adjustment studies to fit integral measurements and reactor spectrum measurements.

Spectrum measurements give direct information about the flux in the Doppler energy region (1 Kev) relative to the average over the fission cross-section of the medium. These measurements are valuable in reducing the uncertainty in Doppler effect predictions.

As a result of fitting to reactor spectrum measurements a reduction of 30% in the inelastic scattering of U238 in the energy range 50 Kev to 150 Kev has been found to be required.

There are still large uncertainties in reactor spectrum measurements. For example, there are uncertainties in the energy scale of proton recoil spectrum measurements and in the detector efficiency in Time-of-Flight spectrum measurements.

Ribon: Do you think that the 30% decrease that you applied to ^{238}U inelastic cross sections between 50 and 150 keV is consistent with microscopic data ?

reply: The standard deviation of the inelastic cross section evaluation used in our calculations was estimated to be $\pm$ 20% so the adjustment is by more than one standard deviation. This was one of the very few items of nuclear data which were adjusted by more than one standard deviation.